

**BLOCKING MYOSTATIN SIGNALING PATHWAY WITH MYOSTATIN
PROPEPTIDE AND FOLLISTATIN: NOVEL APPROACHES TO IMPROVE
SKELETAL MUSCLE HEALING**

by

Jinhong Zhu

M.D., BengBu Medical School, 1998

MS, University of Pittsburgh, 2005

Submitted to the Graduate Faculty of
Swanson School of Engineering in partial fulfillment
of the requirements for the degree of
Doctor of Philosophy

University of Pittsburgh

2009

UNIVERSITY OF PITTSBURGH
SWANSON SCHOOL OF ENGINEERING

This dissertation was presented

by

Jinhong Zhu

It was defended on

November 24, 2008

and approved by

Stephen Badylak, Professor, Surgery and Bioengineering

Bruno Péault, Professor, Pediatrics, Cell Biology, and Bioengineering

Yong Li, Assistant Professor, Orthopedic Surgery and Pathology

Dissertation Director: Jonny Huard, Professor, Orthopedic Surgery, Molecular Genetics, and

Bioengineering

Copyright © by Jinhong Zhu

2009

**BLOCKING MYOSTATIN SIGNALING PATHWAY WITH MYOSTATIN
PROPEPTIDE AND FOLLISTATIN: NOVEL APPROACHES TO IMPROVE
SKLETAL MUSCLE HEALING**

Jinhong Zhu, PhD

University of Pittsburgh, 2009

The complete recovery of injured skeletal muscle has posed a constant challenge for orthopaedic physician. Once injured, skeletal muscle is able to undergo regeneration from satellite cells; nevertheless, in the serious injured muscle, the formation of fibrosis often impedes effective muscle regeneration and resulted in an incomplete muscle healing. Therefore, to develop biological approaches to improve muscle healing, it is crucial to better understand the mechanisms of the skeletal muscle fibrosis.

In the current studies, we found that myostatin (MSTN), a member of TGF- β family, plays a role in the formation of skeletal muscle fibrosis, besides the other putative fibrosis stimulator, TGF- β 1. *In vitro*, MSTN directly stimulated the proliferation of fibroblasts and their productions of fibrotic proteins. *In vivo*, after laceration injury, gastrocnemius muscles of MSTN^{-/-} mice showed less fibrosis and better muscle regeneration than wide-type (WT) counterparts. Considering MSTN as a therapeutic target of skeletal muscle healing, we found that inhibitors of MSTN, MSTN propeptide (MPRO) and follistatin, effectively blocked MSTN signaling and improved skeletal muscle healing after injured. We used adeno-associated virus (AAV)-mediated MPRO cDNA to successfully deliver MPRO *in vivo* and improve skeletal muscle healing of normal mice after laceration, and ameliorate dystrophic pathology of

mdx/SCID mice. Furthermore, our results demonstrated FLST overexpression (FLST/OE) mice exhibited decreased fibrosis and increased muscle regeneration in injured skeletal muscle as compared to wild-type (WT) mice. Moreover, muscle progenitor cells (MPCs) isolated from MSTN^{-/-} and FLST/OE mice significantly regenerated more myofibers than MPCs obtained from WT mice, when transplanted into dystrophic muscles.

Collectively, our results suggested that MSTN directly stimulated fibrosis in the injured skeletal muscle; blocking MSTN signaling with MPRO or FLST improved skeletal muscle healing after laceration injury; blocking MSTN signaling in donor MPCs significantly enhanced the success of cell transplantation into dystrophic muscles. Our studies not only uncover some of the mechanisms implicated in skeletal muscle fibrosis and regeneration, and help the development of new therapeutic approach for promoting the healing of injured or diseased skeletal muscle, but also render a new sight of how to obtain robust genetically modified cell populations for cell therapy.

DESCRIPTORS

Cell Transplantation

Decorin

Dystrophin

Fibrosis

Follistatin

Muscle Progenitor Cells

Muscle Regeneration

Myostatin

Myostatin Propeptide

Transforming Growth factor- β 1

	USING MSTN-/- MICE AND MSTN PROPEPTIDE (MPRO), AN INHIBITOR OF MSTN.....	15
2.3	OBJECTIVE #3: TO EVALUATE THERAPEUTIC EFFECT OF FLST ON INJURED SKELETAL MUSCLE.....	16
2.4	SIGNIFICANCE.....	17
3.0	RELATIONSHIPS BETWEEN TGF-β1, MYOSTATIN, AND DECORIN: IMPLICATIONS FOR SKELETAL MUSCLE FIBROSIS	18
3.1	INTRODUCTION	18
3.2	METHODS.....	19
3.2.1	Isolation of Fibroblasts from Skeletal Muscle.....	19
3.2.2	Cell Culture	20
3.2.3	Western Blot Analysis.....	21
3.2.4	Quantitative RT-PCR	22
3.2.5	Enzyme-Linked Immunosorbent Assay.....	23
3.2.6	Immunocytochemistry.....	23
3.2.7	Animal Model.....	24
3.2.8	Immunohistochemistry.....	25
3.2.9	Statistical Analysis	25
3.3	RESULTS.....	26
3.3.1	Effects of MSTN on Fibroblasts	26
3.3.2	Reduced Fibrosis and Enhanced Skeletal Muscle Regeneration in MSTN-/- Mice.....	28
3.3.2.1	Reduced fibrosis in injured MSTN-/- mice	28
3.3.2.2	Improved muscle regeneration in injured MSTN-/- mice.....	28
3.3.2.3	Elevated DCN expression in injured MSTN-/- mice	30
3.3.3	Relationship between TGF- β1 and MSTN	30
3.3.4	DCN Counteracts the Effect of MSTN.....	34

3.3.5	Inhibitory Effects of DCN on MSTN may be Mediated by FLST	36
3.4	DISCUSSION.....	36
3.4.1	Fibrotic Roles of MSTN in Vitro and in Vivo	37
3.4.2	Improved Muscle Healing in the Injured MSTN ^{-/-} Muscle.....	38
3.4.3	Relationships between TGF- β 1 and MSTN.....	39
3.4.4	Inhibitory Effects on DCN on MSTN.....	40
3.5	CONCLUSIONS	42
4.0	AAV-MEDIATED MYOSTATIN PROPEPTIDE IMPROVED SKELETAL MUSCLE HEALING IN NORMAL MICE AND ATTENUATED DYSTROPHIC PATHOLOGY IN <i>MDX/SCID</i> MICE	43
4.1	INTRODUCTION	43
4.2	METHODS.....	45
4.2.1	Construction of an AAV Vector Carrying Mouse MPRO Gene	45
4.2.2	Transduction of AAV2-MPRO/GFP <i>in Vitro</i>	45
4.2.3	Western Blot	46
4.2.4	Transduction of AAV2-MPRO or GFP into WT Mice	46
4.2.5	Isolation of Muscle Progenitor Cells from WT and MSTN ^{-/-} Mice and Cell Transplantation.....	47
4.2.6	Intramuscular Transduction of AAV2-MPRO/GFP into <i>Mdx/SCID</i> Mice Followed by WT MPC Transplantation	49
4.2.7	Immunohistochemistry.....	50
4.2.8	Statistics	51
4.3	RESULTS	52
4.3.1	MSTN ^{-/-} Muscles Exhibited Increased Neovascularization	52
4.3.2	Delivery of AAV2-MPRO Inhibits MSTN Activity <i>in Vitro</i>	54
4.3.3	AAV2 Delivered-MPRO Inhibits MSTN Activity <i>in Vivo</i>	55
4.3.4	Long Term Beneficial Effects of MPRO on Muscle Healing	59

4.3.5	Lack of MSTN Signal in Donor MPCs Elevated Efficiency of Cell Transplantation in <i>Mdx/SCID</i> Mice.....	61
4.3.6	AAV-MPRO Improved Cell Transplantation and Reduced Severity of Muscular Dystrophy Efficiency in <i>Mdx/SCID</i> Mice.....	63
4.4	DISCUSSION.....	67
4.4.1	Increased Vascularity in the Injured MSTN ^{-/-} Skeletal Muscles and AAV-MPRO Treated Injured Skeletal Muscles	68
4.4.2	Blocking MSTN ^{-/-} Signaling in Muscle Progenitor Cells Improve Cell's Regenerative Capacity.....	69
4.4.3	Improved Success of Cell Transplantation by Blocking MSTN Signaling in Host Dystrophic Muscle.....	71
4.5	CONCLUSION	74
5.0	FOLLISTATIN IMPROVES SKELETAL MUSCLE HEALING	76
5.1	INTRODUCTION	76
5.2	METHODS.....	78
5.2.1	Animal Model.....	78
5.2.1.1	Histology	78
5.2.1.2	Immunohistochemistry.....	79
5.2.1.3	MSTN immunostaining.....	79
5.2.1.4	CD31 immunostaining.....	79
5.2.2	Muscle Progenitor Cell Isolation and Transplantation into Skeletal Muscle	80
5.2.2.1	Isolation of MPCs	80
5.2.3	Flow Cytometry.....	80
5.2.3.1	Cell transplantation.....	81
5.2.4	Statistics	81
5.3	RESULTS	82
5.3.1	Healing after Injury Is Enhanced in FLST/OE Skeletal Muscle.....	82

5.3.1.1	Increased regeneration in the injured FLST/OE skeletal muscle ..	82
5.3.1.2	Decreased fibrosis in the injured FLST/OE skeletal muscle	84
5.3.1.3	Decreased MSTN and increased vascularity in the injured FLST/OE skeletal muscle	85
5.3.2	Comparison of WT and FLST/OE-MPCs	88
5.3.2.1	<i>In vivo</i> muscle regeneration of MPCs	88
5.3.2.2	<i>In vitro</i> characterization of MPCs	90
5.4	DISCUSSION.....	91
5.4.1	Mechanism Involved in the Reduced Fibrosis in the Injured FLST/OE Muscle	92
5.4.2	Cellular Mechanism by Which FLST Promotes Skeletal Muscle Regeneration after Injury	93
5.5	CONCLUSION	96
6.0	OVERALL CONCLUSION.....	97
6.1	FUTURE DIRECTION AND LIMITATION.....	98
6.1.1	Determine If Blocking MSTN in Injured Skeletal Muscle Leads to Functional Recovery	98
6.1.2	Correlation between Angiogenesis and Improved Muscle Healing	99
6.1.3	Limitation	100
APPENDIX A	101
APPENDIX B	104
BIBLIOGRAPHY	109

LIST OF TABLES

Table 1. The Sequences of Primer Pairs for Q-RT-PCR	22
-----------------------------------------------------------	----

LIST OF FIGURES

Figure 1-1 A Schematic Illustration of Injured Skeletal Muscle	4
Figure 1-2 Muscle Regeneration from RZ inside Preserved Basal Membrane	5
Figure 3-1 MSTN Stimulated Proliferation and ECM Production of Fibroblasts	27
Figure 3-2 Inhibition of MSTN Facilitates Skeletal Muscle Healing after Injury.....	29
Figure 3-3 Interaction between TGF- β 1 and MSTN <i>in vitro</i>	32
Figure 3-4 DCN Attenuated the Effects of MSTN on Fibroblasts and Myoblasts.....	33
Figure 3-5 DCN Stimulated Expression of FLST and FLST Promoted Myogenic Differentiation of Myoblasts.....	34
Figure 3-6 Relationship between Decorin, TGF- β 1, Myostatin, and Follistatin	42
Figure 4-1 Schematic Illustration of Preplate Technique	48
Figure 4-2 Earlier Neovascularization in the Injured MSTN ^{-/-} Muscle.....	52
Figure 4-3 Increased Vascularity in Injured MSTN ^{-/-} Muscle at 4 weeks after Laceration	53
Figure 4-4 <i>In Vitro</i> AAV-MPRO Transduction.....	55
Figure 4-5 AAV-MPRO Improved Skeletal Muscles Healing at 4 Weeks after Injury	57
Figure 4-6 Increased Angiogenesis in AAV-MPRO Treated Injured Skeletal Muscle.....	58
Figure 4-7 AAV-MPRO Showed Long-Term Beneficial Effects on Injured Skeletal Muscle	60
Figure 4-8 Donor MSTN ^{-/-} MPCs Exhibited a Higher Regenerative Capacity in the Host Dystrophic Muscle	62
Figure 4-9 Muscle Progenitor Cell Characterization and Transplantation.....	64
Figure 4-10 Improved Dystrophic Pathology in <i>mdx</i> /SCID Mice after AAV-MPRO Treatment	66

Figure 4-11 Schematic Representation of How Transduction of the AAV-MPRO into Host Dystrophic Muscle Improves Efficiency of Cell Transplantation.....	73
Figure 5-1 Transgenic FLST/OE Skeletal Muscle Exhibited Better Muscle Regeneration after Injury.....	83
Figure 5-2 The Muscle of FLST/OE Transgenic Mice Developed Less Fibrosis after Injury	85
Figure 5-3 Decreased MSTN Expression and Increased Vascularity in Injured FLST/OE Skeletal Muscles	87
Figure 5-4 FLST OE MPCs Are Superior to WT MPCs in Regenerating Skeletal Muscle.....	89
Figure 5-5 <i>In Vitro</i> Characterization of WT- and FLST/OE-MPCs	90

ACKNOWLEDGEMENTS

Throughout the past 5 years, many people have contributed to the accomplishment of my Ph.D dissertation. I will be forever grateful for the guidance and support that Dr. Johnny Huard, my advisor, provided to me during my graduate study. I truly admire his dedication and willingness to help, attributes that undoubtedly contributed to the success of my thesis project. I am also very thankful to Dr. Johnny Huard, for his great contribution to my research and the many insightful comments and suggestions he offered throughout my thesis studies. I appreciate that Dr. Yong Li mentored me at my first few years when he was a group leader in muscle group. I am also very fortunate to have Dr. Stephen Badylak, Dr. Bruno Péault, Dr. Yong Li, on my dissertation committee; their expertise in molecular biology was invaluable to my understanding and the development of my thesis.

I would like to highly appreciate that Dr. Xiao Xiao provided adeno-associated virus, and that Dr. Se-Jin Lee generously offered the breeder of myostatin knockout and follistatin overexpression mice. I also am grateful to Lynne Bauer, who bred and took care of all transgenic mice to keep my experiments in line. These precious mice have been the solid foundation of my research.

There are many others who have helped me throughout the last couple of years whom I want to thank. Burhan Gharaibeh, the laboratory manager, is an amazing person who went through a lot of troubleshooting with me in respect to the utility of fluorescence microscopy, Northern Eclipse software, and helped with the determination of sex of neonatal mice using

anatomical sex technique. I also want to thank all the members of the Stem Cell Research Center for their continuous support, especially those I often interacted with, Masa Nozaki, Bo Zheng, Aiping Lu, Ying Tang, Mitra Lavasari, Tom Payne, Karen Corsi, Wei Shen, Ken Urish... I also value the friendships that arose from our collaborations. Keep up the great work!

James Cummins, Matthew Bosco, and Michele Keller, worked behind the scenes to solve problems and make arrangements for me. They have provided wonderful administrative assistance in the laboratory,

More important, I thank my family for all their love and support. Mom, Dad, brothers, sisters in law, and nephews, thanks for everything that you have taught me and for all of your support throughout my life. Most importantly, I would like to give special thanks to my dear husband, Jianqun Ma, because he is the best husband that a woman can dream of, gentle and full of affection. My husband received the highest education in China, having both M.D. and Ph.D. He is a successful thoracic surgeon and associated professor in China. To come here to stay with me, he not only have to make a great sacrifice on his career, the quality of material life, but also have to overcome language obstacle and explore a different research field which was brand new for him. My husband is a very intelligent, diligent, and energetic person. Since we work in the same laboratory, he has helped me a lot with animal experiments. After he finishes at work, he always tries his best to cook delicious Chinese foods for us. Without him, I couldn't have finished so well. While I am accomplishing my Ph.D degree, we are lucky to have our son joining our family. Although we haven't met him yet, he is such a blessing and joy to us. My dear husband, thank you, and I love you and our son very much. Without you, my success is meaningless.

Moreover, I would like to acknowledge Henry J. Mankin Endowed Chair for Orthopaedic Research at the University of Pittsburgh, the William F. and Jean W. Donaldson Chair at Children's Hospital of Pittsburgh, the Hirtzel Foundation, and the NIH (R01 AR47973 awarded to Johnny Huard).

1.0 INTRODUCTION

Although skeletal muscle injuries are extremely common, accounting for up to 30% of all sports-related injuries, the treatments that are currently available are often conservative and ineffective such as RICE principle (rest, ice, compression, and elevation), non-steroid anti-inflammatory drugs (NSAIDs), therapeutic ultrasound, and hyperbaric oxygen. More and more evidence has shown that administration of NSAIDs delays inflammation and regeneration and increases fibrosis¹⁻⁵. Neither therapeutic ultrasound nor hyperbaric oxygen therapy has had beneficial effects on the final outcome of muscle healing^{6,7}. Injured muscle can undergo regeneration spontaneously from satellite cells, a reservoir of myogenic progenitor cells for the repair and maintenance of skeletal muscle, but the ensuing formation of fibrous scar tissue often impedes efficient muscle regeneration, resulting in incomplete healing^{8,9}. As a result, previously injured muscle continues to show muscle atrophy or loss of function, including loss of muscle extensibility and strength. Moreover, there is significant morbidity associated with these injuries, such as the development of painful contractures and the increased risk for repeat injury, by and large as a result of extensive fibrosis.

To improve the healing of injured muscle, researchers have administered growth factors that can promote muscle regeneration, including insulin-like growth factor-1 (IGF-1), basic-fibroblast growth factor (bFGF), and nerve growth factor (NGF), to injured skeletal muscles¹⁰⁻¹³. Treatment with such growth factors—particularly IGF-1—enhanced muscle

regeneration and strength to some extent; however, fibrosis still predominated and prevented complete recovery of the injured muscle. Injured muscle exhibits active muscle regeneration before the formation of thick and extensive connective tissue^{9, 14, 15}. However, many newly formed myofibers express not only desmin, a myogenic marker, but also vimentin, a fibroblast marker. Some of the regenerating myofibers are TGF- β 1 positive as soon as 3 days after injury¹⁶. With the development of fibrosis, the vimentin- or TGF- β 1-positive regenerating myofibers become smaller and gradually disappear, which ultimately are replaced by mononucleated fibrotic cells and scar tissue^{11, 16}. Therefore, apart from the enhancement of muscle regeneration, the prevention of fibrosis is key effort to improve skeletal muscle healing.

Transforming growth factor- β 1 (TGF- β 1) is a potent fibrogenic cytokine in many tissues and organs, including the lungs, kidneys, liver, heart, and skin¹⁷⁻²⁰. To date, it has been widely accepted that TGF- β 1 is also associated with fibrosis in skeletal muscle²¹⁻²³. Elevated TGF- β 1 levels are observed in dystrophic skeletal muscle and shortly after skeletal muscle injury^{16, 21-23}. Research has shown that elevated expression of TGF- β 1 accounts for the initiation and development of fibrosis in muscular dystrophies^{21, 22}. TGF- β 1 has been proven to effectively induce myofibroblastic differentiation of fibroblasts both *in vitro* and *in vivo*, the induction of which is responsible for excessive accumulation of fibrous tissue^{24, 25}. Members of our research group have shown that TGF- β 1 plays a significant role in both the initiation of fibrosis and the inducement of myofibroblastic differentiation of myogenic cells in the injured muscles^{16, 26}. The use of antifibrosis therapies such as TGF- β 1 neutralizing antibody, interferon-gamma (IFN- γ), suramin, relaxin, decorin, or losartan can improve the healing of the injured muscles both histologically and physiologically²⁷⁻³²; however, none of these approaches can completely prevent fibrosis, and the precise mechanisms of fibrosis remain unclear. For instance, it warrants

further investigation whether TGF- β 1 acts along or requires interaction with other molecules during the development of muscle fibrosis. It is likely that other molecules also positively regulate fibrosis. In this project, we have been engaging in searching potential molecules that participates in the skeletal muscle fibrosis, helping better understand mechanisms involved in the fibrosis of the injured skeletal muscle, and developing novel biological approaches to the injured skeletal muscles based on new therapeutic target that we have identified in the current project.

1.1 LITERATURE REVIEW

1.1.1 Wound Healing

Muscle injury and repair have been widely investigated. Muscle injuries occur after either direct trauma (e.g., rupture or laceration) or indirect trauma (e.g., excessive stress, contusion, or strain). Regardless of the type of injury, injured muscles undergo a sequential series of events during the wound healing process including: inflammatory response, necrosis, muscle regeneration, and remodeling^{8, 9, 33, 34}. Immediately after injury, the inflammation process is initiated through the hematoma formation resulting from ruptured blood vessels within the muscle tissue. Simultaneously, the damaged muscle is subjected to degeneration and necrosis as a result of the disintegration of the muscle membrane. A leak in the muscle membrane leads to the activation of intracellular autodegradative pathways by an influx of calcium and the cytotoxin secreted by invading neutrophils. Numerous inflammation cells also invade the injured site during this early phase. The repair phase begins with phagocytosis of damaged tissue. Normally quiescent satellite cells known as myogenic precursor cells are activated. During the removal of tissue debris,

activated satellite cells (myoblasts) withdraw from their self-renewal cycle, readily differentiate, and either fuse with each other (grey arrow) to form multinucleated myotubes or fuse with pre-existing myofibers (white arrowhead) ^{14, 33, 35, 36} (**Figure 1.1; Figure 1.2**). In the meantime, extracellular matrix (ECM) components are synthesized by fibroblasts, and capillary ingrowth is initiated. During the remodeling phase, regenerating myofibers undergo maturation and scar tissue remodels, events that lead to functional recovery of the injured muscle ³⁴. During skeletal muscle healing, an appropriate amount of ECM must be present to serve as a scaffold for fusing myoblasts ^{35, 37} and for the transmission of loads across the tissue defect. However, muscle regeneration and the deposition of ECM are concomitant and competitive events. Excessive connective tissue can form a dense mechanical barrier ³⁸ that interrupts the milieu that is necessary for myofiber growth and prevents regenerated muscle myofibers from growing and elongating. Fibrosis is characterized by an excessive number of abnormally active fibroblasts, the excess accumulation of collagen, disorganized ultrastructural morphology of the connective tissue, and an abnormal proportion of matrix components ³⁹.

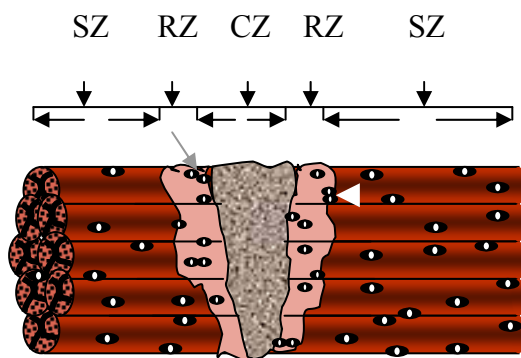


Figure 1-1 A Schematic Illustration of Injured Skeletal Muscle

After injury, the defect (central zone (CZ)) caused by contraction of disrupted myofibers is immediately filled by a hematoma. Subsequent necrosis extends 1 to 2 mm along the damaged myofibers (necrosis zone (NZ) or regeneration zone (RZ)) from the injured site. The remaining myofibers survive the trauma (survival zone (SZ)). After removal of necrotic myofibers through phagocytosis, muscle regeneration occurs within RZ. Simultaneously, recruited fibroblasts begin to deposit ECM in the CZ. The regenerating myofibers reach out of the survived basal lamina of the original myofibers and penetrate the connective tissue within the CZ. However, condensed scar resulting from fibrosis prevents myofibers from lengthening and growing within the CZ ³³.

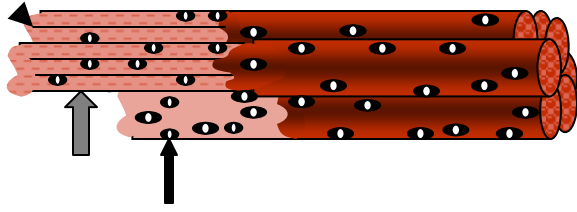


Figure 1-2 Muscle Regeneration from RZ inside Preserved Basal Membrane

During the repair phase, macrophages enter degenerating myofibers to scavenge contractile filament bundles and other necrotic debris, leaving the original basal lamina (thick arrow) as a scaffold that aids in muscle regeneration. After removal of necrotic tissue, spindle-shaped myoblasts (thin arrow) migrate toward and stay beneath the preserved basal lamina, and then fuse to form small multinucleated myofibers (arrowhead).³³

1.1.2 TGF- β 1

Fibrosis prevents full recovery of the injured muscle^{8, 40}. TGF- β 1 plays a major role in the fibrogenesis in a variety of fibrotic diseases and damaged tissues, including skeletal muscle¹⁶⁻²³. After muscle injury, the injury site contains a high level of TGF- β 1¹⁶. Li et al. (2004) found that, after muscle injury, some newly regenerating myofibers express TGF- β 1 protein. The TGF- β 1-positive regenerated myofibers are gradually replaced by mononucleated cells and TGF- β 1-positive scar tissue. Moreover, Li et al. showed that direct injection of TGF- β 1 into skeletal muscle causes early TGF- β 1 autocrine expression within myofibers and fibrosis 2 weeks after injection¹⁶. Antifibrotic agents that interfere with different steps of TGF- β 1 signaling cascades, including decorin, suramin, and IFN- γ , greatly improve muscle healing after injury²⁹⁻³². Decorin directly interacts with TGF- β 1 and prevents TGF- β 1 from binding to its receptors. Suramin, an inhibitor of growth factor receptor activation, competitively prevents TGF- β 1 from binding to the growth factor receptor, and by doing so inhibits the fibrotic effects of TGF- β 1^{31, 32}. IFN- γ negatively regulates the TGF- β 1 signaling pathway by directly inhibiting TGF- β 1-induced phosphorylation of Smad3 and its attendant cascades, and induces the expression of inhibitory

Smad7. Smad7 interferes with the interaction between Smad2/3 and the TGF- β type I receptor, and the complex formation among phosphorylated Smad2/3 and Smad4, thereby interrupting Smad signaling⁴¹.

Not only does TGF- β 1 stimulate fibrosis, it also exerts an inhibitory effect on myogenic differentiation of myoblasts, including the C2C12, L6, Sol 8, L6E9, C-2 and BC3H1 cell lines⁴²⁻⁴⁴. TGF- β 1 also inhibits the proliferation and differentiation of muscle satellite cells⁴⁵. In contrast with control cells, which formed multinucleated myotubes, TGF- β 1-treated satellite cells remained mononucleated and developed distinct networks of stress fibers⁴⁵. Similarly, MSTN strongly inhibits proliferation and differentiation of both myoblasts and myogenic satellite cells⁴⁶⁻⁴⁸.

1.1.3 Myostatin

Myostatin (MSTN), a member of transforming growth factor- β 1 (TGF- β 1), is the key negative regulator of fetal and adult skeletal muscle growth, expressed almost exclusively in the skeletal muscle⁴⁹. MSTN knockout (MSTN^{-/-}) mice are characterized by a dramatic and widespread increase in skeletal muscle mass⁴⁹. MSTN gene is highly conserved across different species arranging from zebra fish to human⁴⁹⁻⁵⁷. Deficiency of MSTN function causes a remarkable increase in skeletal muscle mass from hypertrophy^{50, 55, 57} or both hypertrophy and hyperplasia^{49, 51-53, 56}. Recombinant MSTN and overexpressed MSTN from C2C12 myoblasts carrying amplified copies of a MSTN expression construct can inhibit both proliferation and differentiation of C2C12 myoblasts *in vitro*^{46, 48, 58, 59}. MSTN inhibits C2C12 myoblast proliferation by up-regulating p21, a cyclin-dependent kinase (CDK) inhibitor and decreasing the level and activity of Cdk2 protein. As a result, C2C12 myoblasts treated by MSTN were arrested

in the G0 phase of cycle^{46, 58}. MyoD, Myf5, MRF4, and myogenin are transcription factors of the basic helix-loop-helix-family of myogenic regulatory factors (MRFs). MRFs play genetic hierarchy roles in the skeletal muscle development. MyoD and Myf5 are responsible for the determination of the myogenic lineage whereas myogenin and MRF4 are involved in the regulation of the process of terminal differentiation⁶⁰. MSTN decreases the expression of myoD, Myf5 and myogenin proteins during differentiation^{48, 59}.

Like the TGF- β s, MSTN contains nine cysteine residues in the C-terminal region that is responsible for the activity of MSTN. After secretion, a precursor protein of MSTN undergoes proteolytic cleavage processing, and the resulting C-terminal regions are capable of forming a dimer linked by a disulfide bond⁴⁹. TGF- β 1 and MSTN share some downstream steps in the signaling pathway. The signaling cascades of TGF- β superfamily members are classified into activin/TGF- β and bone morphogenetic protein (BMP)/growth and differentiation factor (GDF) pathways⁶¹⁻⁶³. In the former type of pathway, TGF- β , activin, and nodal-related ligands initially bind to type II receptors (T β RII and ActRII, respectively) and, which results in the formation of a complex containing 2 copies each of receptor II and receptor I (T β RI is known as activin receptor-like kinase (ALK): ALK5, ALK7, or ALK4). Activated type I receptors then induce the phosphorylation of Smad2 and/or Smad3, which further associated with Smad4. The complex of Smad2 and/or Smad3 and Smad4 translocates into nucleus and thereby launch the transcription of Smad2/Smad3-dependent target genes. In contrast, BMP/GDF-like ligands bind to BMPRII or ActRII/IIB. The resulting complex induces phosphorylation of Smad1, Smad5, and/or Smad8, which also form complex with Smad4, and thereby regulates the expression of BMP target genes. Recent studies have shown that, like TGF- β 1 signaling, MSTN signal propagation requires the participation of Smad2 and Smad3 rather than the participation of Smad1, Smad5,

and Smad8^{56, 64, 65}. The binding of MSTN to ActRIIB recruits a type I receptor—either activin receptor 4 (ALK4 or ActRIB) or ALK5 (T β RI)—that then phosphorylates Smad2 and Smad3 and activates a TGF- β -like signal transduction pathway^{56, 64, 65}. MSTN signaling cascades are negatively regulated by the inhibitory Smad7 rather than by Smad6⁶⁴.

Currently, research on MSTN mostly focuses on regulation of MSTN during skeletal muscle development. The potential role of MSTN in fibrogenesis has not been clarified and requires further investigation.

1.1.4 Decorin

Decorin (DCN), a small chondroitin-dermatan sulphate leucine-rich proteoglycan, is composed of a core protein and a single glycosaminoglycan chain^{66, 67}. Three different small proteoglycan with leucine-rich repeats (i.e., decorin, biglycan, and fibromodulin) are able to bind and inactivate TGF- β 1⁶⁸. Decorin has been studied widely, primarily because it is ubiquitous in the ECM and has antifibrogenic properties.

DCN is an inhibitor of TGF- β 1. TGF- β 1 stimulates the growth of Chinese hamster ovary (CHO) cells. However, the overexpression of decorin resulting from transfection of decorin cDNA suppresses the proliferation of transfected CHO cells compared with non-transfected CHO cells^{66, 69}. Further experiments revealed the formation of complexes between core protein of decorin and TGF- β 1^{69, 70}, and then TGF- β 1 was inactivated; however, the activity of TGF- β 1 dimer was restored after it was released from the complex⁶⁹. TGF- β induces synthesis of decorin in many cell types, which suggests that decorin may play a role in the negative feedback of TGF- β ^{31, 69}. Decorin has been used as an antifibrogenic agent in lung, liver, kidney, and muscle tissue because of its biologic binding and neutralizing of TGF- β 1^{28, 29, 39, 66, 71, 72}. Members in our

research group found that decorin can improve skeletal muscle healing by promoting muscle regeneration and decreasing fibrosis^{28, 29}. In order to further investigate the mechanisms by which decorin exerts beneficial effects on skeletal muscle healing, whether decorin also inhibits MSTN was examined in this study.

1.1.5 Myostatin Propeptide

Analogous to TGF- β 1, MSTN is synthesized as a precursor protein constituting of a signal sequence, an N-terminal propeptide domain, a C-terminal domain. After two proteolytic cleavages to remove signal sequences and propeptides, two C-terminal domains form a disulfide-linked dimer, which is active form of MSTN^{46, 49}. However, two released propeptide molecules are able to non-covalently bind to one MSTN dimer and inhibit its biological activity^{56, 73-75}. Different research groups have shown that overexpression of MSTN propeptide (MPRO) in transgenic animals inhibits binding of MSTN to its receptor and consequently generates increased muscling^{56, 57, 76}. Moreover, repeated intraperitoneal injections of recombinant MPRO into *mdx* mice, an animal model of DMD, attenuate pathophysiology of dystrophic muscle and improve its function⁷⁷. Therefore, MPRO offers a therapeutic strategy for blocking MSTN in the injured and diseased muscles.

1.1.6 Follistatin

Follistatin (FLST), a secreted glycoprotein, initially invoked attentions due to its ability to antagonize activin activity in reproduction associated sites^{78, 79}. Later on, it was found that FLST is able to neutralize other several members of TGF- β family such as BMP-2, BMP-4, and BMP-

⁷⁸⁰, GDF-11⁸¹, including MSTN⁸². Transgenic FLST overexpression mice exhibit dramatic increase in muscle mass, which is comparable to that seen in MSTN^{-/-} mice⁵⁶. Systemic administration of FLST reduces MSTN-induced wasting⁷³. FLST reversed MSTN-mediated inhibition of muscle cell differentiation, and MSTN-inhibited expression of Pax-3 and MyoD in muscle cells was blocked as well. Those suggested that FLST also effectively inhibited activity of MSTN *in vitro*⁸². Yeast and mammalian two-hybrid studies revealed that FLST associated with MSTN directly⁸². The Affinity (KD) of FLST for MSTN was as high as 5.84×10^{-10} M as indicated by interaction kinetics of these two molecule. FLST-MSTN coupling was very stable. Collectively, FLST appears to be a promising approach to improve skeletal muscle healing through blocking MSTN.

1.1.7 Duchenne Muscular Dystrophy

Duchenne muscular dystrophy (DMD) is an X-linked recessive hereditary disease resulting from a mutation in the dystrophin gene, which consequently produce the dysfunctional production of dystrophin protein⁸³⁻⁸⁷. Dystrophin, which resides in the sarcolemma of skeletal muscle fibers, works in concert with dystrophin-associated proteins (DAPs), a large oligomeric complex of glycoproteins, to form an assembly that connects the intracellular cytoskeleton and the contractile myofilament apparatus to the extracellular matrix (ECM)^{84, 86, 88-91}. Without functional dystrophin, the membranes of myofibers become susceptible to damage during contraction, as a result of which dystrophin deficiency muscle undergo extensive necrosis. Over time, DMD patients suffer repeated degeneration and functionally flawed regeneration of skeletal muscle, and, as the disease progresses, myogenic progenitor cells are gradually depleted. The resulting extensive fibrosis and the development of regenerating myofibers with varying

diameters (as opposed to characteristic uniformity of normal skeletal muscle) leads an exacerbating cycle of skeletal muscle wasting⁹². According to statistics, approximately 1 in every 3,500 boys is subjected to the devastating effects of DMD and a consequently compromised life quality and life span⁸⁵.

The search for therapies for DMD has primarily focused on the development of gene and cell therapies. The focus of gene therapy is to construct optimal vectors capable of transferring genes into dystrophic muscles to express functionally competent dystrophin, while cell therapy focuses on transplanting healthy donor cells (e.g., myoblasts) into dystrophic muscle to proliferate, fuse with dystrophin-deficient muscle, and generate myofibers which express functional dystrophin. Ultimately, cell therapy seeks to provide a growing reservoir of functional dystrophin and restore the structural strength and integrity of skeletal muscle⁹³.

1.1.7.1 Cell Therapy

Initial animal experiments and clinical trials have revealed that myoblast transplantation does result in an engraftment of dystrophin-positive myofibers; unfortunately, however, this engraftment is transient and causes only a minimal improvement in muscle strength^{16, 94-104}. Moreover, this restoration of dystrophin-expressing myofibers in DMD hosts did not always result in a functional improvement of muscle^{99, 100, 103-106}. This limited success is attributed to several probably factors, including host immune rejection, poor cell survival, a limited dissemination of cells following transplantation, and an unfavorable microenvironment^{95, 107-112}. While tissue engineers and biomedical scientists remain optimistic about the promises that cell therapies hold for treating DMD, critical limitations need to be overcome in order to successfully restore the long-term muscle integrity and function of these patients.

1.1.7.2 Regeneration Capacity of Muscle-Derived Stem Cells

An alternative type of cell that appears to be better-suited for the cell-based therapy of musculoskeletal diseases such as DMD is the muscle-derived stem cells (MDSC). Compared to myoblasts, MDSCs are less immunogenic¹¹³, which likely contributed to enhances engraftment following transplantation into immunocompetent hosts; in one study, MDSCs injected into dystrophic skeletal muscle generated ten times more dystrophin-positive myofibers compared to myoblasts¹¹³. MDSCs are also significantly more versatile compared to myoblasts; several studies indicate that MDSCs are multipotent, as they can differentiate toward myogenic, hematopoietic, osteogenic, chondrogenic, adipogenic, neural, and endothelial lineages¹¹³⁻¹¹⁹. Finally, their proliferative capacity is ideal for permitting tissue engineers to obtain adequate numbers of undifferentiated stem cells for cell-based therapy. Further studies are underway to determine the efficacy of these cells for such therapies.

While there have been exciting advancements in the treatment of DMD with stem cell therapy, this therapy may best be served in combination with gene therapy. For instance, *ex vivo* gene therapy provides a feasible alternative in which autologous cells are isolated from healthy tissue, genetically modified to secrete a protein of interest (e.g., myostatin propetide), expanded *in vitro*, and re-implanted either systemically or locally¹²⁰. The protein carried by donor cell may favor donor cells to form more dystrophin positive myofibers in host muscle than non-modified cells without genetic modification. While this approach may provide superior cell transplantation and long-term results, further studies are ongoing¹²¹.

1.1.7.3 Benefit of blocking the myostatin signal in myoblast transplantation

Since MSTN negatively regulates proliferation and differentiation of muscle cells, suppression of MSTN signaling pathway might be an effective way to boost the efficiency of cell

transplantation in the skeletal muscle. Tremblay's group generated a transgenic domain negative activin receptor IIB (dnActRIIB) mouse that acquired double-muscling phenotype due to dnActRIIB's inactivating MSTN. They reported that transplantation of myoblasts isolated from dnActRIIB mice into *mdx* mice led to improved success of cell transplantation, indicated by significantly larger dystrophin-positive engraftment resulted from dnActRIIB myoblasts than normal myoblasts¹²². In the current study, we took the advantage of WT, MSTN^{-/-}, and FLST overexpression (FLST/OE) mice. Using modified preplate technique, we isolated up to 7 populations of muscle progenitor cells (MPCs) from each type of WT, MSTN^{-/-}, and FLST/OE mice. And then, whether blockade of MSTN signal in donor cells might have beneficial effect on MPC transplantation was extensively examined.

2.0 PROJECT OBJECTIVES

2.1 OBJECTIVE# 1: TO DETERMINE POTENTIAL RELATIONSHIP BETWEEN TGF- β 1, MSTN AND DECORIN IN INJURED SKELETAL MUSCLE

MSTN caught our interests due to the dual roles that it plays in the skeletal muscle. First, MSTN is known as the most potent inhibitor of the development and growth of the skeletal muscle⁴⁹. Second, MSTN also showed its potential in inhibiting fibrosis in the skeletal muscle. *Mdx* mice, with MSTN deficiency, (*MSTN*^{-/-}/*mdx*) not only show less muscle damage, better regeneration, but also less collagenous tissue deposition than their *mdx* counterparts¹²³. However, since skeletal muscle regeneration and fibrosis compete with each other. It is unclear whether the decreased fibrosis in *MSTN*^{-/-}/*mdx* mice is secondary to enhanced regeneration, or whether MSTN may directly promote fibrosis. Therefore, the efforts to clarify the role of MSTN in the skeletal muscle fibrosis are warranted. Although it is widely accepted that TGF- β 1 is a putative growth factor in triggering fibrotic cascades in injured and diseased skeletal muscles; however, in order to develop effective biological approaches to the injured skeletal muscle, it is crucial to understand the mechanisms underlying fibrosis, especially to identify other potential candidates that participate in triggering fibrosis. We hypothesized that MSTN enhances the formation of fibrosis in the injured skeletal muscle. If this hypothesis is proven, we would further hypothesize that neither TGF- β 1 nor MSTN induces fibrosis alone in the skeletal muscle, and

instead these two molecules may synergistically activate fibrotic cascades, regarding to the similarities shared by TGF- β 1 and MSTN. Finally, among different antifibrotic agents that we have demonstrated to improve skeletal muscle healing, decorin is superior to others, because it is able to directly upregulate regeneration by stimulate myogenesis, and downregulate fibrosis by blocking TGF- β 1. We were intrested in whether decorin inhibits MSTN as it did TGF- β 1. Therefore, that was also investigated in this study.

2.2 OBJECTIVE #2: TO INVESTIGATE HOW SKELETAL MUSCLE HEALING CAN BE IMPROVED BY BLOCKING MSTN SIGNALING USING MSTN^{-/-} MICE AND MSTN PROPEPTIDE (MPRO), AN INHIBITOR OF MSTN

In the objective#1, we observed improved skeletal muscle healing in MSTN^{-/-} mice revealed by the enhanced muscle regeneration and reduced fibrosis when compared to WT mice. However, how blocking MSTN signaling benefits skeletal muscle healing remains unclear. Based on information in the literature, the development of fibrosis appears to be negatively related to the extent of blood supply¹²⁴. Our preliminary results showed that improved muscle healing in MSTN^{-/-} mice coincided with higher vascularity than seen in WT mice. Transgenic mice have been very useful tool and widely used by researcher, however, problems rise in efforts to translate promising results collected from transgenic animals to clinic. To circumvent those obstacles, we therefore used adeno-associated virus (AAV) to deliver MSTN propeptide cDNA into gastrocnemius muscle of WT mice to restrict expression of exogenous MPRO within the certain skeletal muscle. With this model, we investigated whether inhibition of MSTN by MPRO reduces fibrosis, promotes neovascularization and muscle regeneration in injured skeletal

muscle. Moreover, we also examined whether with the removal of MSTN, muscle progenitor cells (MPCs) isolated from MSTN^{-/-} skeletal muscle possesses stronger muscle regeneration capacity than MPCs obtained from WT skeletal muscle. Our laboratory has developed a modified preplate technique^{113, 125}, with which, we are able to isolate muscle progenitor cells from mice^{113, 125-127}, pig, and human (unpublished data). Blocking MSTN signaling with different inhibitors (e.g., MPRO, FLST) has been shown to improve muscle regeneration and reduce fibrosis in *mdx* mice. We further explored whether inhibiting MSTN in the host *mdx*/SCID mice by AAV-MPRO enhances regeneration capacity of transplanted muscle progenitor cells.

2.3 OBJECTIVE #3: TO EVALUATE THERAPEUTIC EFFECT OF FLST ON INJURED SKELETAL MUSCLE

Furthermore, we developed biological approaches to block skeletal muscle fibrosis with the use of follistatin. FLST, a secreted protein, is able to bind and antagonize the action of MSTN. We investigated whether transgenic FLST overexpression (FLST/OE) mice develop less fibrosis and more muscle regeneration in the injured skeletal muscle than do WT mice. If so, we would isolate MPCs from skeletal muscles of WT mice and transgenic FLST/OE, mice. When these resulting muscle progenitor cells (MPCs) are transplanted in dystrophic muscle in *mdx* mice, they can fuse with each other or into host myofibers to regenerate dystrophin-positive engraftment consisting of myofibers formed from donor cells. The number of dystrophin-positive myofibers is an index to indicate how efficiently MPCs participate in skeletal muscle regeneration^{125, 128}. Using these cell populations, we would compare the influence of gain

function of FLST genes on muscle cell's ability to regenerate skeletal muscle, when they are transplanted into dystrophic muscle.

2.4 SIGNIFICANCE

The overall goal of this project was to further establish the role of MSTN in the skeletal muscle fibrosis, explore whether TGF- β 1 and MSTN synergistically act together to induce fibrosis, and how inhibition of MSTN results in improved muscle healing. Those findings help us to clarify the mechanisms of fibrosis in injured skeletal muscle, which eventually lead to an optimal approach to treat injured muscle. Moreover, we also would like to determine whether MPRO or FLST, antagonists of MSTN, can effectively block the activity of MSTN *in vivo*, thus enhance muscle healing. Positive results will provide us an alternative avenue to improve muscle healing through targeting MSTN.

3.0 RELATIONSHIPS BETWEEN TGF- β 1, MYOSTATIN, AND DECORIN: IMPLICATIONS FOR SKELETAL MUSCLE FIBROSIS

3.1 INTRODUCTION

MSTN, a member of the TGF- β superfamily, was initially identified as a negative regulator of the growth and development of skeletal muscle⁴⁹. Recent studies have shown that MSTN, may also be involved in fibrosis formation within the skeletal muscle¹²³. *Mdx* mice (an animal model for Duchenne muscular dystrophy) in which expression of the MSTN gene has been ablated (MSTN^{-/-}/*mdx*) not only showed better skeletal muscle regeneration, but also exhibited decreased fibrosis when compared to *mdx* mice (MSTN^{+/+}/*mdx*)¹²³. These results strongly suggest that MSTN plays an important role in muscle fibrosis; however, a direct link between MSTN and fibrosis has yet to be identified. To investigate this possibility, we evaluated the effect of MSTN on fibroblasts, cells responsible for the synthesis of ECM components, and the fibrosis formation in injured skeletal muscle. Due to the fact that TGF- β 1 plays a major role in the formation of fibrosis, we hypothesized that a relationship between TGF- β 1 and MSTN exists. Because decorin (DCN) has been shown to strongly inhibit fibrosis formation in various tissues via blocking of TGF- β 1 activity^{28, 29 39, 72, 129, 130}, we investigated the potential for DCN to inhibit the activity of MSTN as it does for TGF- β 1. Our findings demonstrated that MSTN is involved with the formation of fibrosis and interacts with TGF- β 1, and that DCN has the ability to

counteract the action of MSTN. These results contribute to a better understanding of the mechanism of skeletal muscle healing, and indicate that MSTN represents a potential pharmacological target for anti-fibrogenic therapy.

3.2 METHODS

3.2.1 Isolation of Fibroblasts from Skeletal Muscle

The preplate technique was used to isolate fibroblasts from skeletal muscle¹¹³. Collagen-coated flasks were used in the isolation process since fibroblasts adhere more readily to collagen than myoblasts. After 6-week-old female C57BL/6J mice were sacrificed, their gastrocnemius muscles (GMs) were removed and minced into coarse slurry. The muscle slurry was digested with 0.2% collagenase (type XI) for 1 h, followed by a dispase digestion (grade II, 240 mL) for 30 minutes, followed by a 0.1% trypsin digestion for a final 30 minutes at 37°C. The extracted muscle cells were resuspended in proliferation medium (PM) consisting of Dulbecco's modified Eagle's medium (DMEM; Invitrogen, Carlsbad, CA), 10% horse serum (HS; Invitrogen, Carlsbad, CA), 10% fetal bovine serum (FBS; Invitrogen, Carlsbad, CA), 1% penicillin/streptomycin (P/S; Invitrogen, Carlsbad, CA), and 0.5% chicken embryo extract (CEE; Accurate Chemical & Scientific Corporation, Westbury, NY) and plated onto collagen-coated flasks. A population of preplated cells (PP1), consisting of mostly fibroblasts that attached within the first 2 hours, was collected and used, in these experiments, as skeletal muscle derived fibroblasts.

3.2.2 Cell Culture

The NIH3T3 fibroblast cell line and the C2C12 myoblast cell line were purchased from the American Type Culture Collection (ATCC, Manassas, VA). The cell lines or isolated PP1 fibroblasts were maintained in PM consisting of DMEM, 10% FBS, and 1% P/S until further needed. PP1 fibroblasts were plated onto collagen coated 96-well plates for cell proliferation analysis and onto 6-well plates for the evaluation of α -smooth muscle actin (α -SMA), fibronectin (FN), collagen (type I α 1, II α 2, and III α 1), and MSTN expression. Following an overnight incubation, PM was replaced with serum-free medium supplemented with a serum replacement (Sigma, St. Louis, MO) consisting of heat-treated bovine serum albumin, heat-treated bovine transferrin, and bovine insulin. This serum replacement does not contain growth factors, steroid hormones, glucocorticoids, or cell adhesion factors. We further supplemented this media with varying concentrations of recombinant human MSTN (Leinco Technologies, Inc. St. Louis, MO) for proliferation assays (0, 100, 500, or 1000 ng/mL) and for western blot analysis (0, 100, or 500 ng/mL). After incubation for 48 h, an MTT (3-[4,5-dimethylthiazol-2-yl]-2,5-diphenyltetrazolium bromide) cell proliferation assay kit (Roche Diagnostics, Germany) was used to measure cell proliferation (n=6) following the instructions from the manufacturer. Western blot analysis was used to examine α -SMA, fibronectin, and MSTN expression. Some of the above procedures were repeated using NIH3T3 fibroblasts to confirm the effect of MSTN on fibroblasts. C2C12 myoblasts, a widely used myogenic cell line^{46, 48, 131}, were used to examine whether DCN neutralized the inhibitory effect of MSTN on cell differentiation. We seeded C2C12 myoblasts in 12-well plates in PM at a density of 10,000 cells/well. Following an overnight incubation, PM was replaced with fresh differentiation medium (DM) containing DMEM, 2% HS, and 1% P/S. We maintained a total of four sets of cultured cells. The control set

received only DM while the other sets received DCN alone, MSTN alone, or 1 $\mu\text{g}/\text{mL}$ of MSTN combined with 0-50 $\mu\text{g}/\text{mL}$ DCN ($n = 3$). Cells were cultured for 5 more days during which DM, MSTN, and DCN were changed every other day. Following a similar procedure, we examined whether recombinant follistatin (FLST) protein stimulated myogenic differentiation of C2C12 myoblasts ($n = 3$), and whether soluble TGF- β 1 receptor type II (100 ng/mL , and 1000 ng/mL) (T β RII) (R&D Systems, Inc. Minneapolis, MN) was able to attenuate MSTN-inhibited myoblast differentiation ($n = 3$).

3.2.3 Western Blot Analysis

After culturing, the cells were lysed with T-PER® Tissue Protein Extraction Reagent with the addition of protease inhibitors (Pierce, Rockford, IL). Equal amounts of cellular protein were loaded into each well and separated by 10% sodium dodecyl sulfatepolyacrylamide gel electrophoresis (SDS-PAGE). Nitrocellulose membrane blotting was performed under standard conditions, which was followed by a 2h blocking in 0.05% Tween-20 phosphate buffered saline containing 5% nonfat milk at room temperature. The following primary antibodies were used for immunoblotting: mouse anti- β -actin IgG (1:8,000) (Sigma, St Louis, MO), mouse anti-GAPDH IgG (1:5,000) (Abcam Inc, Cambridge, MA), rabbit anti-MSTN IgG (1:3,000) (Chemicon, Temecula, CA), mouse anti- α -SMA IgG (1:1,000) (Sigma, St Louis, MO), mouse anti-fibronectin (FN) IgG (1:3,000), and rat anti-TGF- β 1 IgG (1:1000) (BD PharMingen, San Jose, CA).

3.2.4 Quantitative RT-PCR

Quantitative RT-PCR (Q-RT-PCR) was used to examine the mRNA expression levels of procollagen (type I α 1, I α 2, and III α 1) in PP1 fibroblasts treated with MSTN (100, 200, and 500 ng/mL) for 12, 24, and 48h. The mRNA was extracted using an Rneasy Plus kit (Qiagen Inc. Valencia CA). The cDNA templates for Q-RT-PCR were synthesized using a RETROscript® kit (Ambion Inc., Austin, TX). Q-RT-PCR was carried out in an ABI Prism 7000 Sequence Detector (Applied Biosystems, Foster City, CA) with SYBR Green PCR Master Mix Reagent (Applied Biosystems, Foster City, CA) as a detector. All target gene expressions were normalized to 18s rRNA levels. The primer pair of procollagen III α 1 was from a previous study¹³². The primer pairs are displayed in Table 1.

Table 1. The Sequences of Primer Pairs for Q-RT-PCR

Gene Name	Primer pairs (S: sense primer, A: Anti-sense primer)	PCR products (bp)
Procollagen type I alpha 1 (BC050014)	S: 5'-GAAGAACTGGACTGTCCCAAC-3' A: 5'-CCTCGACTCCTACATCTTCTG-3'	103
Procollagen type I alpha 2 (AK075707)	S: 5'-TCTGGTAAAGAAGGCCCTGTG-3' A: 5'-GTCCAGGGAATCCGATGTTG-3'	106
Procollagen type III alpha 1 (AK041115)	S: 5'-AGGCTGAAGGAAACAGCAAA-3'(45) A: 5'-TAGTCTCATTGCCTTGCGTG-3'	116
TGF-beta 1 (BC 013738)	S: 5'-CTAATGGTGGACCGCAACAAC-3' A: 5'-CACTGCTTCCCGAATGTCTGA-3'	99
18s rRNA	Prprietary of ABI	N/A

3.2.5 Enzyme-Linked Immunosorbent Assay

Enzyme linked immunosorbent assay (ELISA) was performed to determine whether recombinant MSTN protein stimulated TGF- β 1 secretion in C2C12 myoblasts. C2C12 myoblasts were plated into a 48-well plate and exposed to a range of MSTN concentrations from 0 to 500 ng/ml. Fresh recombinant MSTN protein was added every two days. Cell supernatants were collected at 2 and 4 days (n = 5). These supernatants were centrifuged to remove cell debris and stored at -80°C until the ELISA was performed. The Mouse/Rat/Porcine TGF- β 1 immunoassay kit (R&D Systems, Inc., Minneapolis, MN) was used to quantitatively measure the secreted TGF- β 1 levels in cell culture supernatants, according to the manufacturer's protocol.

3.2.6 Immunocytochemistry

In order to monitor the differentiation capacity of the myogenic cells, they were fixed in cold methanol for 2 minutes after induction of differentiation in 12-well plates. Following a phosphate buffered saline (PBS) wash, the cells were blocked with 10% HS (Vector Laboratories, Inc., Burlingame, CA) for 30 minutes, and then incubated with an anti-myosin heavy chain (MyHC) antibody (Sigma, St Louis, MO) in 2% HS overnight. A negative control was performed by omitting the primary antibody. The next day, after several PBS rinses, the cells were incubated with the secondary antibody goat anti mouse IgG conjugated with Cy3 (Sigma, St Louis, MO) for 1 hour. Hoechst 33258 dye was used in each experiment to stain cell nuclei. Fusion index (ratio of nuclei in myotubes to all nuclei) was calculated (%) to evaluate myogenic differentiation.

3.2.7 Animal Model

All experimental animal protocols were approved by the Animal Research and Care Committee in the Children's Hospital of Pittsburgh (protocols 15-3 & 17-05). C57BL/6 wild-type (WT) (Jackson Laboratories, Bar Harbor, ME) and MSTN^{-/-} mice (7 to 8 weeks of age) were used in this study. All MSTN^{-/-} mice used were offspring of MSTN^{-/-} homozygotes, and PCR was used to confirm the genotype of all MSTN^{-/-} mice. The RT-PCR test was randomly used to confirm the lack of MSTN gene transcription in MSTN^{-/-} mice throughout the experiments. The skeletal muscle mass of MSTN^{-/-} mice and WT mice were also compared to confirm the desired phenotype. The mice were anesthetized with isoflurane controlled under an IMPAC6 anesthetic delivery machine (VetEquip, Pleasanton, CA). Both GMs of each mouse were laterally lacerated to create an injury model as previously described^{29, 30, 32}. A surgical blade (no. 11) was used to make a lateral laceration through 50% of the muscle width and 100% of the muscle thickness in the area of the GM with the largest diameter. We harvested the mouse GMs at 2 and 4 weeks post-surgery. There were 6 to 8 mice (12 to 16 GMs) in the WT and MSTN^{-/-} mouse groups for both time-points. The muscles were isolated, removed, and snap-frozen in 2-methylbutane precooled in liquid nitrogen. After Masson's trichrome staining (IMEB Inc., Chicago, IL), Northern Eclipse software (Empix Imaging, Inc., Cheektawaga, NY) was used to measure areas of fibrotic tissue in the injured sites. In each sample, three representative non-adjacent sections were chosen. The ratio of the fibrotic area to the cross sectional area was used to estimate the extent of fibrosis formation. To determine the skeletal muscle's regeneration efficiency, minor axis diameters (the smallest diameter) of regenerating muscle fibers were measured using Northern Eclipse software on cross-sections of GMs. The diameters of over 350 consecutively centronucleated myofibers were measured in each GM.

3.2.8 Immunohistochemistry

Frozen GMs were sectioned at 10 μ M thickness and immunohistochemical analysis was performed to detect DCN expression. Tissue sections were fixed in 4% formalin for 5 minutes followed by two 10-minute washes with PBS. The sections were then blocked with 10% HS for 1 hour. The rabbit anti-DCN IgG (LF-113, National Institute of Dental Research, Bethesda, MD) primary antibody was diluted 2:100 in 2% HS and incubated with sections overnight at 4°C) to stain tissue sections of WT and MSTN^{-/-} GMs 2 weeks after laceration. The following day, the sections were washed three times with PBS and then incubated with the secondary antibody, goat anti-rabbit IgG conjugated with Cy3 (Sigma, St. Louis, MO).

3.2.9 Statistical Analysis

All of the results from this study are expressed as the mean \pm standard deviation (SD). The differences between means were considered statistically significant if $P < 0.05$. The Student's *t*-test was used to compare the difference in skeletal muscle regeneration, and fibrosis formation between MSTN^{-/-} and WT mice, and the myogenic differentiation capacity between MSTN^{-/-} and WT LTP cells. All other data were analyzed by analysis of variance (ANOVA) followed by post hoc Tukey's multiple comparison test. Error bars on the figures represent the SD, * represents $P < 0.05$, and ** represents $P < 0.01$.

3.3 RESULTS

3.3.1 Effects of MSTN on Fibroblasts

MTT proliferation tests showed that, after 48 h of incubation, MSTN significantly stimulated the proliferation of PP1 and NIH3T3 fibroblasts in a dose-dependent manner (**Figure 3-1A**). Alpha-smooth muscle actin (α -SMA), the actin isoform originally found in contractile vascular smooth muscle cells, has been the most reliable marker of myofibroblasts to date ²⁴. Western blot analysis indicated that MSTN (100 and 200 ng/mL) increased α -SMA expression in PP1 and NIH3T3 fibroblasts (**Figure 3-1B**). Q-RT-PCR revealed that MSTN stimulated procollagen (type I α 1, I α 2, and III α 1) mRNA expression at 48 h (**Figure 3-1C**). Additionally, MSTN stimulated the expression of fibronectin (FN) protein, a component of extracellular matrix (ECM), in PP1 fibroblasts (**Figure 3-1 D**).

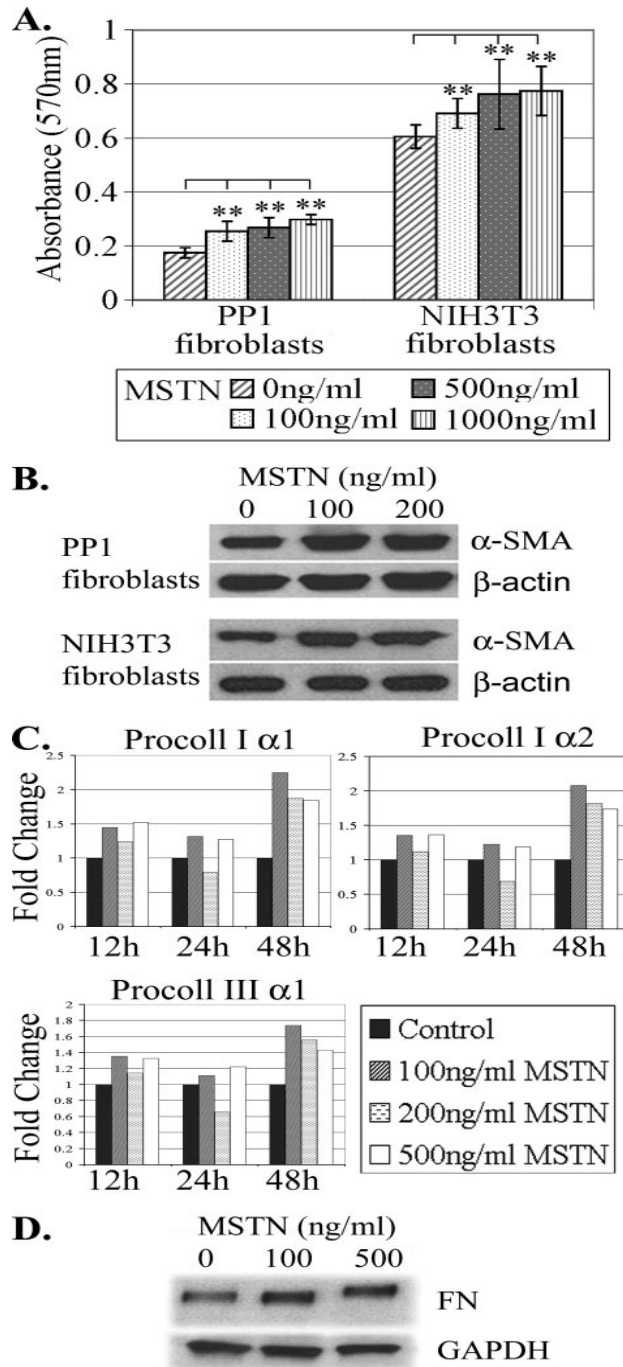


Figure 3-1 MSTN Stimulated Proliferation and ECM Production of Fibroblasts

A, both muscle-derived fibroblasts (PP1) and NIH3T3 fibroblasts were cultured with MSTN, varying in concentration from 0 to 1000 ng/ml for 48 h. Cell proliferation was determined by MTT assay. These results are presented as absorbance values ($n = 6$) of purple formazan crystal at 570 nm, which directly correlates to the number of living cells. Fibroblasts were cultured in DM for 2 days with the addition of various concentrations of MSTN. Expressions of different proteins were analyzed by Western blot. B, the expression of α -SMA in PP1 fibroblasts or NIH3T3 fibroblast is shown. C, Q-RT-PCR analysis of procollagen (types I α 1, I α 2, and III α 1) mRNA expression in PP1 fibroblasts treated with MSTN. Results are presented as the ratio against the gene expression in the control. D, expression of FN in PP1 fibroblasts after MSTN treatment (*, $P < 0.05$; **, $P < 0.01$).

3.3.2 Reduced Fibrosis and Enhanced Skeletal Muscle Regeneration in MSTN^{-/-} Mice

3.3.2.1 Reduced fibrosis in injured MSTN^{-/-} mice

At 2 weeks following injury, we observed extensive deposition of collagenous tissue in the WT and MSTN^{-/-} mice (data not shown). After 4 weeks, the deepest area of the injured site was filled with regenerating myofibers of large diameter, and the fibrotic region was limited to the superficial zone of the laceration site (**Figure 3-2A**). We observed fewer fibrotic connective tissue deposits between regenerating myofibers in the injured muscle of MSTN^{-/-} mice compared to the prominent scar region in the injured WT mouse muscle (**Figure 3-2A**). Quantification of fibrotic tissue (i.e., the ratio of the fibrotic area to the cross-sectional area) revealed that there was a significantly smaller fibrous area in MSTN^{-/-} skeletal muscle as compared to WT skeletal muscle at 2 weeks ($11.5 \pm 3.5\%$ vs. $15.3 \pm 3.1\%$; $P < 0.01$) and at 4 weeks (2.1 ± 0.4 vs. 6.3 ± 2.1 ; $P < 0.01$) after injury (**Figure 3-2B**).

3.3.2.2 Improved muscle regeneration in injured MSTN^{-/-} mice

We used the minor axis diameter (smallest diameter) of centro-nucleated regenerating myofibers to evaluate skeletal muscle regeneration after laceration injury. At 2 weeks after GM laceration, regenerating myofibers were relatively small (data not shown). At 4 weeks, some large, mature myofibers could be observed among the small, centronucleated, regenerating myofibers (**Figure 3-2C**). Quantification showed that MSTN^{-/-} regenerating myofibers had diameters 38.8% larger than WT myofibers ($36.1 \pm 2.5 \mu\text{m}$ vs. $26.0 \pm 2.2 \mu\text{m}$; $P < 0.01$) at 2 weeks after laceration, and the mean diameter of regenerating myofibers in MSTN^{-/-} mice remained 21.1% larger than the mean diameter of regenerating myofibers in the WT mice ($37.7 \pm 2.7 \mu\text{m}$ vs. $31.1 \pm 1.8 \mu\text{m}$; $P < 0.01$) 4 weeks after injury (**Figure 3-2D**).

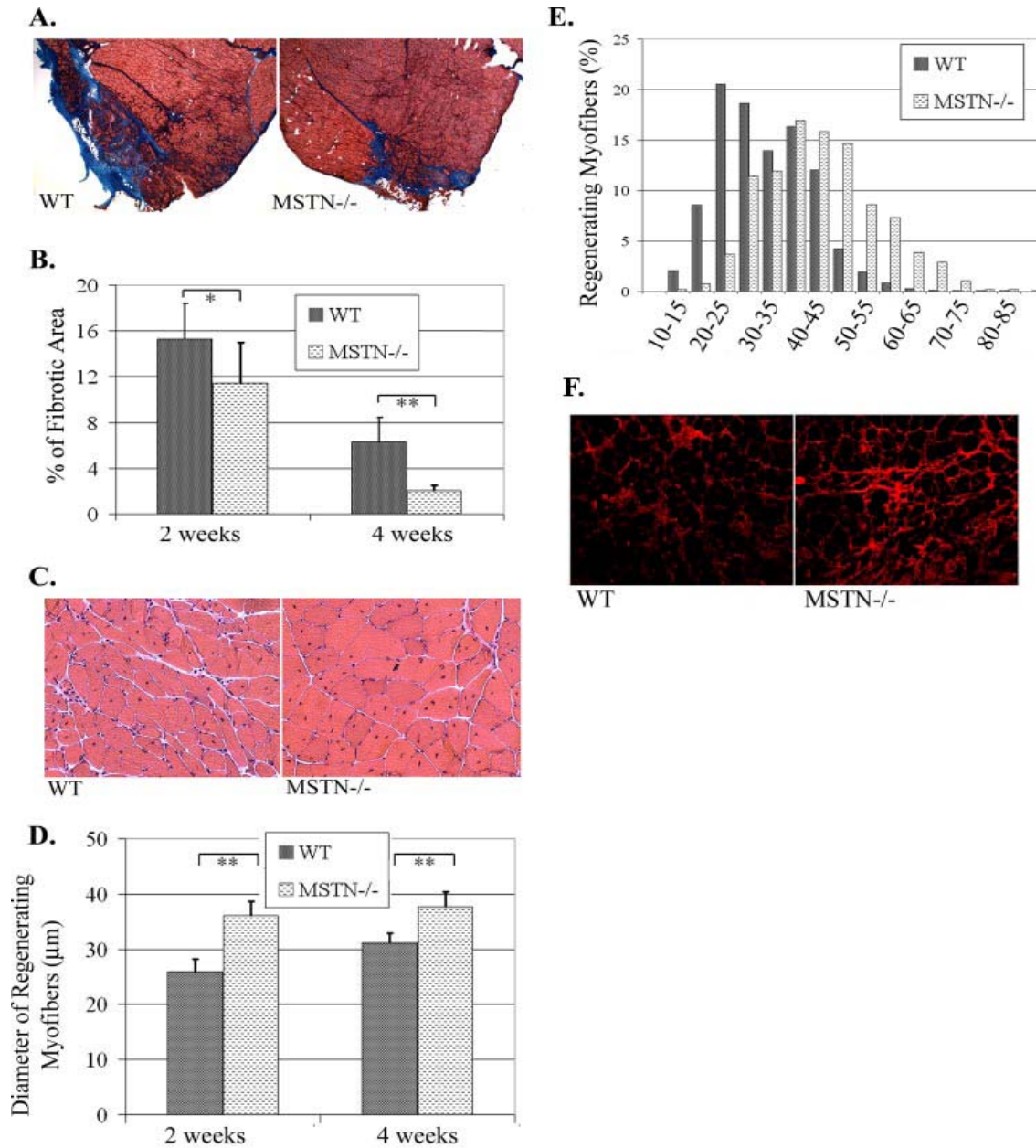


Figure 3-2 Inhibition of MSTN Facilitates Skeletal Muscle Healing after Injury

A, sections from injured WT and MSTN^{-/-} GMs were stained with Masson's trichrome-staining protocol 4 weeks after laceration to determine fibrotic tissue levels. As a result, collagenous tissue is stained blue. B, quantification of fibrotic tissue of WT *versus* MSTN^{-/-} GMs 2 and 4 weeks after laceration. C, myofibers in WT and MSTN^{-/-} GMs were visualized by hematoxylin and eosin staining 4 weeks after laceration. Regenerating myofibers were distinguished by their centralized nuclei. D, quantification of the diameters of regenerating myofibers. E, the distribution of regenerating myofiber diameters at 4 weeks after laceration injury. F, increased DCN immunostaining in injured skeletal muscle of MSTN^{-/-} mice compared with WT mice 2 weeks after laceration. DCN (red) is detected in the ECM between myofibers. (Magnifications: in C and F, x200; in A, x100; *, $P < 0.05$; **, $P < 0.01$.)

The mean diameter of regenerating myofibers in MSTN^{-/-} mice was significantly higher than the mean diameter of the regenerating myofibers in WT mice (**Figure 3-2D**). The distribution of the regenerating myofiber diameters showed that there was an increase in the percentage of larger regenerating myofibers in MSTN^{-/-} mice compared to WT mice (e.g., approximately 7.38% of regenerating myofiber diameters in MSTN^{-/-} mice fell into a range of 50 to 55 μm vs. 1.92% of those in WT mice (**Figure 3-2E**).

3.3.2.3 Elevated DCN expression in injured MSTN^{-/-} mice

To investigate the underlying mechanism for improved muscle healing in MSTN^{-/-} mice, we examined the expression of DCN, a molecule that has been shown to decrease fibrosis and enhance muscle regeneration in injured MSTN^{-/-} skeletal muscle^{16, 29}. Immunohistochemical staining revealed that there was more abundant DCN expression in the regenerating skeletal muscle of MSTN^{-/-} mice than that of WT mice 2 weeks after injury (**Figure 3-2F**). This higher level of DCN expression may be related to the increased regeneration and decreased fibrosis shown in the injured muscle of MSTN^{-/-} mice.

3.3.3 Relationship between TGF- β 1 and MSTN

Western blot analysis showed that the levels of MSTN in C2C12 myoblasts treated with different concentrations of TGF- β 1 were elevated in a dose dependent manner when compared to non-treated controls, suggesting that TGF- β 1 stimulates MSTN expression in C2C12 myoblasts (**Figure 3-3A**). After incubation with increasing concentrations of recombinant MSTN protein, MSTN was shown to stimulate TGF- β 1 expression in C2C12 myoblasts especially with the highest dose at 4 days poststimulation (**Figure 3-3B**). Furthermore, ELISA showed that MSTN

significantly increased TGF- β 1 secretion by C2C12 myoblasts in a dose-dependent manner at 2 and 4 days. After 4 days of stimulation with MSTN (500 ng/mL), C2C12 myoblasts secreted approximately twofold more TGF- β 1 as compared to control cells (**Figure 3-3C**). Q RT-PCR revealed that MSTN (100, 200, and 500 ng/ml) also increased TGF- β 1 mRNA expression 48 *h* post-stimulation (**Figure 3-3D**). PP1 fibroblasts did not express detectable MSTN protein. However, after treatment with MSTN (100 and 200 ng/ml) for 48 *h*, PP1 fibroblasts began to express MSTN as indicated by western blot analysis (**Figure 3-3E**). MSTN also stimulated MSTN expression in C2C12 myoblasts (**Figure 3-3E**). MSTN-induced MSTN autocrine expression in PP1 fibroblasts is reduced by soluble TGF- β 1 receptor type II (T β RII) which blocks the TGF- β 1 signaling pathway (**Figure 3-3F**). Moreover, our results indicated that soluble T β RII was also able to restore MSTN inhibited C2C12 myoblast differentiation (**Figure 3-3G**). We also examined whether exogenous TGF- β 1 recombinant protein was able to stimulate autocrine expression of TGF- β 1 in MSTN^{-/-} muscle cells as it does in C2C12 myoblasts¹⁶. We observed that exogenous TGF- β 1 could induce its autocrine expression in WT primary myoblasts but not on primary MSTN^{-/-} myoblasts (**Figure 3-3H**).

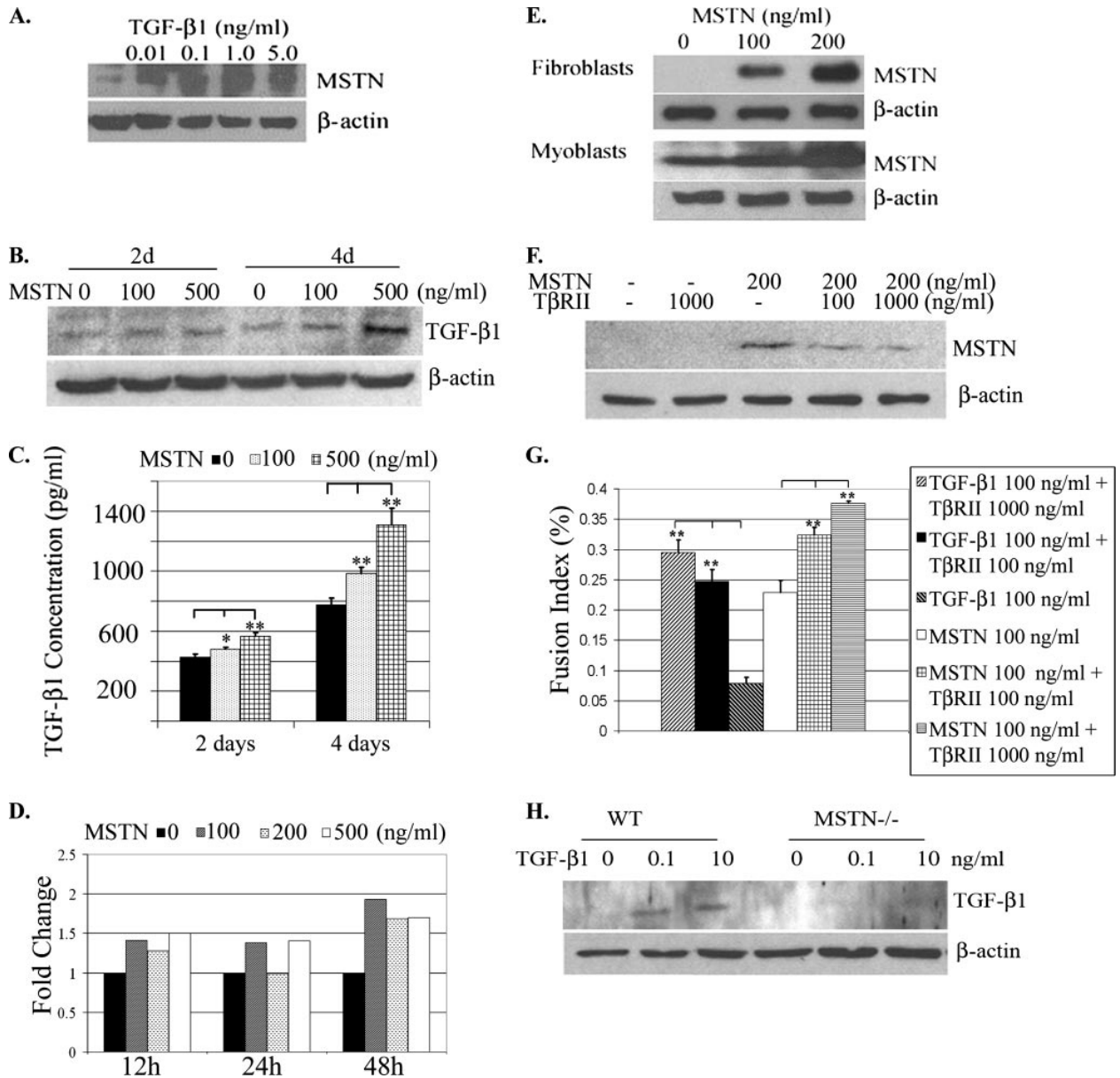


Figure 3-3 Interaction between TGF-β1 and MSTN *in vitro*

A, Western blot analysis of MSTN expression in C2C12 myoblasts treated with different concentrations of TGF-β1 ranging from 0 to 5.0 ng/ml for 48 h. B, C2C12 myoblasts were treated with different concentrations of MSTN in DM. Cell lysates were collected at 2 and 4 days to examine TGF-β1 expression by Western blot; C, while the conditioned medium was collected at the same time points, the levels of TGF-β1 in the medium were also analyzed by ELISA. D, Q-RT-PCR for TGF-β1 after MSTN treatment (100, 200, and 500 ng/ml) in PP1 fibroblasts. E, the level of MSTN expression in PP1 fibroblasts and C2C12 myoblasts treated with MSTN recombinant protein. F, Western blots were used to determine MSTN expression level in PP1 fibroblasts after cells were treated with either MSTN or both MSTN and soluble TβRII for 48 h. G, C2C12 myoblasts were cultured in DM with different treatments, TGF-β1, MSTN, TGF-β1 and TβRII, or MSTN and TβRII, for 4 days. Fusion indexes were used to access impacts of treatments on C2C12 myoblast differentiation. H, myoblasts isolated from WT, and MSTN^{-/-} GMs were grown for 48 h under stimulation by TGF-β1. Western blot analysis was used to detect TGF-β1 expression in WT and MSTN^{-/-} cells (*, $P < 0.05$; **, $P < 0.01$).

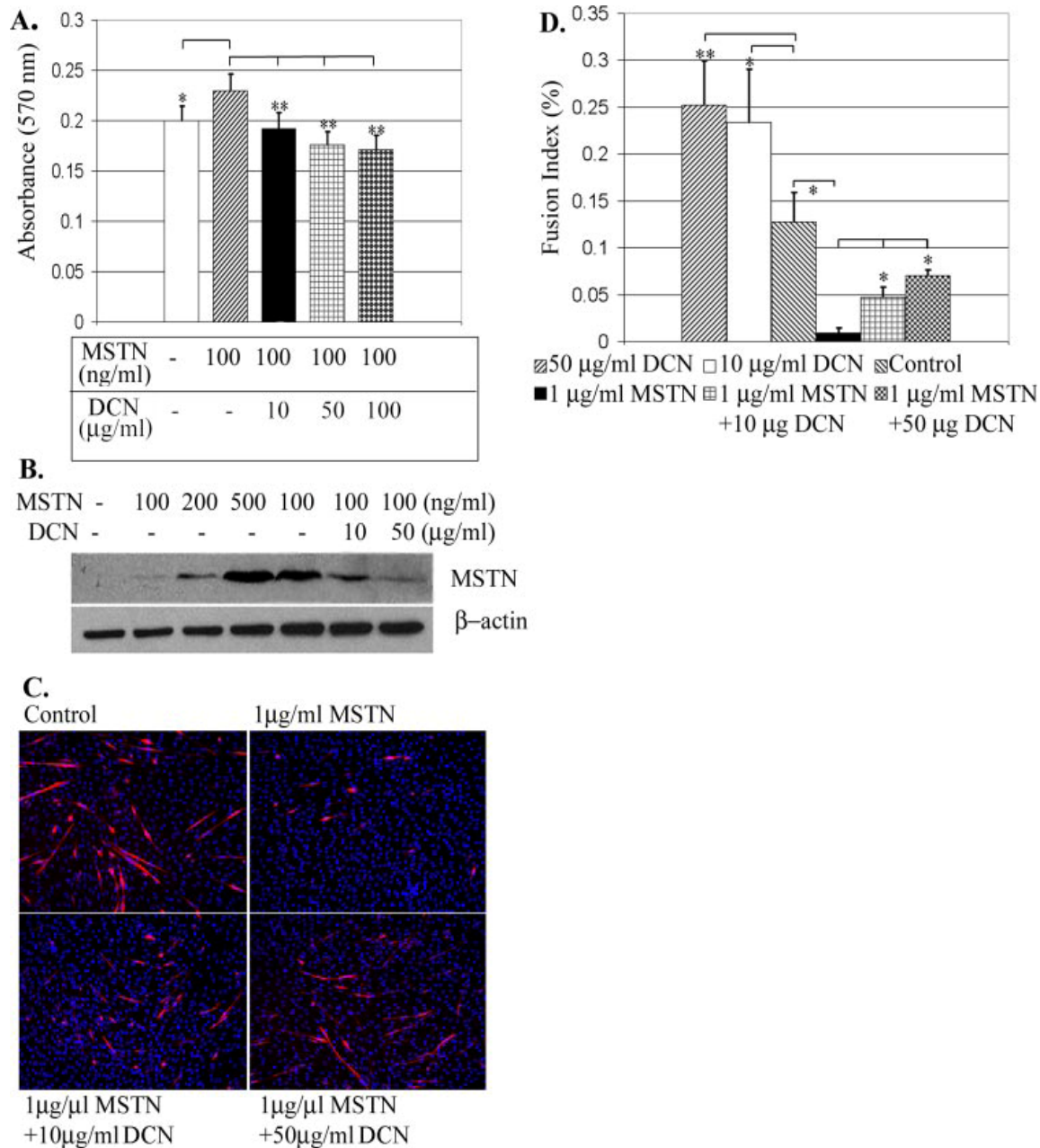


Figure 3-4 DCN Attenuated the Effects of MSTN on Fibroblasts and Myoblasts

A, PP1 fibroblasts were treated for 48 h with 100 ng/ml MSTN or combinations of MSTN and DCN. Non-treated cell cultures were used as a control. MTT assay was performed to assess cell proliferation. B, after incubation of PP1 fibroblasts with MSTN, or a combination of MSTN and DCN, Western blot analysis was performed to determine whether DCN reduced the autocrine expression of MSTN in PP1 fibroblasts stimulated with MSTN. C, C2C12 myoblasts were cultured without treatment, with 1µg/ml MSTN alone, or co-incubated with 1µg/ml MSTN and different concentrations of DCN for 5 days. Myotubes were monitored by anti-skeletal myosin heavy chain immunostaining; nuclei were stained by Hoechst 33258 (magnification, x100). D, fusion indexes were determined to estimate the differentiation capacity of C2C12 myoblasts in response to different treatments.

3.3.4 DCN Counteracts the Effect of MSTN

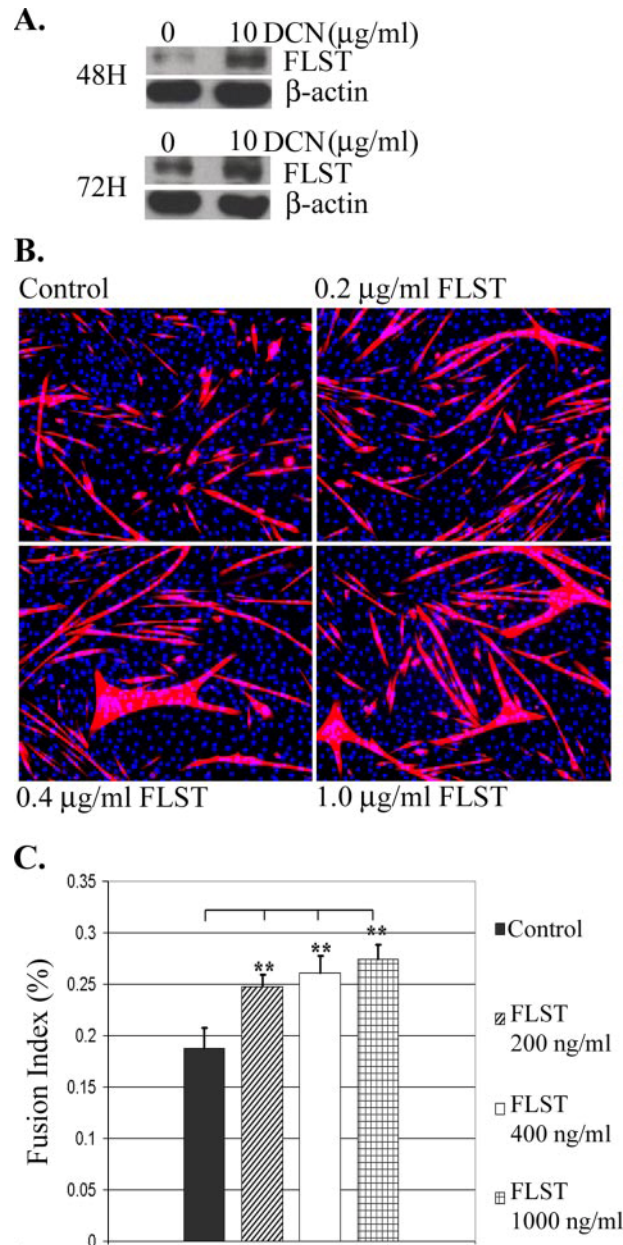


Figure 3-5 DCN Stimulated Expression of FLST and FLST Promoted Myogenic Differentiation of Myoblasts

A, DCN increased the expression of FLST in C2C12 myoblasts 48 and 72 h after treatment. B, immunofluorescence analysis of myotubes. C2C12 myoblasts were maintained in DM for 5 days in the presence of different concentrations of FLST. Myotubes were double-labeled with an antibody recognizing skeletal myosin heavy chain and with the fluorescent nuclear dye Hoechst 33258 (magnification, $\times 100$). C, fusion indexes were calculated to evaluate the degree of C2C12 myoblast differentiation upon FLST stimulation.

As previously shown in **Figure 3-1A**, 0.1 $\mu\text{g/ml}$ MSTN significantly stimulated PP1 fibroblast proliferation. This dosage was selected to examine whether DCN could reduce the proliferative influence of MSTN on PP1 fibroblasts. After PP1 fibroblasts were incubated with MSTN and exposed to varying concentrations of DCN for 48 h, MTT assay revealed that the addition of DCN significantly repressed MSTN's stimulatory effect on PP1 proliferation in a dose-dependent manner as expected (**Figure 3-4A**). These findings are comparable to a previous report showing that DCN blocked the stimulatory effect of TGF- β 1 on PP1 fibroblasts²⁹. Our earlier results indicated that MSTN induced its own expression in an autocrine manner in PP1 fibroblasts (**Figure 3-3E**). Therefore, we examined the ability of DCN to block the MSTN autocrine expression in PP1 fibroblasts. As previously shown, PP1 fibroblasts, which were not treated with MSTN, failed to express detectable MSTN protein, while PP1 fibroblasts treated with MSTN showed a high level of MSTN expression in comparison to the control (**Figure 3-3E, 3-4B**). However, DCN decreased MSTN autocrine expression by PP1 fibroblasts in a dose-dependent manner (**Figure 3-4B**). Our previous experiments showed that 1 $\mu\text{g/ml}$ MSTN almost completely inhibited myoblast differentiation (data not shown). Therefore, we chose this dose to assess whether DCN treatment could reverse MSTN-inhibited myogenic differentiation in C2C12 cells. Except for the control cells, the cultures were treated with DCN alone, MSTN alone, or 1 $\mu\text{g/ml}$ MSTN combined with increasing concentrations of DCN (0-50 $\mu\text{g/ml}$). Following a 5-day incubation, DCN treated-groups (data not shown) and controls showed widespread myosin heavy chain (MyHC)-positive myotubes, whereas cells treated with MSTN alone contained only a few myotubes (**Figure 3-4C**). The addition of DCN reversed the inhibition of MSTN on myogenic differentiation, as indicated by the increase in the number and size of myotubes in comparison to the MSTN-treated group (**Figure 3-4C**). Measurements

showed that DCN treatment promoted C2C12 myoblast differentiation by significantly increasing fusion indexes in a dose-dependent manner (**Figure 3-4D**), suggesting that DCN attenuated the inhibitory effect of MSTN and thereby, stimulated myoblast fusion.

3.3.5 Inhibitory Effects of DCN on MSTN may be Mediated by FLST

To further explore whether DCN regulated MSTN activity via an intermediate molecule, we investigated the effect of DCN on the expression of follistatin (FLST), which is able to bind to MSTN and suppress its activity⁸². We found an up-regulation of FLST expression by C2C12 myoblasts 48 and 72 h after addition of 10 µg/ml DCN (**Figure 3-5A**). Our results also revealed the ability of FLST to stimulate myogenic differentiation, which was demonstrated by the presence of larger myotubes containing more nuclei in comparison to the control group (**Figure 3-5B**). In a dose-dependent manner, FLST treatment led to a significant increase in fusion index (**Figure 3-5C**) compared to the control group, suggesting that FLST promotes myogenic differentiation and accelerates the maturation of myotubes.

3.4 DISCUSSION

MSTN has been drawing more and more attention due to mounting evidence indicating that inhibition of MSTN significantly improves skeletal muscle diseases such as muscle dystrophy. But, the role of MSTN in injured skeletal muscle and its relationships with other molecules such as TGF-β1 and DCN (important key factors in muscle healing) remain unknown.

3.4.1 Fibrotic Roles of MSTN in Vitro and in Vivo

Recent studies reported by Yamanouchi *et al.* highlight the expression of MSTN in fibroblasts in injured skeletal muscle¹³³, suggesting that fibroblasts may be a source of MSTN. Previously, we have shown that TGF- β 1 significantly promotes proliferation of PP1 fibroblasts²⁹. Here, our *in vitro* study shows that MSTN activates fibroblasts by stimulating fibroblast proliferation and inducing their expression of α -SMA analogous to that of TGF- β 1 in an autocrine manner. Like TGF- β 1¹³⁴, MSTN may transiently attract fibroblasts into an injury site, further inducing them to express MSTN in an autocrine fashion; they then differentiate into myofibroblasts, thereby accelerating the deposition of the ECM. Researchers widely believe that prolonged presence and excessive activity of myofibroblasts is associated with the abnormal accumulation of ECM components in injured and diseased tissue^{135, 136}. Moreover, MSTN has been shown to induce procollagen (type I α 1, I α 2, and III α 1) mRNA and FN protein expression by PP1 fibroblasts. Given the results collected in our *in vitro* study, we hypothesized that a lack of MSTN in knockout mice would decrease the proliferation of fibroblasts and reduce their production of collagenous tissue in injured skeletal muscle. This was made evident by a significant decrease in the formation of fibrosis in MSTN^{-/-} mice at 2 and 4 weeks after injury when compared to WT mice. McCroskery *et al.*, recently confirmed the correlation of MSTN expression to the formation of fibrosis by showing less fibrosis formation in the notexin-damaged tibialis anterior (TA) muscle in MSTN^{-/-} mice 4 weeks after injury as compared to WT mice¹³⁷. Moreover, we found an elevated expression level of DCN, an inhibitor of TGF- β 1, in injured MSTN^{-/-} skeletal muscles compared to injured WT muscles at 2 weeks after injury. In accordance with this result, increased DCN mRNA has been observed in regenerating MSTN^{-/-} muscle¹³⁷. Increased DCN

might inhibit the effect of TGF- β 1, thereby partially explaining the reduced fibrosis and enhanced regeneration in injured MSTN^{-/-} muscle.

3.4.2 Improved Muscle Healing in the Injured MSTN^{-/-} Muscle

Satellite cells serve as a reservoir of myogenic progenitor cells for the repair and maintenance of skeletal muscle. MSTN negatively regulates self-renewal and differentiation of satellite cells⁴⁷, and decreases the expression of members of the basic helix-loop-helix muscle regulatory factors (MRF) (MyoD, Myf5, mrf4, myogenin)^{48, 58}. MSTN^{-/-} mice show an increased number of satellite cells activated and differentiated toward a myogenic lineage⁴⁷. In this study, our data demonstrates that MSTN^{-/-} mice contain regenerating myofibers with significantly larger diameters than WT mice at 2 and 4 weeks after GM laceration. The increased number of satellite cells in MSTN^{-/-} mice could, in part, explain the enhanced regeneration revealed by the larger diameter of regenerated myofibers in MSTN^{-/-} mice compared to WT mice. Indeed, it has been reported that blocking MSTN signals by isolating myoblasts from transgenic mice carrying the mutated MSTN receptor results in improved success of myoblast transplantation in *mdx* mice compared to normal myoblasts¹²². Furthermore, high levels of MSTN protein have been reported within necrotic fibers in the skeletal muscles of rats damaged by notexin¹³⁸, and western blot analysis revealed the upregulation of MSTN protein at early time-points following notexin-induced injury in rat skeletal muscle¹³⁹. Interestingly, it has been shown that MSTN interferes with the chemotaxis of macrophages *in vitro*¹³⁷; recombinant MSTN protein significantly reduces the migration of macrophages and myoblasts toward chemoattractants *in vitro*, which likely promotes skeletal muscle regeneration¹³⁷. These results suggest that MSTN could impede recruitment of macrophages and myoblasts into the injured site *in vivo*.

Macrophages infiltrate damaged tissue to remove debris that could hinder muscle regeneration. Macrophages also secrete a variety of growth factors and cytokines that have chemotactic and/or mitogenic effects on muscle precursor cells thereby accelerating muscle regeneration¹⁴⁰⁻¹⁴⁴. Compared with WT mice, MSTN^{-/-} mice have shown elevated recruitment of macrophages and myoblasts and an accelerated inflammatory response after muscle injury¹³⁷. These results suggest that the earlier initiation of skeletal muscle regeneration in the injured skeletal muscle of MSTN^{-/-} mice compared to the injured muscle of WT mice may be due, in part, to accelerated removal of muscle debris. During skeletal muscle healing (following active muscle regeneration at early time-points after injury) fibrosis initiates about one week post injury, and peaks at four weeks^{8, 40, 145}. Li *et al.*¹⁶ reported that some regenerating myofibers probably differentiate into myofibroblasts to contribute the formation of fibrosis. This correlation between fibrosis development and intense MSTN signaling—and TGF- β 1 expression¹⁶ in the early phase of healing may suggest the differentiation of regenerating myotubes/myofibers into myofibroblasts. Consequently, MSTN protein might modulate the muscle fiber regeneration process through the early events of phagocytosis and inflammation¹³⁸ and later control myofiber maturation. In this way, MSTN seems to act as a regulatory molecule that is produced by the tissue to specifically suppress and control the size of muscle growth and development¹⁴⁶.

3.4.3 Relationships between TGF- β 1 and MSTN

As members of the TGF- β superfamily, TGF- β 1 and MSTN share many similarities in structure, signaling pathway, and function^{64, 65}. It has also been shown that TGF- β 1 plays a critical role in skeletal muscle fibrosis after injury^{16, 28-30, 32, 147-149}. Since both TGF- β 1 and MSTN promote fibrosis, it is very important to understand the potential relationships between these two

molecules. Recent reports demonstrated that exogenous TGF- β 1 strongly stimulated the expression of MSTN in C2C12 myoblasts ¹³¹. In fact, our *in vitro* data shows that TGF- β 1 increases MSTN expression in C2C12 myoblasts (and vice-versa), and TGF- β 1 and MSTN are found to co-localize in the same myofibers shortly after MSTN injection or after injury. We found that MSTN is able to induce its autocrine expression in both fibroblasts and myoblasts. In the presence of soluble T β RII, MSTN autocrine expression in fibroblasts is decreased. We have known that MSTN inhibits C2C12 myoblast differentiation. When TGF- β 1 receptors type II (T β RII) is blocked by soluble T β RII, MSTN's ability to inhibit C2C12 myoblast differentiation is reduced. Apart from that, quantitative RT-PCR results show that MSTN also stimulates TGF- β 1 mRNA expression in PP1 fibroblasts. Our previous study has shown that TGF- β 1 is able to induce autocrine expression of TGF- β 1 in C2C12 myoblasts ¹⁶, nevertheless, our present data revealed that TGF- β 1 failed to induce its autocrine expression in MSTN-/- primary muscle cells. Taken together, these results show that TGF- β 1 and MSTN may target different cell membrane receptors ⁶⁵, but can also bind to the same receptor, suggesting that their signaling appears to be somehow related. It is likely, then, that the inducement of skeletal muscle fibrosis by TGF- β 1 is partially mediated by its interaction with MSTN. However, the mechanism by which TGF- β 1 interacts with MSTN to cause fibrosis warrants further investigation.

3.4.4 Inhibitory Effects on DCN on MSTN

DCN, a small chondroitin-dermatan sulphate leucine-rich proteoglycan, exists ubiquitously in the ECM. Due to its binding to and inhibition of TGF- β 1, DCN has been used as a potent antifibrosis agent in various organs and tissues ^{28, 29, 39, 72, 129, 130}, including skeletal muscle ^{28, 29}. However, DCN's ability to regulate MSTN activity is still unknown. DCN, which is composed of a core

protein and a single glycosaminoglycan chain^{66,67}, has the ability to bind to TGF- β 1 due to the fact that the core protein of DCN contains two binding sites for TGF- β 1⁷⁰. Similarly, Miura *et al.* have shown that DCN, or the core protein of DCN, directly binds to active MSTN molecules to block MSTN-mediated inhibition of C2C12 myoblast proliferation¹⁵⁰. The actual location of the MSTN binding site in the DCN core protein and evidence that shows whether TGF- β 1 and MSTN competitively bind to DCN is topics for further investigation. Of further interest is the possibility that DCN may regulate MSTN by influencing another intermediate molecule like FLST, an antagonist of MSTN⁸². Our results not only show that DCN reduces the effects of MSTN on fibroblasts and myoblasts, but also indicates that it stimulates the expression of FLST in C2C12 myoblasts. Exogenous FLST then stimulates C2C12 myoblast differentiation, which is probably due to FLST's neutralization of endogenous MSTN. These results indicate that the effect of DCN on MSTN may be related to the up-regulation of FLST, which would consequently suppress MSTN activity. Nevertheless, more experiments, for example, the effect of DCN on FLST knockout cells, need to be done to establish the role of FLST in DCN inhibited MSTN activity. Furthermore, we have shown that TGF- β 1 probably plays a role in the MSTN signaling pathway since TGF- β 1 soluble receptor antagonizes, at least in part, the effect of myostatin on muscle cells. Overall, DCN probably regulates MSTN activity via three ways: (i) directly binding MSTN; (ii) indirectly downregulate MSTN by binding to TGF- β 1; and, (iii) indirectly down-regulating MSTN by stimulating FLST expression.

3.5 CONCLUSIONS

In summary, our results suggest the following: (i) MSTN stimulates the formation of fibrosis in skeletal muscle after injury; (ii) TGF- β 1 and MSTN up-regulate the expression level of each other; and, (iii) DCN is capable of inhibiting MSTN activity as it does for TGF- β 1 (**Figure 3-6**). These results, combined with the fact that TGF- β 1 plays a key role in skeletal muscle fibrosis and that DCN reduces fibrosis in injured skeletal muscle, suggest that TGF- β 1 and MSTN probably act together; they synergistically amplify the fibrotic process in injured or diseased skeletal muscles resulting in greater fibrosis than either could induce individually. Our findings may help to further increase the understanding of the mechanism by which MSTN^{-/-} mice show decreased fibrosis and enhanced regeneration after injury and suggest that the inhibition of MSTN might be a new therapeutic approach for improving skeletal muscle healing through enhancement of regeneration and reduction of fibrosis.

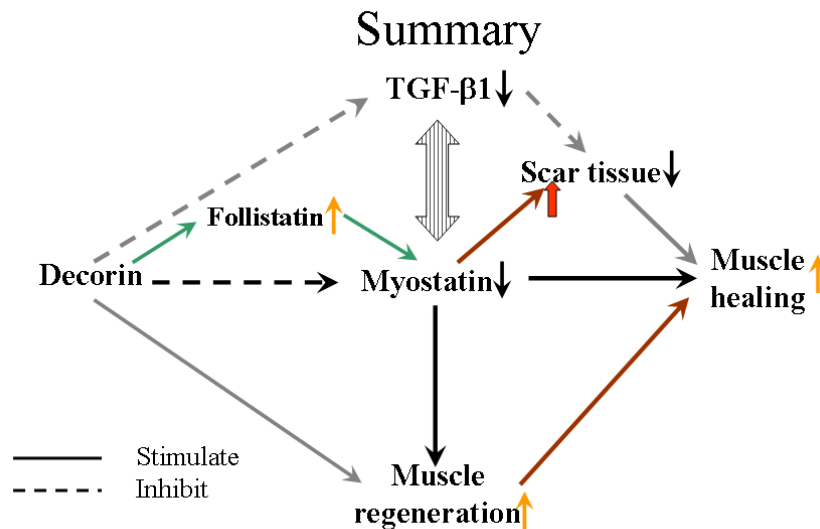


Figure 3-6 Relationship between Decorin, TGF- β 1, Myostatin, and Follistatin

4.0 AAV-MEDIATED MYOSTATIN PROPEPTIDE IMPROVED SKELETAL MUSCLE HEALING IN NORMAL MICE AND ATTENUATED DYSTROPHIC PATHOLOGY IN *MDX/SCID* MICE

4.1 INTRODUCTION

Since MSTN negatively regulates the growth and development of fetal and adult skeletal muscle⁴⁹, various therapeutic strategies for treating muscle dystrophies or muscle wasting have been developed to target MSTN. The *mdx* mouse is a model for Duchenne and Becker muscular dystrophy which mimics dystrophic pathology of muscular dystrophic patients, such as repeated muscle damage and regeneration, along with accumulating fibrotic and fatty tissues. Research has shown that *mdx* mice with MSTN knockout are physically stronger, with a greater muscle mass, less fibrosis, and a superior capacity for skeletal muscle regeneration¹²³. Similar functional and histopathological improvements were observed in *mdx* mice treated with MSTN blocking antibody and recombinant myostatin propeptide (MPRO)^{77, 151}. Subsequently, a variety of inhibitors of MSTN have been identified, including a MSTN blocking antibody, MSTN MPRO^{56, 57, 73, 152}, follistatin (FLST)^{56, 73}, follistatin-related genes¹⁵², growth and differentiation factor-associated serum protein-1¹⁵³, and soluble activin type IIB receptor (ACVR2B)¹⁵⁴.

Several groups, including ours, have found that MSTN positively regulates the formation of skeletal muscle fibrosis, much as is the case with TGF- β 1^{123, 127, 137, 155}. Consistent with this

are the findings that recombinant MSTN protein stimulates fibroblast to proliferate and synthesize TGF- β 1, and fibrotic proteins such as fibronectin, and collagen types I and III¹²⁷. *In vivo*, injured MSTN^{-/-} skeletal muscles not only exhibit improved muscle regeneration, but also develop significantly less fibrosis after injury than their wide-type controls; this is in part because MSTN carries out a signal transduction similar to the pro-fibrotic signaling of TGF- β 1⁶⁵; in fact, it appears that TGF- β 1 and MSTN act synergistically^{127, 131} to induce fibrosis in the injured muscle¹²⁷. MSTN is therefore an ideal therapeutic target for enhancing the regeneration and reducing the fibrosis of the injured and diseased skeletal muscle.

Different research groups have shown that an overexpression of MPRO in transgenic animals increases muscle regeneration⁵⁵⁻⁵⁷. Although the amount of increase in muscle mass may vary, it appears to be proportional to levels of transgene expression^{56, 57}. It was also found that recombinant MPRO binds to MSTN and antagonizes its biological activity^{74, 75}, so that the local and systemic administration of MPRO can each successfully block MSTN activity and attenuate the severity of skeletal muscle dystrophy^{77, 156, 157}. In this current study, we investigate how skeletal muscle healing improves by eliminating MSTN signaling in MSTN^{-/-} mice. We also use adeno-associated virus serotype 2 (AAV2) to intramuscularly deliver MPRO into skeletal muscle and examine whether a gene transfer-mediated constitutive expression of MPRO improves skeletal muscle healing in normal as well as *mdx*/SCID mice.

4.2 METHODS

4.2.1 Construction of an AAV Vector Carrying Mouse MPRO Gene

The AAV2-MPRO particle, encoding a mouse MSTN propeptide (MPRO) sequence under the control of the cytomegalovirus (CMV) promoter, was generated in following a co-transfection methods described previously¹⁵⁸. We used PCR to amplify MPRO cDNA, and then cloned it into a CMV promoter-driven AAV vector plasmid. A schematic illustration of CMV-MPRO gene cassette is shown in the **Figure 4-4A**. A pair of primers was designed to amplify the gene segment spanning CMV and MPRO gene to detect AAV2-MPRO transcription as indicated in **Figure 4-4 A**. The sequences of primers for cmv-mpro are: forward: AAGCTGCAGAAGTTGGTTCG, backward: AGTGGAGGCGCTCTTGGC. *In vitro* expression of AAV-MPRO in C2C12 myoblasts was examined by RT-PCR.

4.2.2 Transduction of AAV2-MPRO/GFP *in Vitro*

C2C12 myoblasts were plated onto collagen-coated 12-well plates for overnight, and then were infected with an MPRO-carrying vector at a dose of 10^6 AAV2-MPRO viral genome (v.g.)/cell. The cells then were cultured for 4 more days in low serum medium. Following fixation of cells, myosin heavy chain (MyHC) immunostain was performed to monitor myotubes, and the fusion index was calculated by determining the ratio of nuclei within fused myotubes (≥ 2 nuclei) to the total number of nuclei.

4.2.3 Western Blot

Western blot was performed as previously described at the section **3.2.3**. Primary antibodies, mouse anti-MyoD (554130, 1:250; Pharmingen), anti-myogenin (556358, 1:250; Pharmingen), and goat anti-Myf5 (1:100, Santa Cruz Biotechnology, Inc., Santa Cruz, CA), mouse anti- β -actin (loading control, 1:8000, Sigma) was applied on membranes for overnight. Next day, after sufficient wash, membrane was incubated with the horse-radish peroxidase (HRP)-conjugated secondary antibodies (Pierce, Rockford, IL) were diluted to 1:5000 and applied. HRP activity was determined by its reaction with SuperSignal West Pico chemiluminescent substrate (Pierce), and finally positive bands were visualized on X-ray film in a dark room.

4.2.4 Transduction of AAV2-MPRO or GFP into WT Mice

Ten female C57BL/6 wide-type (WT) mice at eight weeks of age were used for these experiments. Fifty μ l of AAV2-MPRO (2.5×10^{12} v.g./ml) was injected into both GMs of five mice, while the same amount of phosphate buffered saline (PBS) was injected into the GMs of the other 5 mice as controls. One month after AAV2 vector transduction, both GMs of each mouse were subjected to laceration injury. Mice were sacrificed at 4 weeks after laceration. The GMs were then harvested, snap-frozen in the liquid nitrogen, and stored in -80° . CD31 staining was used to assess whether an MPRO overexpression would increase angiogenesis in the injured muscle when compared to the WT control.

In a long-term study, GMs of 2 female C57BL/6 WT mice (8 weeks old, $n = 4$) were injected with 50 μ l of AAV2-MPRO (2.5×10^{12} v.g./ml), whereas, the same dose of AAV2-GFP was injected into GMs of 2 female littermates ($n = 4$) as control, similarly, which was followed

by bilateral laceration of GMs at 4 weeks after virus transduction. Mice were then sacrificed at one year post-injury. The GMs were also harvested, snap-frozen in the liquid nitrogen, and stored in -80° . Muscle regeneration and fibrosis were measured for the animals in the both sets of experiments according to a published protocol ¹²⁷.

4.2.5 Isolation of Muscle Progenitor Cells from WT and MSTN^{-/-} Mice and Cell Transplantation

Muscle progenitor cells (MPCs) were isolated based on their properties of slow-adhering to collagen-coated flask using a published modified preplate technique. We isolated 5 WT MPCs from 5 male neonatal C57BL/6J mice as well as 5 populations of MSTN^{-/-} MPCs from 5 male neonatal MSTN^{-/-} mice with the same background as WT mice. We used an anatomical sex technique to determine the gender of neonatal mice. Briefly, new born mice were sacrificed, and both upper and lower limbs were harvested. After removal of skin, bone, cartilage, remaining muscles were subjected to sequential enzymatic digestions including: collagenase type XI, dispase, and trypsin. The resulting muscle cell extracts were then seeded on collagen-coated flasks. Different cell populations were obtained by replating the extracts after different time intervals (2h (PP1), 24h (PP2), 24h (PP3), 24h (PP4), 24h (PP5), and 72h (PP6)). PP1 cells are fibroblasts. The earlier preplate populations (PP2-5) were mainly composed of myoblasts and satellite cells, whereas the late preplate population attached to flask after the last 72h cells (PP6) enriches MPCs ^{113, 125, 126, 159}. Late preplate cells were collected as MPCs, grew at a low density in proliferation medium (PM) consisting of Dulbecco's modified Eagle's medium (DMEM; Invitrogen), 10% horse serum (HS; Invitrogen), 10% fetal bovine serum (FBS; Invitrogen), 1%

penicillin/streptomycin (P/S; Invitrogen), and 0.5% chicken embryo extract (CEE, Accurate Chemical & Scientific Corporation, Westbury, NY) (**Figure 4-1**).

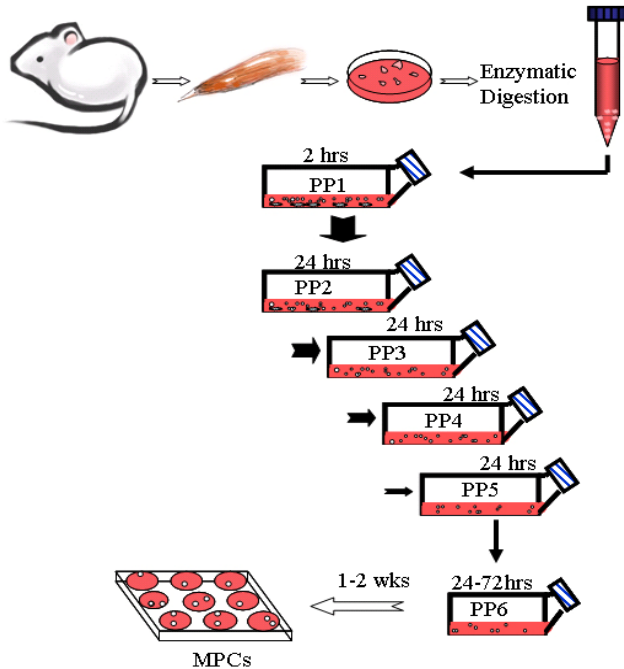


Figure 4-1 Schematic Illustration of Preplate Technique

We expanded WT and *MSTN*^{-/-} MPC population *in vitro* in PM. When cells reach certain numbers, we trypsinized cells, washed them with PBS, and then counted them with a hemocytometer. We transplanted MPC population into GMs of female *mdx*/SCID mice, which were generated by crossing *mdx* (C57BL/10ScSn-*Dmd*^{*mdx*}, Jackson laboratory) and SCID mice (C57BL/6J-*prkdc*^{*scid*}/SzJ mice, Jackson laboratory) at the animal facility of our institution. Each MPC population was transplanted in to 4 legs of *mdx*/SCID so that variability among different gastrocnemius muscles (GMs) and *mdx*/SCID mice can be reduced. Around 300,000 MPCs were transplanted into each GM of female mice. At two weeks after cell transplantation, mice were sacrificed, and GMs were harvested and cyrosectioned. Dystrophin immunostain was performed

and the number of dystrophin-positive was used to evaluate muscle regeneration capacity of transplanted donor cells.

4.2.6 Intramuscular Transduction of AAV2-MPRO/GFP into *Mdx*/SCID Mice Followed by WT MPC Transplantation

To evaluate whether blockade of MSTN signaling in host dystrophic muscle by MPRO can improve regeneration capacity of MPCs, AAV2-MPRO (2.5×10^{12} v.g./ml) in 50 μ l of PBS was injected into both GMs of 3 *mdx*/SCID mice (4 weeks of age, n = 6) 4 weeks prior to cell transplantation; while 3 littermates received the same dose of AAV2-GFP (n = 6) as controls. Muscle progenitor cells (MPCs) isolated from skeletal muscle of wild-type mice C57BL/6 WT mice were transplanted into both AAV-MPRO and AAV-GFP transduced GMs (300,000 cells per GM). Before cell transplantation, The MPCs were trypsinized and characterized by flow cytometry for CD34 and Sca-1 expression. To label these cells, non-specific binding to MPCs were blocked with 10% mouse serum, and then incubate with rat anti-mouse Sca-1 PE and biotinylated CD34 monoclonal antibody (ABCAME) followed by an incubation with streptavidin (SA)-APC (Pharmingen). Control cells were treated with corresponding isotype control antibodies. Before analysis, 7-amino-actinomycin D was added to exclude the nonviables. Flow cytometry with a cell sorter (FACStar Plus or FACSAria; Becton Dickinson) was used to determine percentage of CD34 and Sca-1 positive cells. Moreover, MPCs' desmin expression and myogenic differentiation capacity were evaluated by immunocytochemistry. For examination of desmin, MPCs were plated on 12 well plates at a density of 10,000 cells per well, and cells grew in PM for overnight before staining. Moreover, for myogenic differentiation test, MPCs were plated on 12 well plates (20,000 cells per well) with DMEM supplemented with 2%

FBS (low serum concentration stimulates myotube differentiation) and cultured for 4 days when myotubes were extensively formed. Prior to staining, cells were fixed by pre-cooled methanol for 2 min, blocked with 10% horse serum for 30 min, and then incubated with a mouse anti-desmin antibody, or a mouse anti-myosin heavy chain (MyHC) antibody (1:250, M-4276, Sigma) for 2 hours. The primary antibodies were detected with a secondary anti-mouse IgG antibody conjugated with Cy3 (1:300, C2181, Sigma) for 1h. The nuclei were stained by DAPI staining. The percentage of desmin positive cells was determined. The myogenic differentiation capacity was measured by fusion index.

After two additional weeks post cell transplantation, mice were sacrificed and GMs were harvested for immunohistochemistry and histological examination. MPC transplantation efficiency was measured by the number of dystrophin-positive myofibers in host muscles. Fibrosis was determined by Masson's trichrome staining; muscle regeneration was evaluated after H&E staining; in a separate experiment, *mdx*/SCID mice were sacrificed 3 months post AAV-MPRO/GFP injection.

4.2.7 Immunohistochemistry

To stain CD31 or dystrophin, tissue sections were fixed in 4% formalin for 5 minutes followed by two 10-minute washes with PBS. The sections were then blocked with 10% HS for 1 hour. The rat CD31 primary antibody (BD Pharmingen) was diluted 1:150 in 2% HS, or a rabbit dystrophin primary antibody (1:400, Abcam) and incubated with sections for 1h at room temperature. The sections were washed three times with PBS and then incubated with the corresponding secondary antibody, rabbit anti-rat IgG conjugated with 555 (red, Invitrogen) or

donkey anti-rabbit IgG conjugated with 594 (red, Invitrogen) for 30 minutes. Dapi was used to stain the nuclei.

To perform MPRO and coll IV double-immunostain, tissue sections were fixed and blocked following standard protocol as described above. Sections were then incubated overnight at 4°C in a goat MPRO antibody (2.5 ug/ml, RnD system) that was diluted in 5% donkey serum. The following day, these sections were washed with PBS and incubated with the secondary antibodies, rabbit anti-Goat IgG conjugated with 594 (red, Invitrogen). After finishing MPRO staining, sections were blocked again prior to the use of coll IV primary antibody. Rabbit anti-Coll IV IgG (1:250, Biodesign International, Saco, ME) in 5% serum was applied on section for 1h at RT followed by PBS washes and incubation with donkey anti-rabbit IgG conjugated with 488 (green, Invitrogen).

4.2.8 Statistics

All of the results from this study are expressed as the mean \pm standard deviation (SD) or mean \pm error of the mean (SEM). The differences between means were considered statistically significant if $P < 0.05$. The Student's t-test was used to compare the difference between two groups. Error bars on the graphs represent the SD or SEM. * represents $P < 0.05$, and ** represents $P < 0.01$.

4.3 RESULTS

4.3.1 MSTN^{-/-} Muscles Exhibited Increased Neovascularization

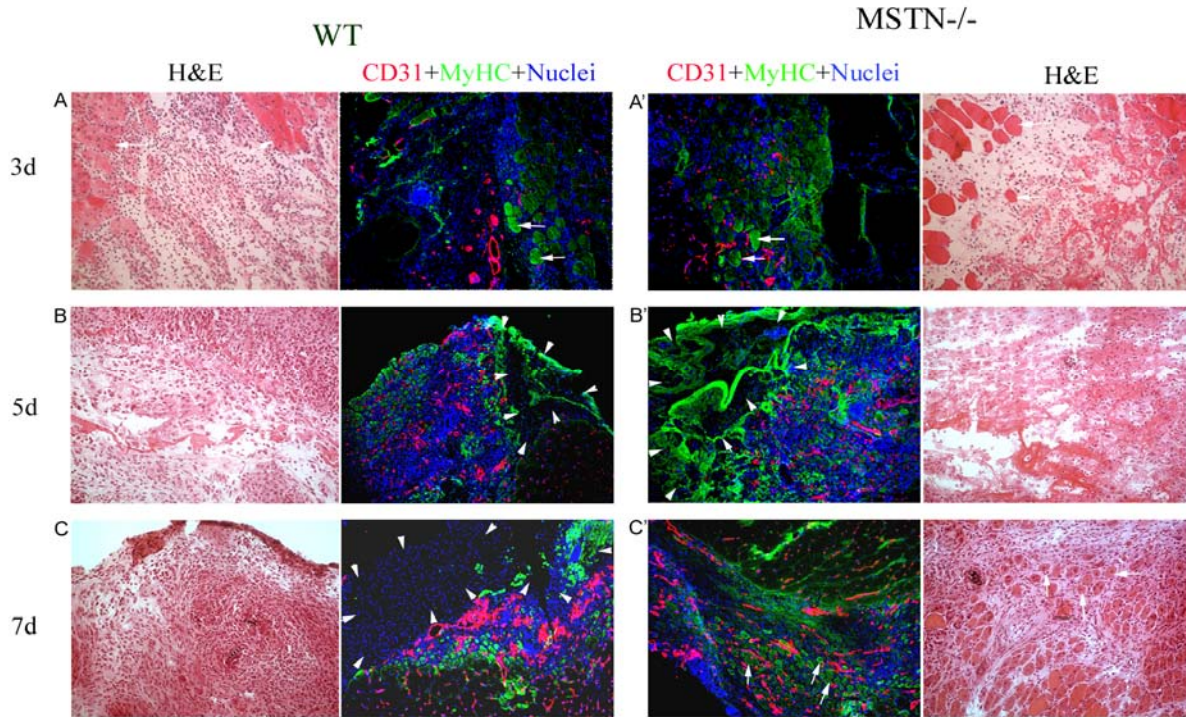


Figure 4-2 Earlier Neovascularization in the Injured MSTN^{-/-} Muscle

At 3, 5, 7 days after laceration injury, frozen sections of injured WT and MSTN^{-/-} muscles were subjected to HE stain and double immunostain: MyHC (green,) and CD31 (red). HE stains parallel to images of immunostaining show the process of muscle healing after injury. (A, A') At day 3, ruptured myofibers degraded, and numerous inflammatory cells invaded into the injured site. A few residues of necrotic myofibers (green, arrows) were detected in the injured WT and MSTN^{-/-} muscle. (B, B') At day 5, muscle degeneration continued, CD31-positive capillary was absent at CZ (arrowheads) of the injured sites. (C) At day 7, CZ of the injured WT muscle was filled with disorganized connective tissue; capillary remained absent from CZ (arrowheads). In contrast, in the MSTN^{-/-} injured muscle (C'), some regenerating myofibers pierce into CZ and the ingrowth of CD31-positive capillaries was also detected.

To investigate the underlying mechanisms by which blocking MSTN signaling promotes skeletal muscle healing, we compared neovascularization between these injured muscles of WT and MSTN^{-/-} mice. CD31 (endothelial maker, red) and myosin heavy chain (MyHC, green) staining were carried out to determined the injured site and the extent of vascularity in the injured muscles.

Day 3 post-laceration, we can observe numerous mononucleated cells and myofiber debris (arrows) in both kinds of injured muscles (**Figure 4-2 A, A'**). At day 5, capillary was absent in central wounds of WT and MSTN^{-/-} muscle as delineated by white arrowheads (**Figure 4-2 B-B'**). At 7 days post-injury, CZ of MSTN^{-/-} muscle had started to be neovascularized through ingrowth of capillaries from periphery of the wound and newly regenerated myofibers had penetrated into central of the wound (arrows, **Figure 4-2 C'**), whereas there remained deficiency of blood vessel in the central wound of WT muscle (arrowheads, **Figure 4-2 C**). Corresponding H&E stain showed the histology of injured muscles at different time points after injury. At 4 weeks, CD31-positive blood vessels were seen irregularly scattered in the injured WT muscle, whereas blood vessels were more evenly distributed in the injured MSTN^{-/-} muscle, suggesting a more mature pattern of neovascularization in injured MSTN^{-/-} muscle. A quantitative analysis demonstrated that injured MSTN^{-/-} muscle showed a significantly higher capillary density than did the WT control (**Figure 4-3**).

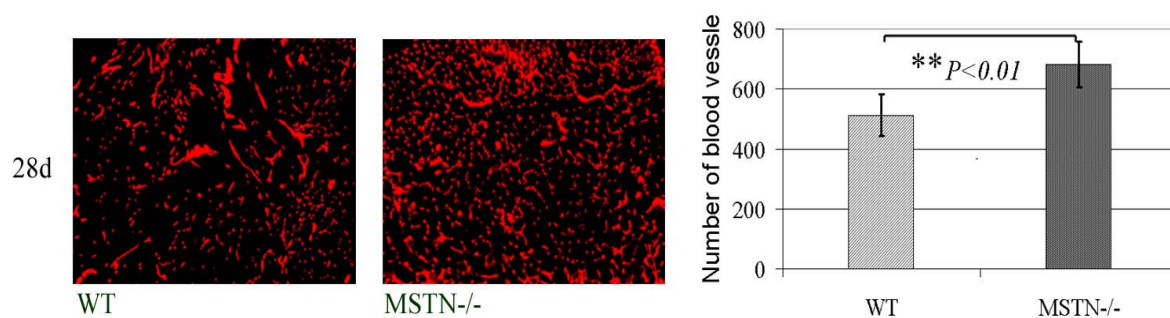


Figure 4-3 Increased Vascularity in Injured MSTN^{-/-} Muscle at 4 weeks after Laceration

CD31 immunostain demonstrate that there is a significant increase in CD31 positive capillaries in injured MSTN^{-/-} muscle compared to control (Mean ± SD; ** $P < 0.01$).

4.3.2 Delivery of AAV2-MPRO Inhibits MSTN Activity *in Vitro*

In this study, we used an adeno-associated virus (AAV) vector serotype 2 to deliver the MPRO to myoblasts *in vitro* and a direct injection of the virus to deliver the MPRO to the gastrocnemius muscle (GM) *in vivo*. *In vitro*, the RT-PCR result indicated that MPRO gene was successfully expressed in C2C12 myoblasts (**Figure 4-4 A**). The MPRO effectively neutralized the MSTN and stimulated the differentiation of C2C12 myoblasts. In contrast to non-transduced C2C12 myoblasts, AAV2-MPRO-transduced myoblasts readily fused into larger myotubes containing numerous myonuclei (**Figure 4-4 B**). The addition of AAV2-MPRO led to a significant increase in the cells' fusion index in culture (**Figure 4-4 B**). Moreover, an overexpression of MPRO stimulated the expression of Myf5 and myogenin in C2C12 myoblasts in differentiation medium without affecting MyoD expression (**Figure 4-4 C**).

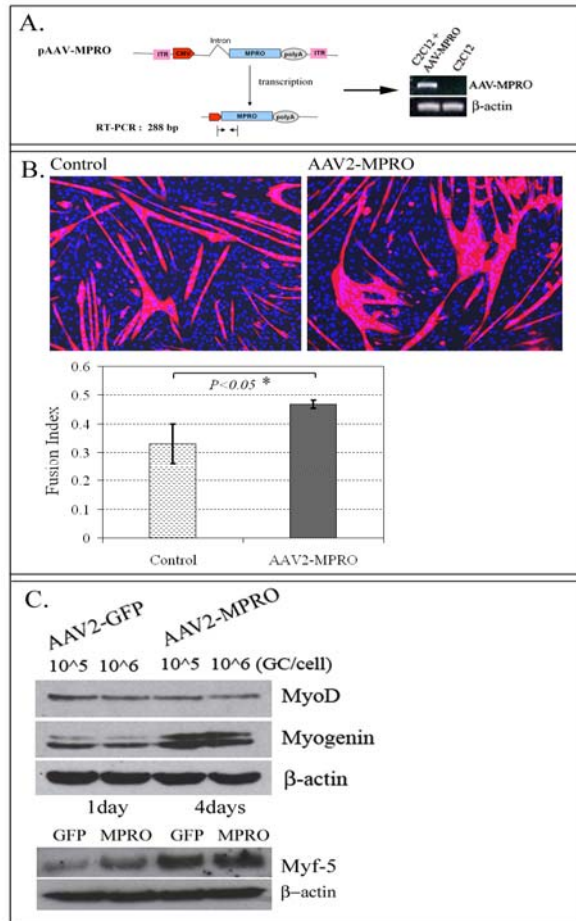


Figure 4-4 In Vitro AAV-MPRO Transduction

(A) The schematic illustration shows the CMV-MPRO construct. The expression of AAV-MPRO by C2C12 myoblasts was detected by RT-PCR. (B) After induction of myogenic fusion in low-serum medium, C2C12 myoblasts expressing AAV-MRPO were fixed and stained with MyHC (red); nuclei were stained with Dapi (blue). AAV-MPRO transduction resulted in the formation of larger MyHC-positive multinucleated myotubes and a significant increase in fusion index (Mean \pm SD; * $P < 0.05$). (C) AAV-MPRO stimulated the expression of myogenic regulatory factors, Myf-5 and myogenin, but not MyoD.

4.3.3 AAV2 Delivered-MPRO Inhibits MSTN Activity *in Vivo*

We then transduced AAV2-MPRO into the murine skeletal muscle to examine whether an AAV-delivered MPRO gene could be stably expressed *in vivo* and improve the skeletal muscle healing after injury. We injected the AAV-MPRO into the GMs of adult BL6J mice; the same amounts of PBS were injected into littermates as the control. Four weeks after the AAV2 vector delivery,

we lacerated both GMs of each mouse. Mice were sacrificed at 4 weeks post-injury. Masson's trichrome histochemistry showed extensive fibrosis infiltration in injured WT skeletal muscle, while fibrosis in injured AAV-MPRO transduced muscle was limited with a reduced amount of fibrotic tissue (**Figure 4-5 A**). An MPRO overexpression significantly suppressed the formation of fibrous scar tissue in the injured AAV2-MPRO transduced GMs as compared to that in the WT counterpart (2.64 ± 1.04 vs. 7.21 ± 1.06 ; mean \pm SD, $** P < 0.01$) (**Figure 4-5 B**). The expression of the MPRO in AAV-MPRO transduced muscles indicated that genes delivered by the AAV were stably expressed in muscle (**Figure 4-5 C**). The weight of AAV2-MPRO transduced-GMs was also significantly higher than that of the WT counterparts (**Figure 4-5 D**). We also observed larger regenerating myofibers in the AAV2-MPRO transduced injured muscle than in the injured WT muscle (**Figure 4-5 E**). The mean diameter of regenerating myofibers in the GMs overexpressing MPRO was increased 26.7% over that in the non-transduced GMs, and the difference was significant (36.79 ± 3.79 vs. 29.03 ± 2.18 ; mean \pm SD, $**P < 0.01$) (**Figure 4-5 F**). Correspondingly, the distribution of diameter of regenerating myofibers revealed that 78% of regenerating myofiber in control muscle had a diameter smaller than 35 μm when compared to 46.28 % of that in AAV2-MPRO transduced muscle; in contrast, 53.7% of regenerating myofibers in injured AAV-MPRO transduced muscle had a diameter in the range of 35 to 70 μm (**Figure 4-5 G**).

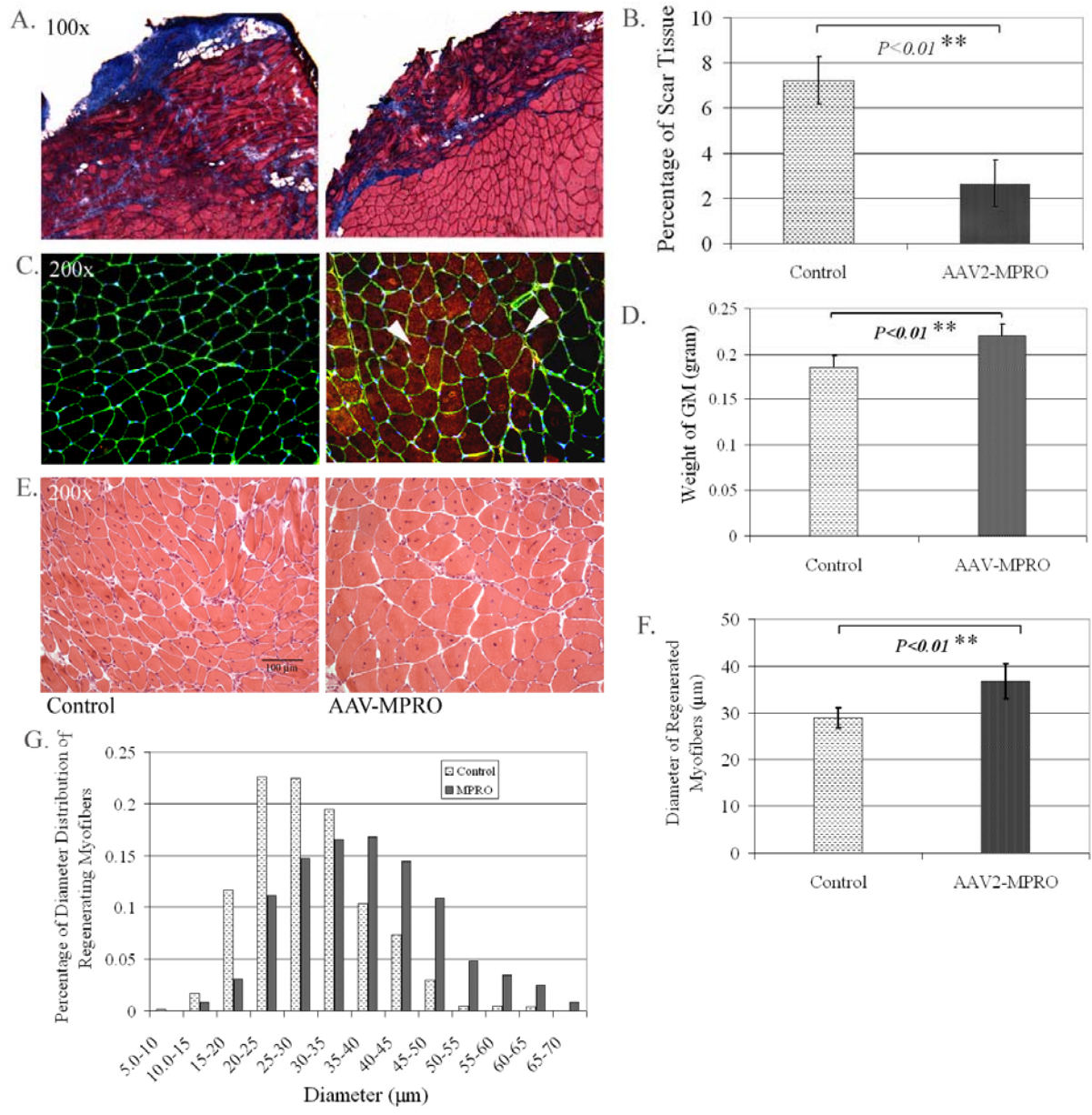


Figure 4-5 AAV-MPRO Improved Skeletal Muscles Healing at 4 Weeks after Injury

(A) Masson trichrome staining show extensive fibrotic tissue (blue) at the injured site of the muscles treated with PBS, whereas fibrotic tissue was mostly limited to the surface of the injured site of AAV-treated injured muscle. (B) Consequently, the fibrosis in the AAV-MPRO treated injured muscle was significantly decreased in comparison to PBS control. (C) Coll IV (green) and MPRO (red) double-staining showed strong MPRO signal in the cytoplasm of fibers of AAV-MPRO transduced muscle. PBS injected muscle was a negative control. (D) When injured muscles were harvested at 4 weeks after injury, we found that AAV-MPRO transduced GMs gained significantly more weight over PBS control. (E) HE stain revealed obvious muscle hypertrophy in AAV-MPRO treated injured muscle. (F) The increase in the diameter of regenerating myofibers resulted from MPRO was significant (Mean \pm SD; ** $P < 0.01$). (G) Frequency histograms show the regenerating myofiber diameter distribution in the AAV-MPRO treated and control muscle.

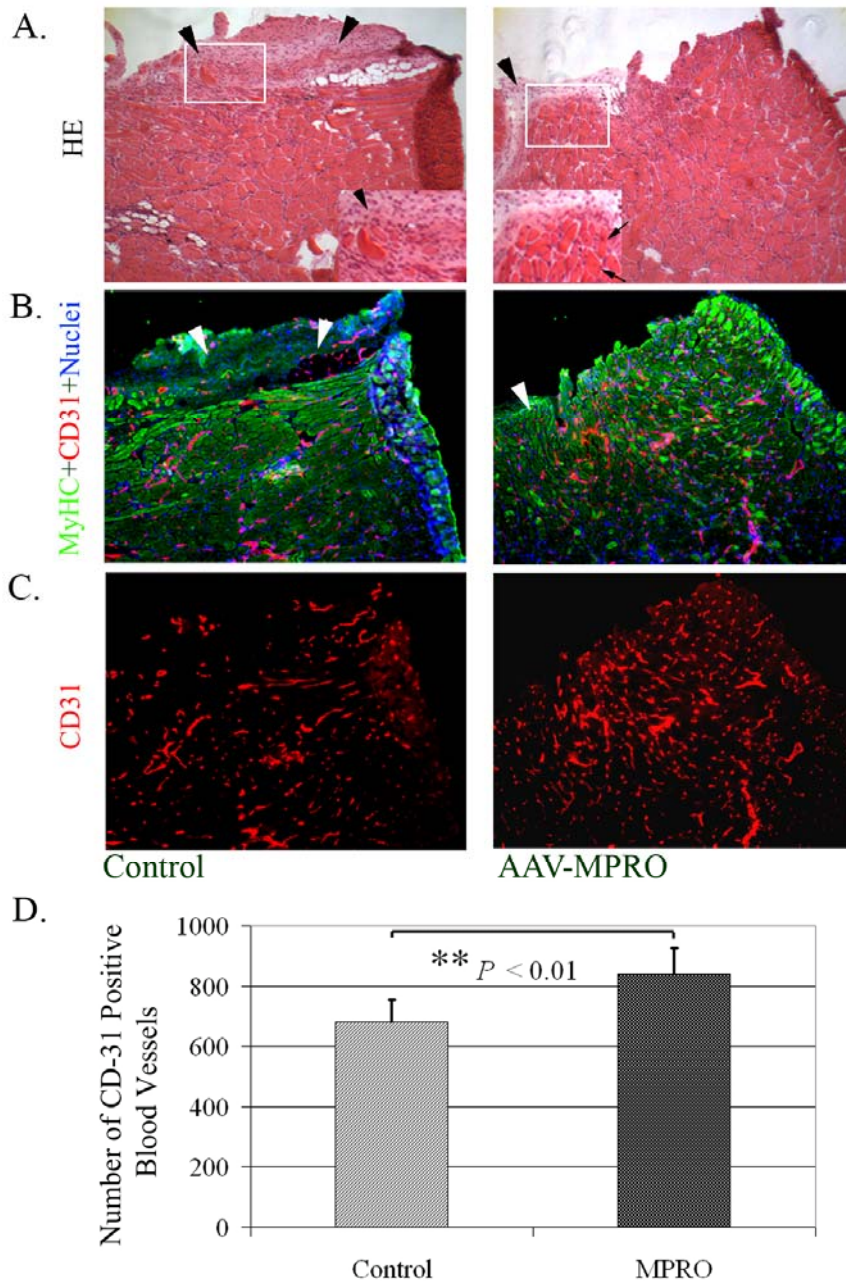


Figure 4-6 Increased Angiogenesis in AAV-MPRO Treated Injured Skeletal Muscle

(A) HE stain show abundant disorganized connective tissue (black arrowheads) in the superficial zone of injured site of AAV-GFP treated muscle, while in the injured AAV-MPRO treated muscle, regenerating fibers (black arrowheads) ingrown into injured site replaced connective tissue. Inserts are enlarged images in the frames. (B) MyHC (green) and CD31 (red) double-immunostaining of parallel slides confirmed the absence of myofibers in injured site (white arrowheads) corresponding to the connective tissue of AAV-GFP treated injured muscle. Moreover, we observe CD31-positive capillaries scattered among the MyHC-positive regenerating myofibers. (C) CD31-staining (red) alone indicated a higher density of CD31 positive capillaries in the AAV-MPRO treated injured muscle than that in AAV-GFP treated muscle. The increase in angiogenesis in the former is significant (Mean \pm SD; ** $P < 0.01$).

In addition, we also found increased vascularity in the AAV2-MPRO-transduced mice after the GM laceration; **Fig.4** shows the representative images from the injured AAV-MPRO transduced muscle and the control. In efforts to clarify the mechanism of how a blockade of the MSTN signal via the MPRO improved muscle healing, we investigated whether the MPRO overexpressing injured muscle exhibited more CD31 positive capillaries. The H & E stain showed the histology of injured skeletal muscles (**Figure 4-6 A**). The MyHC-CD31 double stain showed regenerated myofibers interspersed with CD31 positive capillaries at the injured site (**Figure 4-6 B**). The CD31 stain alone revealed a higher density of capillaries in the MPRO overexpressing injured muscles than in their counterparts (**Figure 4-6 C**). We consequently found significantly more CD31 positive capillaries in the AAV-MPRO transduced injured muscle than in the control at 4 weeks post-injury (**Figure 4-6 D**).

4.3.4 Long Term Beneficial Effects of MPRO on Muscle Healing

In a separate study, we injected the AAV-GFP and the AAV-MPRO into the GMs of different littermates 4 weeks prior to laceration injury, but they were not sacrificed until one year after the muscle laceration. We were able to still detect strong expressions of the GFP and MPRO in the myofibers of the AAV-GFP or MPRO transduced muscles, respectively. We observed the GFP-positive fibers in the AAV-GFP treated muscle, but not in the AAV-MPRO treated muscle (**Figure 4-7A**). Collagen type IV staining shows the outlines of myofibers; MPRO-positive myofibers (arrowheads) indicate a constitutive expression of MPRO in skeletal muscles transduced with the AAV-MPRO, but not in the AAV-GFP control muscle (**Figure 4-7A**). Many regenerating myofibers remained centronucleated in muscles overexpressing GFP or MPRO 1 year post-injury (**Figure 4-7 B**). Many regenerating myofibers remained centronucleated in

muscles overexpressing GFP or MPRO 1 year post-injury (**Figure 4-7 B**). We observed significantly larger regenerating myofibers in the AAV2-MPRO transduced injured muscle than in the controls (**Figure 4-7 B**).

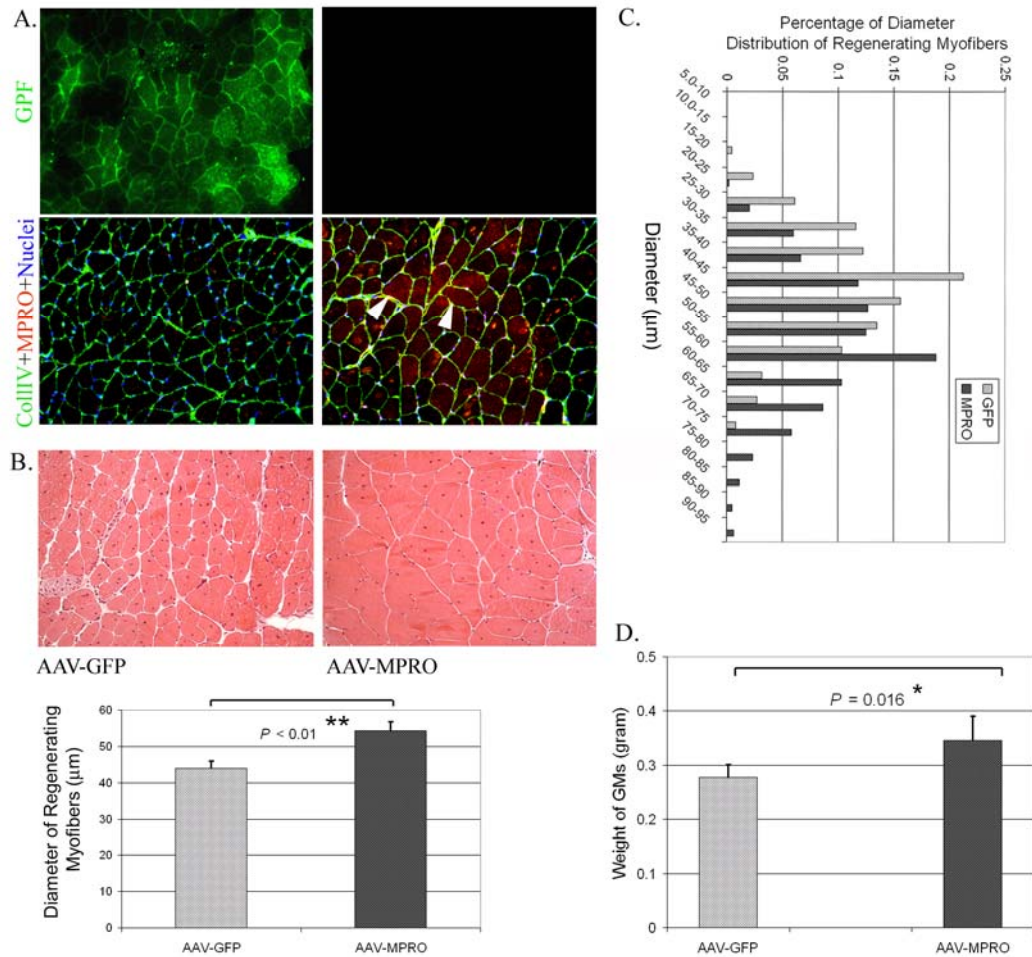


Figure 4-7 AAV-MPRO Showed Long-Term Beneficial Effects on the Injured Skeletal Muscle

(A) Images show the expression of GFP (green) in the AAV-GFP treated muscle at 1 years post injury in contrast to the absence of GFP signal in AAV-MPRO treated muscle. In the lower images, collagen IV immunostaining (green) highlights each individual muscle fibers. MPRO immunostaining reveals MPRO expression in the cytoplasm of myofibers of AAV-MPRO treated muscles, while the AAV-GFP treated muscle serve as a negative control. (B) Constitutive expression of MPRO in the AAV-MPRO treated muscle continued to cause muscle hypertrophy after muscle injury. Larger central nucleated myofibers can be observed in the AAV-MPRO treated injured muscle as compared to the control. The mean diameter of regenerating myofibers in the former was significantly increased. (C) Distribution of diameters of regenerating myofibers in the AAV-GFP and -MPRO treated injured muscle. (D) Weight of injured muscle transduced with AAV-MPRO was higher than the control (Mean \pm SD; * $P < 0.05$).

Frequency histogram indicated that the AAV-MPRO transduced injured muscles contained a greater percentage of regenerating myofibers that have larger diameters; for instance, only 30% of the regenerating myofibers in the control muscle were larger than 50 μm when compared to 61 % in the AAV2-MPRO transduced muscle (**Figure 4-7 C**). The blockade of the MSTN by the MPRO has a long-term effect with a significant increase in the weight of GMs (**Figure 4-7 D**).

4.3.5 Lack of MSTN Signal in Donor MPCs Elevated Efficiency of Cell Transplantation in *Mdx*/SCID Mice

In efforts to search a robust cell population for cell therapy treating DMD, we investigated whether blocking the MSTN signal pathway in donor cells could augment the success of cell transplantation. We therefore isolated MPCs from the skeletal muscle of the MSTN^{-/-} mice to examine their performance in the recipient dystrophic muscle over the WT MPCs. Transplantation of MSTN^{-/-} MPCs into the dystrophic muscle produced more dystrophin-positive regenerated myofibers, as compared to a few myofiber regenerated from WT-MPCs in the control muscle (**Figure 4-8 A**). We isolated five WT MPC populations and five MSTN^{-/-} MPC population from five WT and five MSTN^{-/-} mice, respectively. Each cell population was injected into four legs to minimize the variation among different *mdx*/SCID mice. The mean number of dystropin-positive myofibers derived from the same cell population from four leg specimens was considered as one sample. Regarding the variability among different cell populations, we did observe that some WT MPC population regenerated more myofibers than did other MSTN^{-/-} MPC populations (eg., WT#3 > MSTN^{-/-}#3, 2); however, MSTN^{-/-} #2, which produced the least number of myofibers among the MSTN^{-/-} MPC populations, exceeded

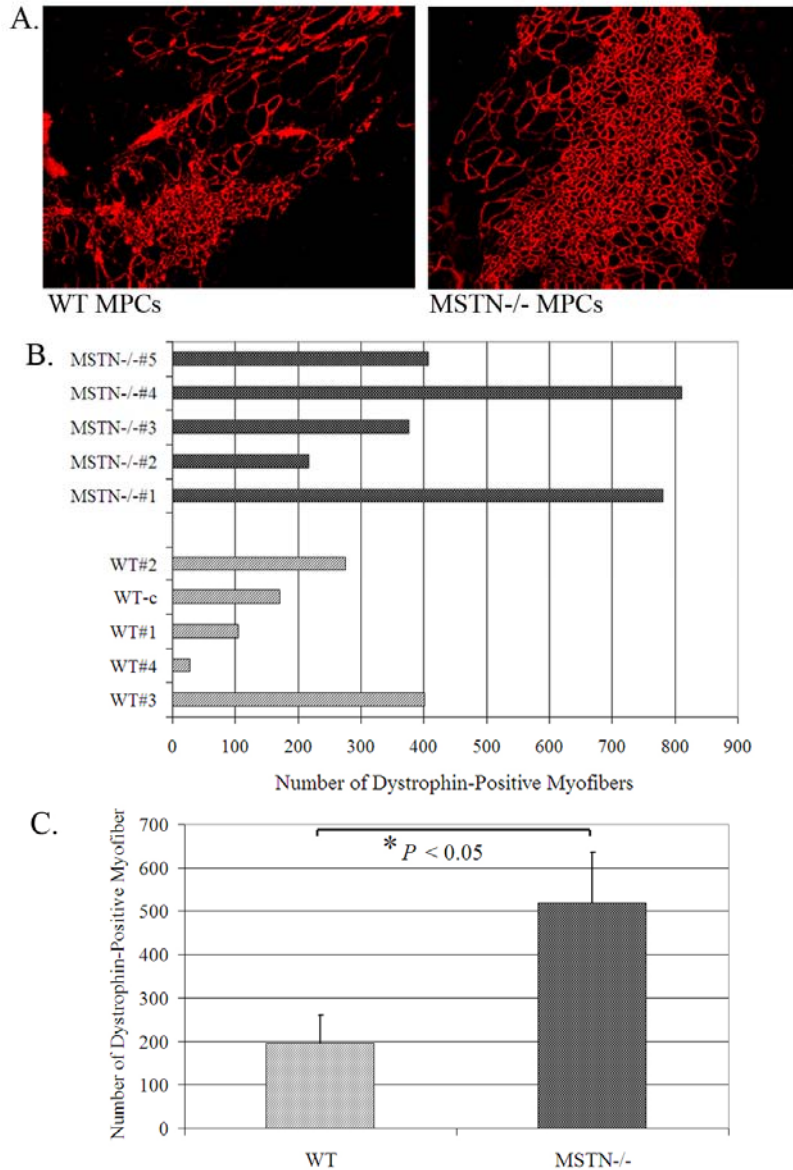


Figure 4-8 Donor MSTN^{-/-} MPCs Exhibited a Higher Regenerative Capacity in the Host Dystrophic Muscle

(A) Representative images show that the MSTN^{-/-} MPCs produced numerous dystrophin-positive myofibers (red) in dystrophic muscle as compared to a few dystrophin-positive fibers seen in dystrophic muscle transplanted with the WT MPCs. (B) Both WT and MSTN^{-/-} MPC populations show a great variation in regenerating muscle fibers, however, the majority of MSTN^{-/-} MPC population regenerated more dystrophin-positive muscle fibers than all WT MPC populations combined. (C) Transplantation of MSTN^{-/-} MPC led to 165% more dystrophin-positive fibers in dystrophic GMs than in control dystrophic GMs transplanted with WT MPCs; blocking the MSTN signal in donor cells led to a significant increase in dystrophin-positive regenerated muscle fibers (Mean ± SEM; * $P < 0.05$).

the results of three WT-MPC populations out of the five total populations (**Figure 4-8 B**). The maximum number of myofibers regenerated from the WT-MPC population was 400, whereas three out of five MSNT^{-/-} population regenerated more than 400 myofibers, and two MSTN^{-/-}

MPC population gave around 800 regenerated myofibers (**Figure 4-8 B**). As a result, overall number of the dystrophin positive regenerated myofibers in MSTN^{-/-} MPC populations surpassed that of the WT cells (195.6 ± 65.357 vs. 518.08 ± 117.64 ; mean \pm SEM, $*P < 0.05$) (**Figure 4-8 C**).

4.3.6 AAV-MPRO Improved Cell Transplantation and Reduced Severity of Muscular Dystrophy Efficiency in *Mdx/SCID* Mice

We further examined whether blocking the MSTN in the dystrophic host muscle can facilitate donor muscle cell transplantation. We transplanted the MPCs isolated from the WT mice into the dystrophic muscles pre-treated with either AAV-GFP or AAV-MPRO 4 weeks prior to cell transplantation. *In vitro* characterization revealed that 70% of MPCs expressed demin, a myogenic marker (**Figure 4-9 A**), suggesting a high myogenic potential of these cells. In the low serum medium, the MPCs readily fused and formed into MyHC positive multi-nucleated myotubes (**Figure 4-9 B, F**). A small portion of this MPC population was CD34 and Sca-1 double positive, which may represent stem cells (**Figure 4-9 C, E**). An *in vivo* characterization showed that these MPC were able to regenerate dystrophin positive myotubes when injected into dystrophic muscle of *mdx/SCID* (**Figure 4-9 F**). Two weeks after cell transplantation, we examined whether blocking MSTN signal by MPRO in host muscle increased the efficiency of muscle cell transplantation in dystrophic muscles. The images in **Figure 4-9 G** showed the representative images of dystrophin positive engraftments in muscles of *mdx/SCID* mice 2 weeks after cell transplantation. We found that normal MPCs injected into the AAV-MPRO transduced dystrophic muscles surpassed the cells injected into the control muscles in regenerating muscle, indicated by more dystrophin-positive regenerating myofibers (**Figure 4-9 G**).

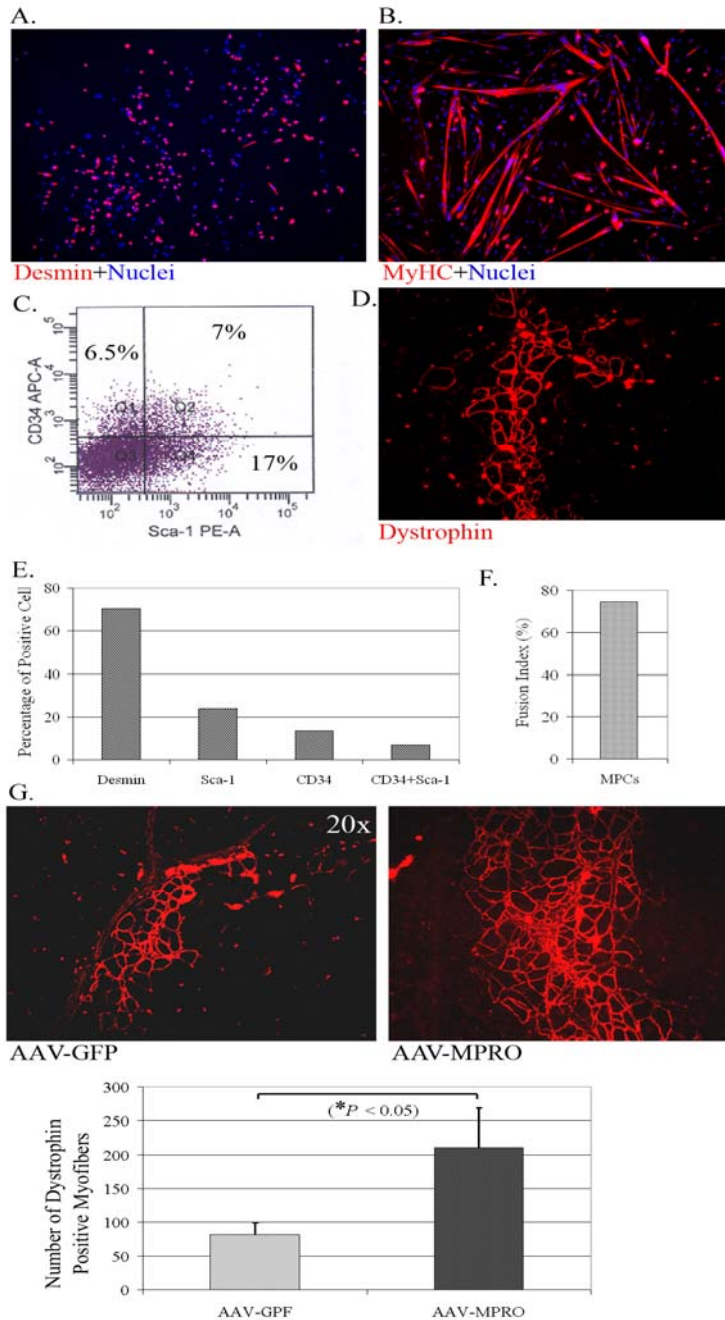


Figure 4-9 Muscle Progenitor Cell Characterization and Transplantation

(A, F) MPC population was highly desmin positive, around 70.4%. (B) In a low serum medium, MPCs easily differentiated and fused into multinucleated myotubes visualized by MyHC (red) and dapi (blue) staining with a fusion index of 74.5% (F). (C, E) Flow cytometry indicated 24% of MPCs are Sca-1 positive, 13.5% CD34, and 7% Sca-1 double positive. (D) *In vivo* characterization showed that MPCs were able to form dystrophin-positive (red) myofibers in dystrophic mice. (G) We injected the same numbers of this MPC population into skeletal muscle of *mdx*/SCID mice transduced with the AAV-GFP and -MPRO respectively; the MPCs transplanted into muscle regenerated more dystrophic positive myofibers than cells in the control muscle. The increase is significant (Mean \pm SEM; * $P < 0.05$).

To explore why MPCs transplanted into the AAV-MPRO treated muscles performed better, we compared the differences in dystrophic pathology between the GMs of *mdx*/SCID mice transduced with AAV-GFP or MPRO. Cryosectioned muscle samples were subjected to H&E and Masson's trichrome staining at 6 weeks after virus transduction. Histological analysis indicated a decreased dystrophic phenotype after the AAV-MPRO treatment. The insets (20x) show whole sections of cross-section of GMs (**Figure 4-10 A**). The arrows in the insets indicate that generally more necrotic foci affected by pathological changes were observed in the AAV-GFP transduced control dystrophic muscle than in the AAV-MPRO treated dystrophic muscle, which were poorly stained by eosin (**Figure 4-10 A**). The enlarged images (40x) revealed that those areas consist of necrotic myofibers, numerous mononucleated cells, connective tissue, or small regenerating myofibers. The necrotic myofibers and cellular filtration can be readily appreciated in a further enlarged image (100x) of the control muscle (arrows and arrowhead), whereas the AAV-MPRO treated muscle exhibited less damages but a lot of regenerating fibers (arrows and arrowhead, **Figure 4-10 A**). Masson's trichrome stain revealed that the degenerative areas were associated with extensive fibrotic tissue (blue). Low (2x) and high (40x) magnification images revealed that the control dystrophic muscles generally contain more fibrotic tissue than did AAV-MPRO treated dystrophic muscles. A higher levels of fibrosis, averaging 7.08% (and varying from 5.32 to 9.02%) by area of GM cross-section affected, is detected in the control muscle as compared to 4.09% (and varying from 2.73 to 6.07%) in the treated muscle. A significant decrease in fibrous scar tissue in the AAV2-MPRO treated muscles was observed as compared to the controls (**Figure 4.10 B**).

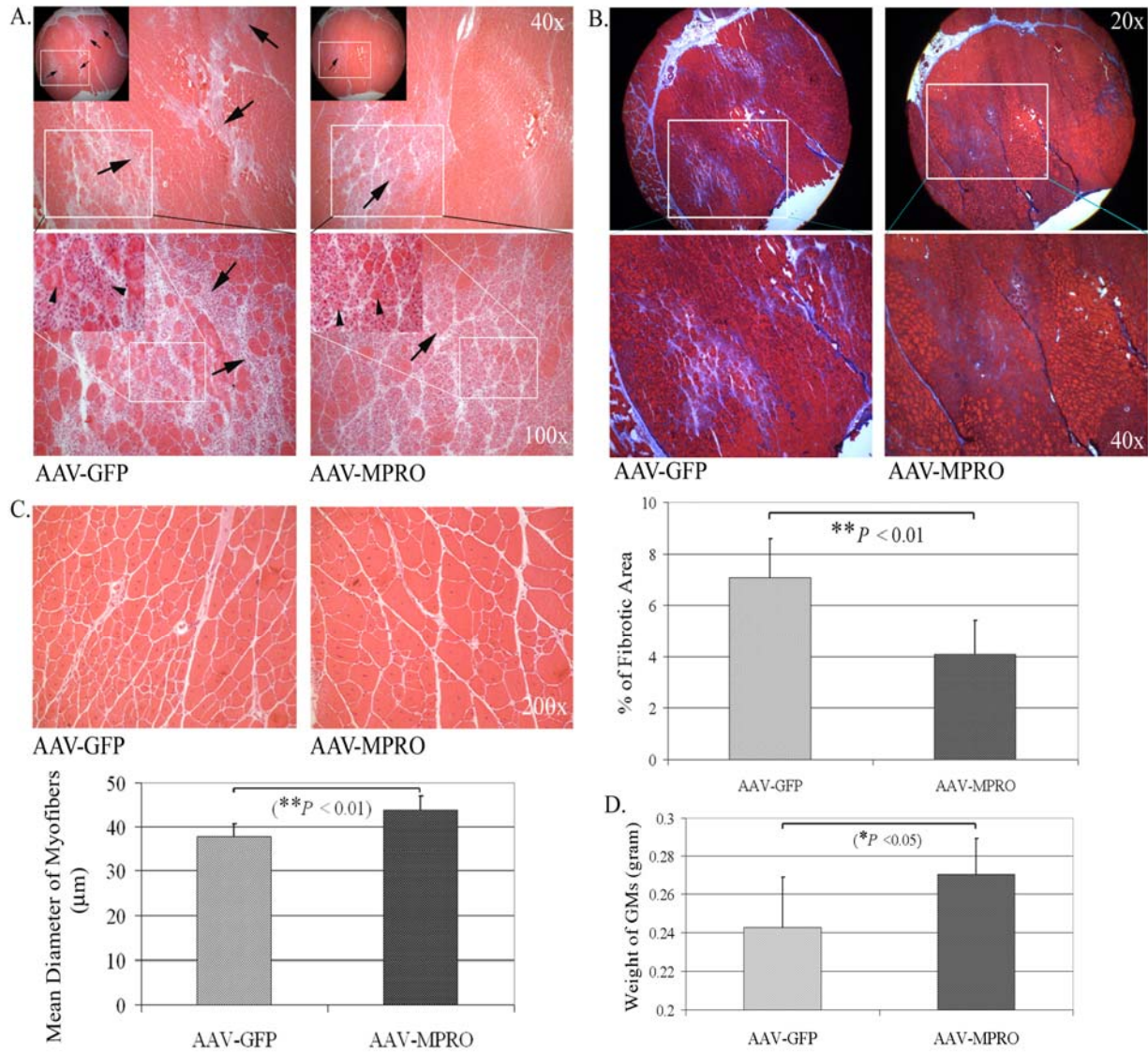


Figure 4-10 Improved Dystrophic Pathology in *mdx*/SCID Mice after AAV-MPRO Treatment

(A) Small inserts 2x in upper images (HE) show overall morphology of cross-sectional dystrophic muscles. Small arrows in inserts point out poorly stained necrotic foci. More necrotic foci were observed in AAV-GFP treated dystrophic muscle than AAV-MPRO treated dystrophic muscle. When necrotic foci were enlarged, we observed necrotic myofibers (arrowheads) and numerous mononuclear cells (arrows) in AAV-GFP treated dystrophic muscle, but abundant small newly regenerated fibers and less cellular infiltration in AAV-MPRO treated dystrophic muscle. (B) Masson's trichrome staining reveal that the necrotic foci were stained blue suggesting accumulation of fibrotic tissue within the foci. (See the additional amplified images.) Measurement of the scar tissue shows that AAV-MPRO treatment led to a significant decrease in fibrosis of dystrophic muscle (Mean \pm SD; * $P < 0.01$). (C) The mean diameter of regenerating myofibers in AAV-MPRO treated muscle is significantly larger than that of AAV-MPRO treated muscle (Mean \pm SD; * $P < 0.01$). (D) Moreover, this AAV-MPRO induced muscle hypertrophy eventually cause a significant increase in muscle weight (Mean \pm SD; * $P < 0.05$).

Moreover, hypertrophy in AAV2-MPRO treated dystrophic muscle is noteworthy. Measuring the diameter of a single fiber demonstrated that the mean diameter of fibers in the AAV-MPRO transduced dystrophic muscles is significantly larger than that of the AAV-GFP transduced counterparts (**Figure 4-10 C**). The AAV2-MPRO transduction-induced muscle hypertrophy eventually led to a significant increase in muscle weight when compared to control (**Figure 4-10 D**). Taken together, improvements in dystrophic muscle by the AAV-MPRO were manifested by decreases in necrotic foci, fibrosis, and increases in muscle weight and single fiber diameter.

4.4 DISCUSSION

After injury, skeletal muscle is able to undergo limited regeneration from myoblasts, satellite cells, myogenic progenitor cells, and stem cells; nevertheless, severely injured muscle usually ends up with incomplete skeletal muscle healing due to the fact that the ensuing formation of fibrosis hinders effective muscle regeneration. Thus, an optimal approach to treat injured muscle should not only be able to enhance muscle regeneration, but also reduce the formation of fibrosis.

The discovery of the MSTN is a significant breakthrough for the development of therapeutic approaches for myopathies. In addition to numerous evidence showing that inhibiting MSTN boosts muscle growth and regeneration under pathological conditions, such as with muscle injury and dystrophy^{77, 123, 127, 137, 151}, MSTN also regulates skeletal muscle fibrosis^{127, 137, 155}. Without MSTN, as seen with MSTN $-/-$ mice, skeletal muscle fibrosis is significantly lower after injury than that observed with WT skeletal muscle^{127, 137}. While fibroblasts are the main source of extracellular matrix (ECM) during the formation of fibrosis, MSTN directly stimulates

the proliferation of muscle fibroblasts and their *in vitro* and *in vivo* production of ECM^{127, 137, 155}. Therefore, MSTN is an excellent therapeutic target for treating injured and diseased muscles. Because the *in vivo* cytokine networks are very complex, however, the underlying mechanism by which MSTN inhibition attenuates muscle fibrosis requires further investigation. For now, it is clear that MSTN and TGF- β 1 synergistically induce fibrosis after skeletal muscle injury; the reduced fibrosis in injured MSTN^{-/-} muscle may result in part, but perhaps not completely, from the absence of MSTN¹²⁷; whether or not this is indeed the case, however, is not yet entirely clear. This may also be related in part to local changes in vascularity.

4.4.1 Increased Vascularity in the Injured MSTN^{-/-} Skeletal Muscles and AAV-MPRO Treated Injured Skeletal Muscles

As the local tissue vascularity promotes muscle regeneration and helps to reduce the amount of fibrosis following injury¹²⁴. It is not surprising that we noted an earlier onset of neovascularization from the time of injury in the MSTN^{-/-} muscle compared to wild type muscle. At 4 weeks after injury, injured MSTN^{-/-} muscle contained significantly more CD31-positive capillaries than controls. The increased vascularity appears to partially account for improved muscle healing in injured MSTN^{-/-} mice. Since the emergence of transgenic animals in the last decade, they have become a powerful and exciting research model to study protein function and molecular mechanisms through taking advantage of “loss or gain of function”. Nevertheless, it is worth mentioning that the irreversible genetic manipulations may result in compensatory upregulation, developmental defects, and others. Changes take place during the prenatal life which may impose undesired effects on adult animals¹⁶⁰. An alternative experimental approach to transgenesis is to use a virus as a gene delivery vehicle carrying the

desired cDNA to certain tissues or organs. The Adeno-associated virus (AAV) is garnering significant interest as a vector for human gene therapy, due to its lessened immunogenicity and ability to efficiently infect differentiated fibers of skeletal muscle and stable long term expression of transferred gene^{147, 161}. In this study, we injected an AAV2-mediated MSTN propeptide cDNA into GMs 4 weeks prior to injury to establish a postnatal, muscle specific MSTN propeptide overexpression model.

Our results suggest that the AAV-MPRO gene could be stably expressed *in vivo* and improve the healing of the injured muscle over a long term. We found that the MPRO gene transfer improved skeletal muscle healing by stimulating muscle regeneration and inhibiting fibrosis 4 weeks after injury, which coincides with higher density of CD31 positive capillaries in the MPRO expressed muscle than in the control. This further suggests that there is a negative correlation between MSTN and vascularity in injured skeletal muscle, which is consistent with what observed in injured MSTN^{-/-} muscle; nonetheless, it is important to note that the mechanisms by which MSTN and vascularity are conversely linked warrant further investigation. Our long term study also shows that there is an abundant expression of the GFP and MPRO in the skeletal muscles at 1 year after gene transfer. By that time fibrosis nearly disappears in all injured muscles, while the hypertrophy of regenerating myofibers in AAV-MPRO transduced muscles was still observed, indicating a continuous beneficial effect on myofibers.

4.4.2 Blocking MSTN^{-/-} Signaling in Muscle Progenitor Cells Improve Cell's Regenerative Capacity

As much of the pathology involved in traumatic skeletal muscle injury is similar to that involved with the pathology of muscular dystrophy, our group has taken a particular interest in the

muscular dystrophy with a special emphasis on cell therapy. Cell therapy has received increasing attention, since accumulating evidence demonstrates that the transplantation of highly proliferative multipotent cells may be able to treat numerous diseases and tissue injuries. One such disease is DMD, a lethal sex-linked recessive, muscle-wasting disease stemmed from a mutation of the dystrophin gene. The absence of a functional dystrophin expression at the sarcolemma of myofiber makes it susceptible to contracting forces, and consequently results in muscle fiber necrosis and muscle weakness. Although finding an effective treatment for DMD will require further research, cell and gene therapies are two therapeutic approaches of great interest to the research community. Theoretically, transplanting cells with a normal dystrophin gene into dystrophic muscle should be able to partially restore dystrophin and improve DMD. Donor myoblasts, especially stem cells, do indeed form dystrophin-positive myofibers in dystrophic muscles of *mdx* mice; significant results, however, have not yet been produced, due to obstacles such as poor dissemination, a limited survival of donor cells.

In order to improve cell therapy for the treatment of diseases such as DMD, it is crucial to have donor cells with high quality of performance. Since MSTN negatively regulates the growth and development of myofibers, blocking the MSTN signaling of donor cells may significantly improve the performance of muscle cells. In studies performed by Tremblay *et al*, myoblasts that were isolated from transgenic mice and carried a dominant negative form of myostatin receptor (dnActRIIB) on average gave rise to 75% more dystrophin-positive fibers in recipient dystrophic tibialis anterior muscle than did WT myoblasts¹²². Similarly, we previously reported that muscle regeneration in *mdx*/SCID mice is superior when their GMs are implanted with MSTN^{-/-} as opposed to WT MPCs¹²⁷. In the present study, we isolated more MSTN^{-/-} MPC populations from different MSTN^{-/-} mice and more extensively compared their competency in

cell transplantation to that of the WT MPC populations. In this comparison, we first found that there exists a broad heterogeneity within both WT MPC populations and *MSNT*^{-/-} in term of the capacity of these cells to regenerate muscle. This heterogeneity likely resulted from variations among mice from which cells were isolated, as well as variations among the host *mdx*/SCID mice. We further compared the regenerative capacity of MPCs between WT and *MSTN*^{-/-} population, and found that the *MSTN*^{-/-} MPCs can produce significantly more dystrophin-positive myofiber than the WT MPCs. These results suggest that genetically modifying donor cells does improve the success of cell transplantation.

4.4.3 Improved Success of Cell Transplantation by Blocking MSTN Signaling in Host Dystrophic Muscle

It appears that over time, there has been an increasing numbers of biomedical investigators who believe that inhibiting MSTN is a therapeutic strategy for treating muscular dystrophy^{77, 151, 162}. Among some of the therapies that have been investigated are the use of an anti-MSTN antibody and of a recombinant MSTN propeptide, both of which produce a histological and functional improvements in *mdx* mice^{77, 151}. Xiao's group recently reported that the same MPRO cDNA as used in this study can be delivered systematically with the AAV-serotype 8 vector to augment the skeletal muscle mass of both normal and *mdx* mice¹⁵⁷. Moreover, MPRO overexpression resulted in less mononuclear cell infiltration and fibrosis as well as lower creatine kinase levels in the dystrophic muscle of *mdx* mice when compared to untreated controls.¹⁵⁷ More interestingly, it has been found that blocking MSTN signal transduction in host *mdx* mice significantly enhances muscle regeneration capacity of donor myoblasts^{122, 163}; Tremblay *et al* have accomplished this by generating transgenic *mdx* mice with a dominant negative form of

MSTN receptor (dnActRIIB),¹²² as well as by overexpressing the MSTN inhibitor, follistatin (FLST)¹⁶³. Normal myoblasts transplanted into these transgenic *mdx* mice outperformed cells transplanted in *mdx* mice that were not transgenically modified^{122, 163}. Of note, however, data were obtained from experiments using genetically engineered *mdx* mice, making it difficult to translate these findings into the clinical trial. Moreover, dnActRIIB and FLST are not MSTN-specific inhibitors, as they also block other growth factors such as activin. By contrast to these studies, our study examines the impact of injected MPCs into dystrophic muscles which are not transgenically modified, but rather, in which MSTN is blocked by AAV-MPRO. Specifically, the AAV-GFP or MPRO construct was injected into the muscles of *mdx*/SCID mice 4 weeks prior to the transplantation of MPCs to investigate whether this AAV-MPRO construct can enhance the muscle regeneration potential of donor cells by blocking MSTN signaling.

Our results indicate that inactivating MSTN in dystrophic host muscle with MPRO significantly improves the regeneration that follows MPC transplantation; when compared to the AAV-GFP transduced control, the MPRO construct yielded significantly more dystrophin-positive myofibers. We further observed that MPRO ameliorates the dystrophic pathology of *mdx* mice by reducing collagen deposition, mononuclear cellular infiltration, and promoting muscle regeneration; these findings were in sharp contrast to the typical findings of dystrophic muscle, in which muscle fibers are gradually replaced by fibrotic and adipose tissue. The extensive fibrosis in dystrophic muscle is a likely cause for an ineffective cell transplantation. It is possible that a favorable microenvironment for donor cells to promote regeneration is created by inhibiting fibrogenesis. Accordingly, we propose three mechanisms (**Figure 4-11**) by which cell transplantation can be improved, based on our experimental findings. First, MPRO prevents MSTN from inhibiting donor cell-mediated myofiber regeneration; in doing so, donor cells may

be better able to adapt, proliferate, differentiate, and form dystrophin-positive myofibers. Second, MPRO inhibits MSTN, thereby reducing fibrosis and promoting muscle regeneration in dystrophic muscle. Finally, the decrease in degenerative foci, fiber necrosis, and moderated cellular infiltration may suggest that there are fewer cytotoxic cytokines and substances being secreted by inflammatory cells (e.g., neutrophil), such as tumor necrosis factor- α (TNF- α),

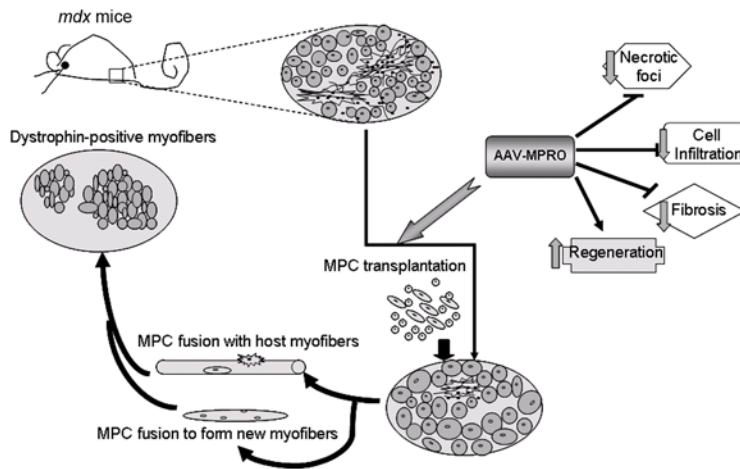


Figure 4-11 Schematic Representation of How Transduction of the AAV-MPRO into Host Dystrophic Muscle

Improves Efficiency of Cell Transplantation

(1) MPRO inhibits the endogenous MSTN and promotes muscle regeneration in the host dystrophic muscle. (2) MPRO reduces fiber necrosis and inflammatory cell infiltration. (3) MPRO reduces fibrosis. The deregulation of MSNT on donor cells ameliorated dystrophic physiology and may facilitate donor cells to form more dystrophin-positive myofiber.

superoxide, hypochlorite, and nitric oxide¹⁶⁴⁻¹⁶⁶ in the AAV-MPRO-treated dystrophic muscle.

Numerous *in vitro* and *in vivo* evidences have demonstrated that inflammatory cells (e.g., neutrophils and macrophages) are detrimental to healthy muscle cells¹⁶⁷⁻¹⁶⁹ and myofibers^{170, 171}

(Figure 4.11).

The primary onset of muscle necrosis in dystrophin-deficient muscle is primarily attributed to the increased susceptibility to damage during contraction. Additionally, typical secondary chronic inflammatory response to progressive muscle necrosis further aggravates the

symptoms of dystrophinopathies; it has been well documented that an excessive inflammatory response can directly cause severe myofiber damage in both dystrophies and myositis¹⁷²⁻¹⁷⁵. In *mdx* mice, abrupt skeletal muscle necrosis begins at 21 days and peaks at 28 days of age¹⁷⁶; with the an administration of TNF- α neutralizing antibody Remicade®, however, there is a delay in the onset of muscle breakdown, as well as a decrease in phagocyte infiltration, fiber necrosis, and centronucleated myofibers in *mdx* mice when compared to controls¹⁶⁴. It has also been shown that depleting neutrophils or inhibiting TNF- α by Etanercept reduces the extent of muscle necrosis in *mdx* mice¹⁶⁵. In a similar fashion, our results indicate that MPRO improves the dystrophic phenotype in *mdx*/SCID mice, ultimately enhancing the efficiency of cell transplantation. Accordingly, improving the microenvironment of host dystrophic muscle in this fashion probably is a feasible approach for enhancing the efficiency of cell transplantation.

4.5 CONCLUSION

Our data show that angiogenesis occurs earlier in the injured MSTN^{-/-} muscle than in the injured normal muscle after laceration injury. The increased angiogenesis appears to partially account for improved muscle healing in injured MSTN^{-/-} mice. Next, we use AAV to deliver MPRO cDNA into GMs to restrict MSTN propeptide overexpression in the certain skeletal muscles of adult mice. Our results suggest that AAV-MPRO gene could be stably expressed in vivo and improve healing process of injured muscle for a long term. We found that MPRO gene transfer improved skeletal muscle healing through stimulating muscle regeneration and inhibiting fibrosis 4 weeks after injury, which coincides with more active angiogenesis in MPRO expression muscle than control. It suggests a negative correlation between MSTN and angiogenesis in

injured skeletal muscle. However, the clear relationship between MSTN and angiogenesis warrants further investigation.

Furthermore, we found that elimination of MSTN expression in MPCs led to an increase in cells' ability to regenerate skeletal muscle in the dystrophic muscle of *mdx* mice. Moreover, Inactivation of MSTN in dystrophic host muscle by MPRO significantly improved the success of MPC transplantation as compared to the AAV-GFP transduced control, evidenced by significantly more dystrophin-positive myofibers in the former. It is probably partially due to the fact that MPRO ameliorated the dystrophic pathology of *mdx* mice by promoting muscle regeneration and reducing collagen deposition, and thereby improve milieu in host dystrophic muscle and favor donor cells' survival and expansion.

Taken together, the combination of gene and cell therapies may represent a type of novel effective approach for treating injured and diseased skeletal muscle. One such specific approach involves the use of the AAV-MPRO to inhibit MSTN in host muscle; it is certainly an approach that has the potential for the future with clinical applications of cell transplantation.

5.0 FOLLISTATIN IMPROVES SKELETAL MUSCLE HEALING

5.1 INTRODUCTION

Our group has identified anti-fibrotic agents which significantly enhance skeletal muscle healing after injury by antagonizing TGF- β 1. These include suramin^{31,32}, γ -interferon³⁰, decorin^{16,28,29}, relaxin^{148,149}, and losartan²⁷. Although much of the pathogenesis following skeletal muscle injury has been attributed to TGF- β 1, we have recently reported that fibrosis is also caused by another agent that limits skeletal muscle healing, namely myostatin (MSTN)¹²⁷. MSTN is a primary negative regulator for the growth and development of fetal and postnatal skeletal muscle^{49,73}. Several groups, including ours, have found that MSTN stimulates fibrosis in injured and diseased skeletal muscle^{123,127,137,177}. This is because the cell surface receptor to which MSTN predominantly binds-- activin type IIB cell surface receptor (ACVR2B)-- activates a downstream TGF- β -like signaling pathway^{56,64,65}. More interestingly, we find the reciprocity between MSTN and TGF- β 1: TGF- β 1 and MSTN reciprocally induce the expression of one another; blocking TGF- β 1 signaling impairs MSTN's biological activity, and vice versa¹²⁷. It suggests that TGF- β 1 appear to act in synergy with MSTN to induce fibrosis in the skeletal muscle.

In addition to impairing skeletal muscle healing by promoting fibrosis, MSTN also inhibits myofiber regeneration in diseases such as Duchene's Muscular Dystrophy (DMD)¹²³ as well as after injury^{127,137}. Specifically in the former, *mdx* mice, an animal model of DMD, were

noted to undergo significantly more myofiber damage and less myofiber regeneration along the diaphragm when compared to MSTN knockout *mdx* mice (MSTN^{-/-}/*mdx*) mice.¹²³ Similarly, following notexin-injury of the TA and laceration of the GM, there was a significantly greater regeneration and significantly less amount fibrosis among the MSTN^{-/-} mice in comparison to WT controls^{127, 137}.

To the end of developing therapies which can antagonize MSTN, research in this area has led to the discovery of a glycoprotein that neutralizes several proteins of the TGF- β family, namely follistatin (FLST). FLST has been found to antagonize both MSTN in skeletal muscle and activin A in reproductive tissues, as well as neutralize several other proteins within the TGF- β family^{80, 81 82}. Several *in vivo* studies on FLST have further shown that the systemic administration of this agent directly inhibits MSTN and also reduces MSTN-induced muscle wasting^{73 82}, while FLST/OE transgenic mice exhibit a dramatic increase in muscle mass, much as is seen to occur in MSTN KO mice⁵⁶.

In this study, we provided *in vivo* and *in vitro* data to support the development of FLST as a therapeutic agent for skeletal muscle injury and disease. Specifically, we hypothesize that FLST/OE transgenic mice will undergo more skeletal muscle regeneration and less fibrosis after laceration of the GM compared to WT controls. We next test that if skeletal muscle healing is superior in the FLST/OE mice compared to WT controls, then the muscle progenitor cells of the FLST/OE muscle will outperform cells of WT muscle, which is likely responsible for this enhanced healing.

5.2 METHODS

5.2.1 Animal Model

In accordance with our IACUC approval by the Children's Hospital of Pittsburgh, we performed bilateral lacerations along the gastrocnemius muscle (GM)^{28-31, 127, 149}, as described at section 3.2.7., of 16 male C57BL/6 wild-type (Jackson Laboratories, Bar Harbor, ME) and 16 male FLST/OE mice, each at 7-8 weeks of age, and harvested these muscles at 2 and 4 weeks after laceration (n=8 per group).

5.2.1.1 Histology

We quantified the percent fibrosis and muscle regeneration from each harvested muscles, as previously described¹²⁷. Briefly, following cryosectioning of these tissues histological staining was performed with Masson's trichrome kit (IMEB Inc., Chicago, IL); we then quantified the percent fibrosis with Northern Eclipse software (Empix Imaging, Inc., Cheektawaga, NY), which measures the area of fibrotic tissue along the sites of injury and divides this by the cross-sectional area of tissue to calculate a percentage. For each limb, we obtained calculations from three representative and non-adjacent sections.

In order to evaluate skeletal muscle regeneration, we stained sections from each harvested muscle with Hematoxylin and Eosin (H&E), and quantified the smallest diameters of centro-nucleated myofibers, which represent regenerating muscle fibers, with Northern Eclipse software; we measured the diameters of over 350 non-consecutive centro-nucleated myofibers for each GM.

5.2.1.2 Immunohistochemistry

Additionally, we performed immunohistochemistry to detect MSTN (red fluorescence) and collagen type IV (green fluorescence) expression along each injured GMs. We also targeted CD31, an endothelial cell marker, with immunohistostaining to monitor angiogenesis in injured muscle, and manually counted CD31-positive microvessels with Northern Eclipse software.

5.2.1.3 MSTN immunostaining

Frozen GMs were sectioned at 10 μ M thickness and immunohistochemical analysis was performed to detect MSTN expression. Tissue sections were fixed in 4% formalin for 5 minutes followed by two 10-minute washes with PBS. The sections were then blocked with 10% HS for 1 hour. Goat anti-MSTN (R&D Systems, Minneapolis, MN) primary antibody was separately diluted 1:100 in 2% HS and incubated with sections overnight at 4°C. Sections were then washed three times with PBS and incubated with a secondary antibody, anti-goat IgG conjugated with biotin (1:200) (Vector Laboratories, Burlingame, CA), for 1 hour at room temperature (RT), followed by a PBS wash. Finally, streptavidin conjugated with 555 (1:500) (Invitrogen, Carlsbad, CA) was applied to each section for an additional hour. Eventually, DAPI dihydrochloride (4', 6-Diamidino-2-phenylindole dihydrochloride; Sigma, St Louis, MO) was used to counterstain the nuclei.

5.2.1.4 CD31 immunostaining

To detect vascularity, we blocked the sections with 10% HS for 1 hour, and applied a rat CD31 primary antibody (BD PharMingen, San Jose, CA) that was diluted 1:150 in 2% HS. This preparation was incubated for 1 hour at RT. The sections were then washed three times with PBS

and incubated with the secondary antibody, rabbit anti-rat IgG conjugated with 555 (Invitrogen), for 30 minutes. Finally, DAPI was used to stain the nuclei.

5.2.2 Muscle Progenitor Cell Isolation and Transplantation into Skeletal Muscle

5.2.2.1 Isolation of MPCs

Using a modified preplate technique^{113, 178}, we isolated a fraction of MPCs with properties of low adhesion to collagen and long-term proliferation. We obtained five populations of WT MPCs from male neonatal C57BL/6J mice, as well as 7 populations of FLST/OE MPCs from male neonatal FLST/OE mice with a background of C57BL/6J mice as described at section 4.2.5.

5.2.3 Flow Cytometry

In order to characterize WT and FLST MPC populations, we utilized flow cytometry specific to the markers CD34, Sca-1 in both WT and FLST/OE MPCs to analyse the percentage of stem cell markers as previously described^{113, 178} to examine whether FLST/OE MPCs contain more stem cells than WT MPCs. Briefly, cultured cells were trypsinized, centrifuged, and washed twice with PBS. We subsequently re-suspended our cell pellets, blocked them with 10% mouse serum (Sigma) for 10 minutes on ice and applied rat anti-mouse monoclonal conjugated antibodies (CD34-PE, Sca-1-APC; BD PharMingen) to incubate on ice for 30 minutes. Following this incubation period, we excluded nonviable cells by adding 7-amino-actinomycin D (7-AAD; Pharmingen) to each sample. Cells were then evaluated with a FACS Caliber flow cytometer (Becton Dickinson) and analyzed with CellQuest software (Becton Dickinson).

5.2.3.1 Cell transplantation

After expanding MPCs *in vitro*, these cells were injected into the GMs of female *mdx*/SCID mice; these mice were bred by crossing *Mdx* (C57BL/10ScSn-*Dmd*^{*mdx*}) and SCID (C57BL/6J-*prkdc*^{*scid*}/SzJ) mice (Jackson laboratory) at our institution's animal facility. Approximately 3×10^5 cells from each cell population were transplanted in each GM, for a total of 4 GMs among recipient female *mdx*/SCID mice. All *mdx*/SCID mice used were littermates, and all were sacrificed 2 weeks post-transplantation. The recipient GMs from these mice were harvested at this time, snap-frozen, and cyosectioned on a later date at thicknesses of 10 μ M. Dystrophin immunostaining was performed to detect dystrophin positive myofibers formed from donor MPCs in dystrophic muscle as elaborated at section 4.2.7.. Dystrophin positive myofibers were then counted to assess the efficiency of cell transplantation in the skeletal muscle of *mdx*/SCID mice.

5.2.4 Statistics

All data are reported as the mean \pm standard deviation (SD) or mean \pm standard error of the mean (SEM), and data analyses have been performed with a Student's t-test for comparisons between two groups as well as with a One-Way ANOVA for comparisons among three or more groups (SPSS Jandel Corporation). For all statistically significant differences observed after a One-Way ANOVA, the appropriate multiple comparison tests have been used to perform a post-hoc analysis. Statistical significance is considered for all *p*-values < 0.05 ; values marked with asterisks (*) and (**) represent $P < 0.05$, $P < 0.01$, respectively.

5.3 RESULTS

5.3.1 Healing after Injury Is Enhanced in FLST/OE Skeletal Muscle

5.3.1.1 Increased regeneration in the injured FLST/OE skeletal muscle

Following laceration, the GMs from WT and FLST/OE mice regenerated as confirmed by visualizing centro-nucleated myofibers and variability of fiber size (i.e., fiber diameter) (**Figure 5-1A**). Regarding the myofiber size, fiber diameters visualized at 7 days after laceration were small, ranging from 5-35 μm . (**Figure 5-1B**). Over time, however, the diameters of regenerating myofibers were increasing and myofibers gradually matured, with the mean diameter of FLST/OE myofibers being significantly larger than that of WT muscle fibers. Compared to WT mice, the mean fiber diameters for FLST/OE mice as measured at post-laceration days 7, 14, and 30 were larger by approximately 25.3% (19.37 ± 0.80 vs. 15.46 ± 0.81 ; $p < 0.01^{**}$), 31.6% (39.77 ± 3.69 vs. 30.22 ± 2.75 ; $p < 0.01^{**}$), 32.5% (45.55 ± 3.03 vs. 34.38 ± 1.56 ; $p < 0.01^{**}$), and 36.3% (64.36 ± 5.4 vs. 47.22 ± 3.49 ; $p < 0.01^{**}$) respectively at 7, 14, 30 days, and 1.5 years after GM laceration, when compared to WT mice (**Figure 5-1C**). The absolute differences (mean diameter of FLST/OE regenerating myofibers minus that of WT regenerating myofibers, green curve) in mean diameters of regenerating myofibers between WT and FLST/OE mice were also increasing (**Figure 5-1C**). Accordingly, healing muscles of FLST/OE mice compared to WT animals contain larger percentage of larger myofibers at each time point. For example, at 7 days 49% of regenerating WT myofibers are smaller than 15 μm , on the contrary, 86% of regenerating

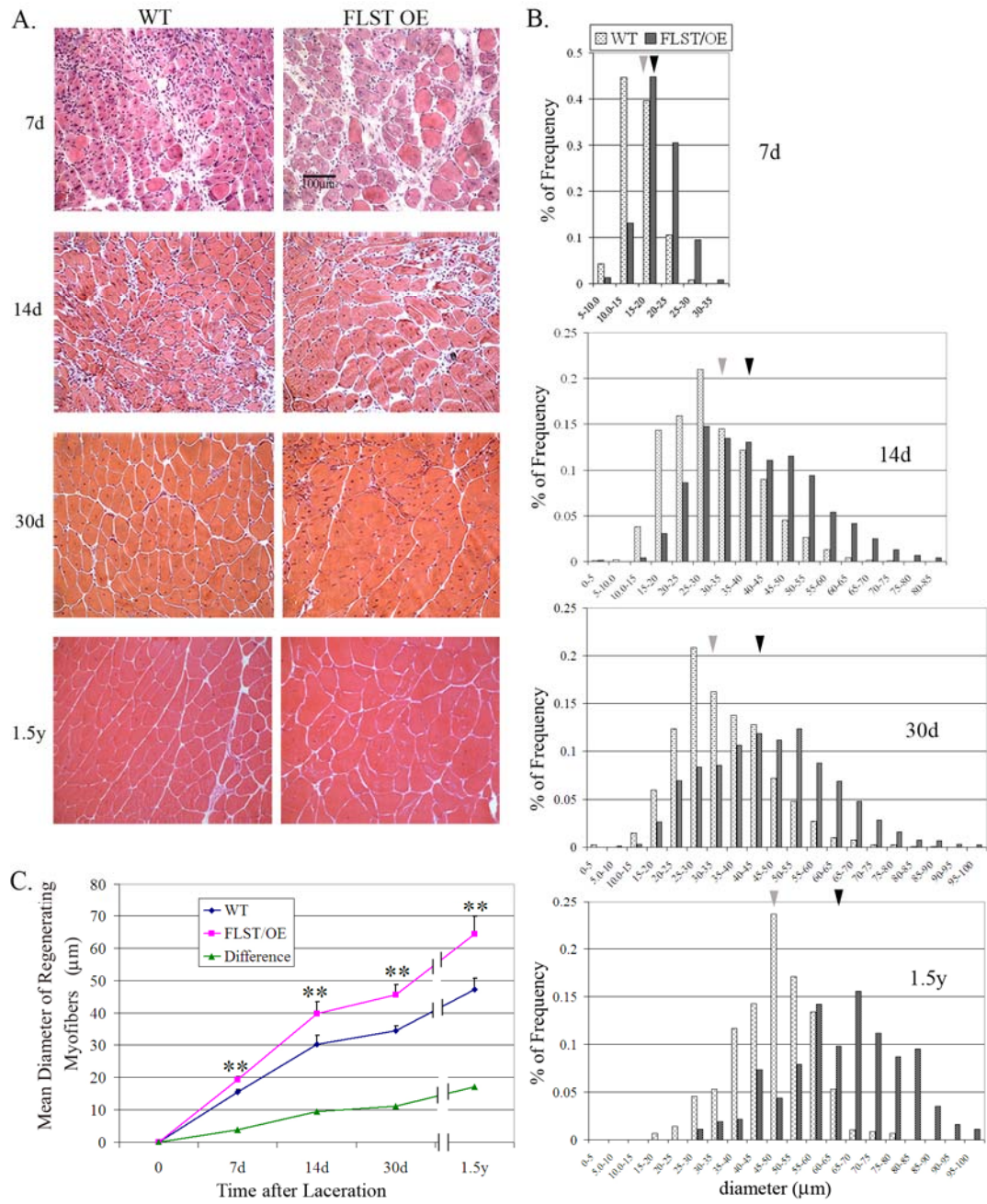


Figure 5-1 Transgenic FLST/OE Skeletal Muscle Exhibited Better Muscle Regeneration after Injury

Injured FLST/OE skeletal muscles showed accelerated regeneration as compared with WT counterparts. A, HE staining of cross section of injured WT and FLST/OE skeletal muscle at 7, 14, 30 days and 1.5 years after laceration injury. Myofibers and nuclei were stained in red and black, respectively. Regenerating myofibers are characterized by centralized nuclei. Black bar represents for 100 μm. B, Distribution of diameters of regenerating myofibers in WT and FLST/OE skeletal muscle 7, 14, 30 days, and 1.5 years after post-injury. Gray bars represent myofibers from WT mice while black bars represent myofibers from FLST/OE mice. Moreover, the gray arrowheads indicates mean diameters of regenerating fibers in WT muscle, while black arrowheads indicates that in FLST/OE muscle. C, Quantitation of diameters of regenerating myofiber. The increases in the mean diameters of regenerating fibers in FLST/OE muscle over that in WT muscle is increasing. (* P < 0.05, ** P < 0.01)

FLST/OE myofibers are larger than 15 μm ; at 14 days, 55% of regenerating myofibers of WT mice are smaller than 30 μm whereas 73% of regenerating myofibers of FLST/OE mice fall in to the category of 30 to 85 μm ; at 30 days, 60% of regenerating myofibers of WT mice are smaller than 35 μm , while 73% of regenerating FLST/OE myofibers larger than 35 μm (**Figure 5-1B**).

5.3.1.2 Decreased fibrosis in the injured FLST/OE skeletal muscle

In addition to noticing differences in myofiber regeneration, we observed significant differences in the deposition of collagenous connective tissue after injury in each group of mice. Specifically at two weeks after laceration, fibrosis developed extensively in WT muscles, but relatively limited in FLST/OE muscles (**Figure 5-2A**). The percentage of fibrosis quantified at 2 weeks post-injury within these tissues, respectively, was $3.54\% \pm 1.71\%$ and $8.71\% \pm 2.36\%$, ($p < 0.01^{**}$) (**Figure 5-2B**). Compared to these values obtained at 2 weeks, our quantification analysis showed a reduction in fibrosis at 4 weeks among GMs of WT and FLST/OE mice (**Figure 5-2 A**); in spite of this, the relative fibrosis formation in WT GMs continued to be significantly larger than FLST OE GM (2.1 ± 1.1 vs. 5.57 ± 1.94 ; $P < 0.01^{**}$) at four weeks post-injury (**Figure 5-2B**). However, fibrosis in both injured GMs of WT and FLST/OE mice disappeared at 1.5 years after injury (data not shown).

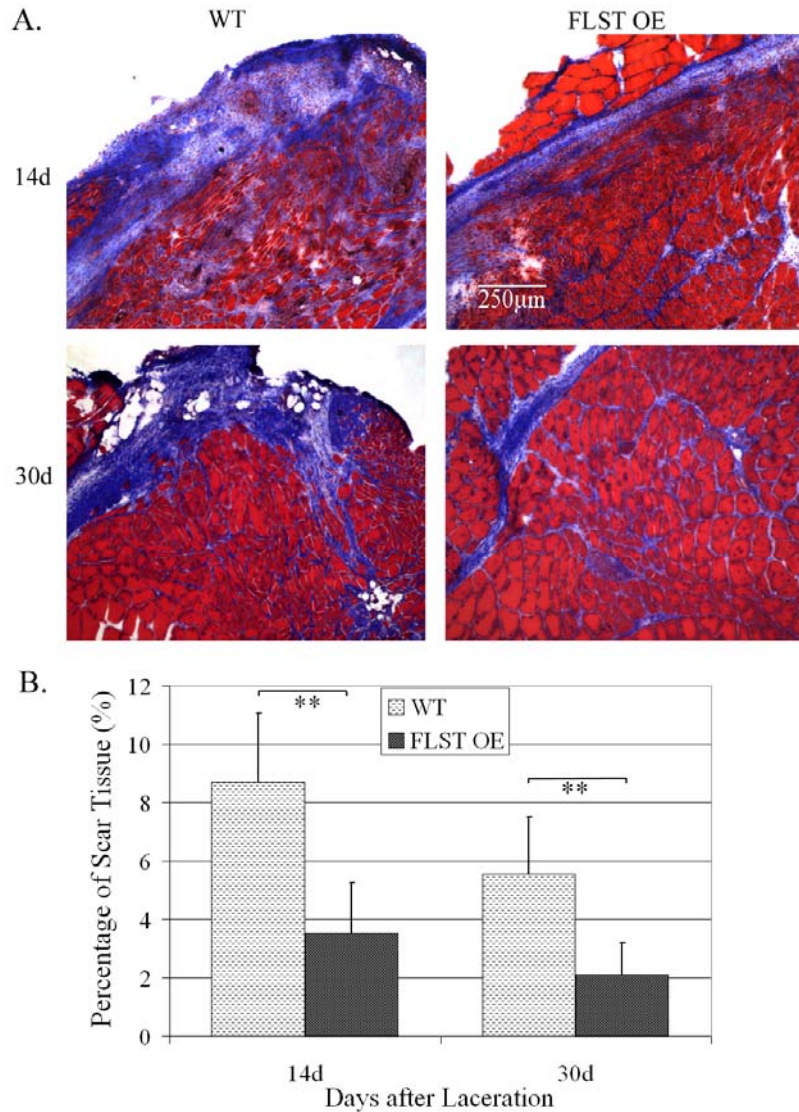


Figure 5-2 The Muscle of FLST/OE Transgenic Mice Developed Less Fibrosis after Injury

Fibrosis in injured FLST/OE muscle was reduced over injured WT muscle. Masson's trichrome staining was performed on sections of injured FLST/OE and WT muscle (myofibers in red; fibrosis in blue). A, Representative images of injured FLST/OE and WT muscle at 14 and 30 days after injury. There is less fibrosis observed in injured FLST/OE muscle than WT muscle. B, Injured FLST/OE muscles developed significantly less fibrosis than did injured WT muscles. (* $P < 0.05$, ** $P < 0.01$)

5.3.1.3 Decreased MSTN and increased vascularity in the injured FLST/OE skeletal muscle

Upon investigating how FLST enhances muscle healing, we found that, in vivo, apart from reported mechanism that FLST's inhibition of MSTN via direct binding^{56, 82}, it also represses MSTN expression in injured FLST/OE muscle. This became apparent at two weeks after injury,

when we noted that FLST/OE muscle expresses less MSTN compared to WT muscle (**Figure 5-3A, B**). Collagen IV (CollIV, green) immunostaining, staining for basal lamina, was used to trace the outline of myofibers. MSTN protein (red) mostly locates in the cytoplasm of regenerating fibers as indicated by CollIV and Centro-nuclei. However, some of MSTN-positive regenerating myofibers lacked the complete basal lamina. When measuring the area and density of MSTN signal in the injured muscles, we found that MSTN signals in the injured FLST/OE muscle were significantly less than observed in WT control. Moreover, it has been found that FLST stimulates angiogenesis both in vitro and in vivo ¹⁷⁹, and a negative correlation has been reported between angiogenesis and fibrosis ¹²⁴. These findings lead us to examine vascularization in the injured FLST/OE and WT muscles. We assessed the vascularity of injured FLST/OE and WT muscles at four weeks following laceration, and observed that FLST/OE muscles have a significantly larger number of CD31-positive microvessels along the zone of injury in comparison to their WT counterparts (**Figure 5-3C, D**). This indicates that increased vascularity may at least be partially responsible for the improved muscle healing that is observed in FLST/OE mice.

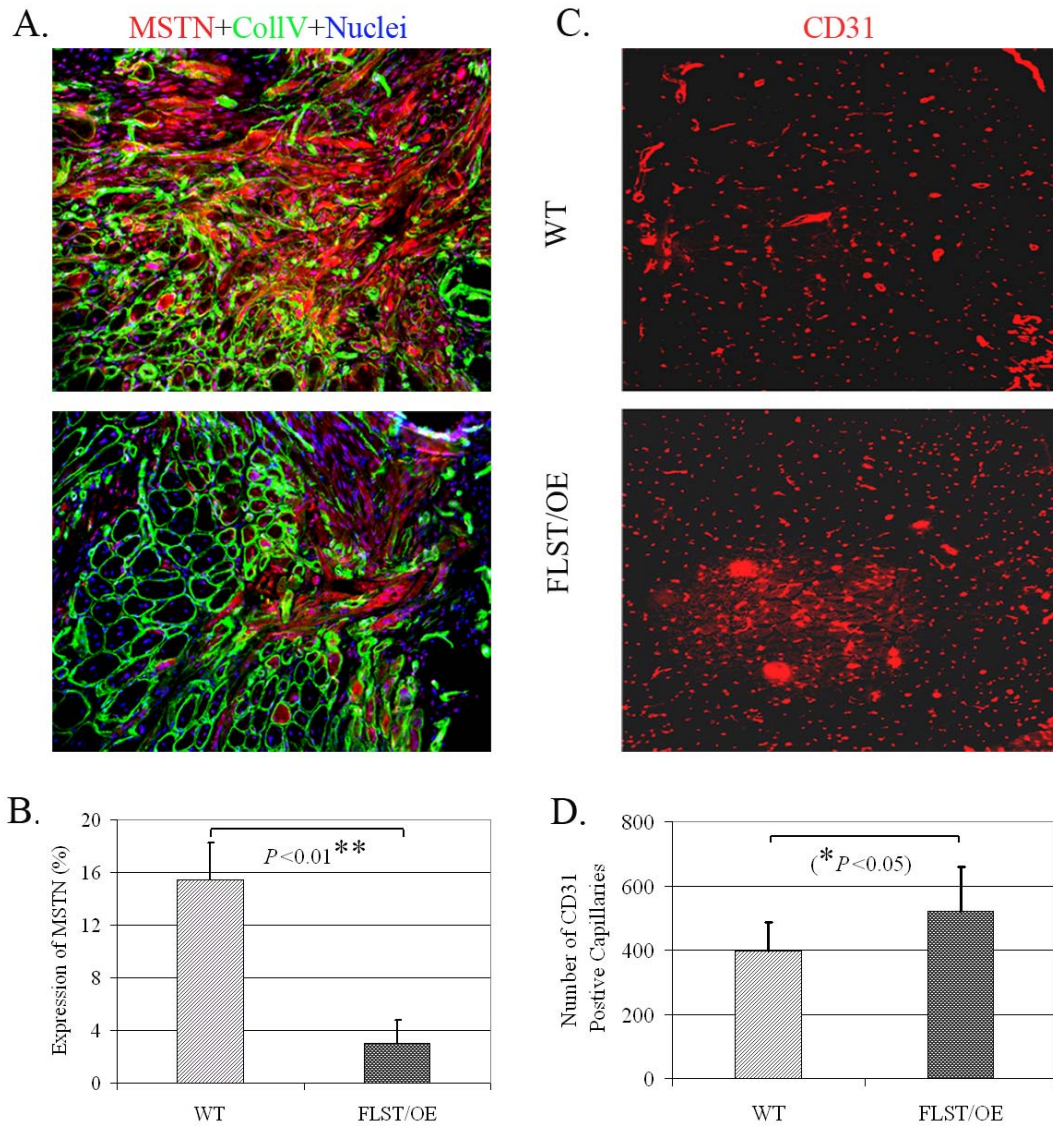


Figure 5-3 Decreased MSTN Expression and Increased Vascularity in Injured FLST/OE Skeletal Muscles

A, Immunohistochemistry was performed to detect MSTN (fluorescence red) and collagen type IV (fluorescence green) expression in injured WT and FLST/OE muscle. Collagen type IV was used to locate basal lamina of myofibers including, necrotic, intact, and regenerating myofibers. MSTN-positive signals were seen with in some of regenerating myofibers with basal lamina and some of myofibers without basal lamina. Injured FLST/OE muscle contained less MSTN staining than did injured WT muscle. B, When we measured the relative area of MSTN positive, we found that there were significantly more MSTN signals detected in injured WT muscle than in injured FLST/OE muscle. C, CD31, an endothelial maker, was stained to monitor capillaries in injured muscle. D, There were a significantly more CD31 positive capillaries in injured FLST/OE muscle than that in injured WT muscle. (* $P < 0.05$, ** $P < 0.01$)

5.3.2 Comparison of WT and FLST/OE-MPCs

5.3.2.1 *In vivo* muscle regeneration of MPCs

Muscle progenitor cells (MPCs) are a population of long-term proliferating cells that regenerate the skeletal muscle of dystrophic mice more efficiently than myoblasts. Since injured FLST/OE muscles underwent better muscle regeneration than did WT controls, FLST/OE MPCs may accordingly be superior to WT MPCs in regenerating muscle. Using a preplate technique that our group has previously described, we isolated these cells from both WT mice and FLST/OE mice and compare their ability to regenerate skeletal muscle in dystrophic muscle. WT- and FLST/OE-MPC populations were injected into GMs of *mdx*/SCID mice, respectively with each population injected into 4 GMs. Quantitation of engraftment with regard to the number of dystrophin-positive myofibers was performed to evaluate cell transplantation efficiency. Despite a high degree of variability in the WT- and FLST/OE-MPCs' abilities to regenerate myofibers *in vivo* (**Figure 5-4A**), there is no WT-MPC population regenerating more than 400 dystrophin-positive fibers, whereas, three of 7 FLST/OE populations regenerated 530 to 810 dystrophin-positive fibers (**Figure 5-4A**); FLST/OE populations are significantly more successful at regenerating dystrophin-positive fibers. Specifically, whereas the WT-MPC population with the greatest amount of dystrophin-positive fiber regenerating was able to regenerate 400 fibers, 3 of 7 FLST/OE populations regenerated between 530 to 810 fibers (**Figure 5-4A**). Overall FLST/OE-MPCs (n = 6) produced significantly larger muscle engraftment than did WT cells (n = 5) (485.5 ± 92.07 vs. 195.6 ± 65.375 ; Mean \pm SEM; $P = 0.023$; t-test) (**Figure 5-4B**). Two representative dystrophin-positive engraftment-derived from FLST/OE- and WT-MPCs (784 vs. 494 dystrophin-positive myofibers), respectively, are shown in **Figure 5-4C**.

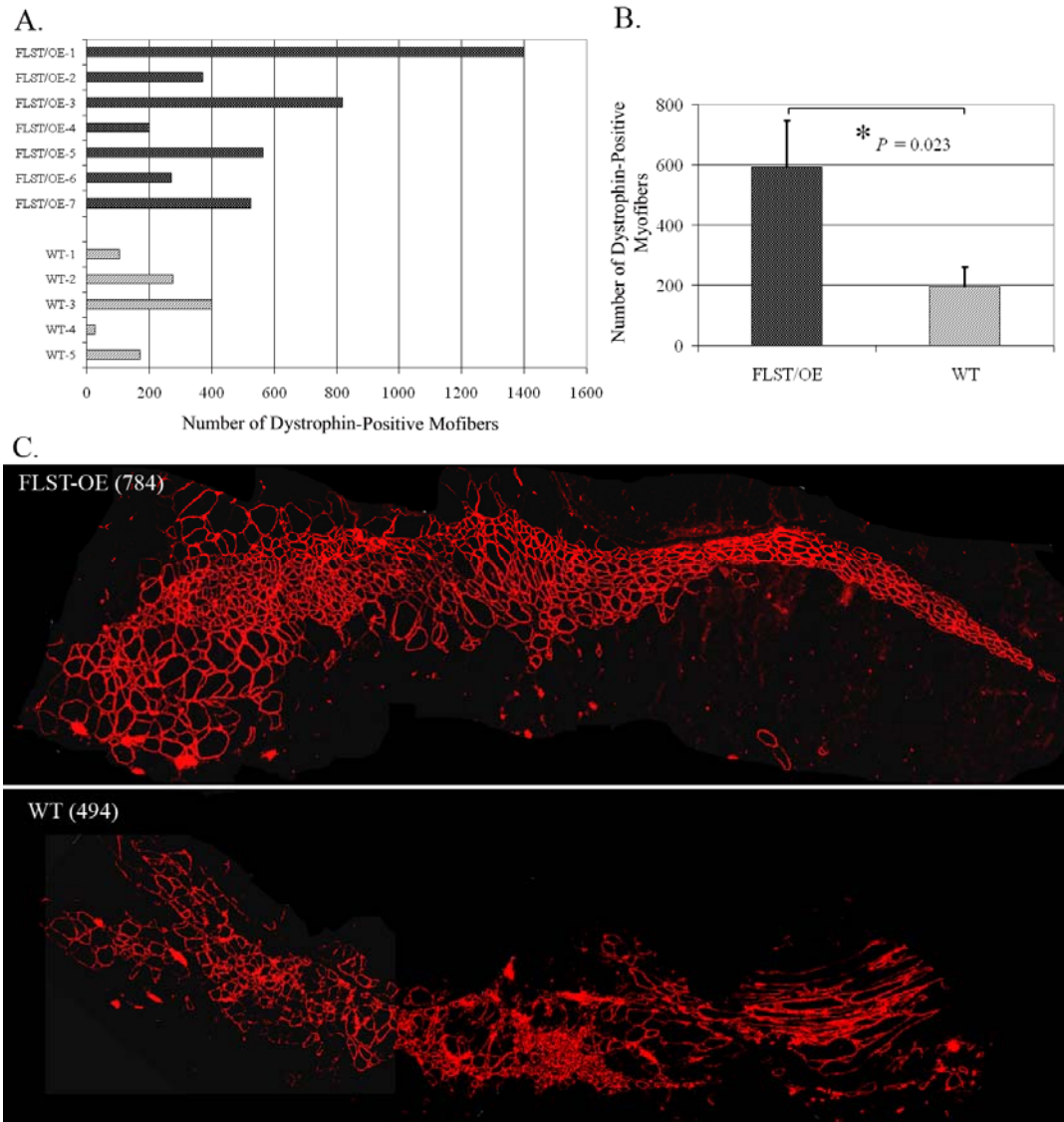


Figure 5-4 FLST OE MPCs Are Superior to WT MPCs in Regenerating Skeletal Muscle

FLST/OE-MPCs regenerated skeletal muscle more efficiently than WT-MPCs, when transplanted into GMs of *mdx*/SCID mice. A, Quantitation of engraftment in terms of number of dystrophin-positive fibers regenerated from FLST/OE- and WT-MPC populations. B, The overall mean dystrophin-positive myofibers was significantly larger for FLST/OE MPCs (592.79 ± 154.9 ; Mean \pm SEM; $n = 7$ FLST/OE-MPC populations; 4 muscles per population) than for WT-MPCs (195.6 ± 65.375 ; Mean \pm SEM; $n = 5$ WT-MPC populations; 4 muscles per population; $P = 0.023^{**}$, *t*-test). C. Representative engraftments showed that transplanted MPCs regenerated dystrophin-positive myofibers (fluorescence red) within dystrophic muscle. FLST/OE-MPCs produced more dystrophin-positive myofibers than did WT-MPCs. (* $P < 0.05$, ** $P < 0.01$)

5.3.2.2 *In vitro* characterization of MPCs

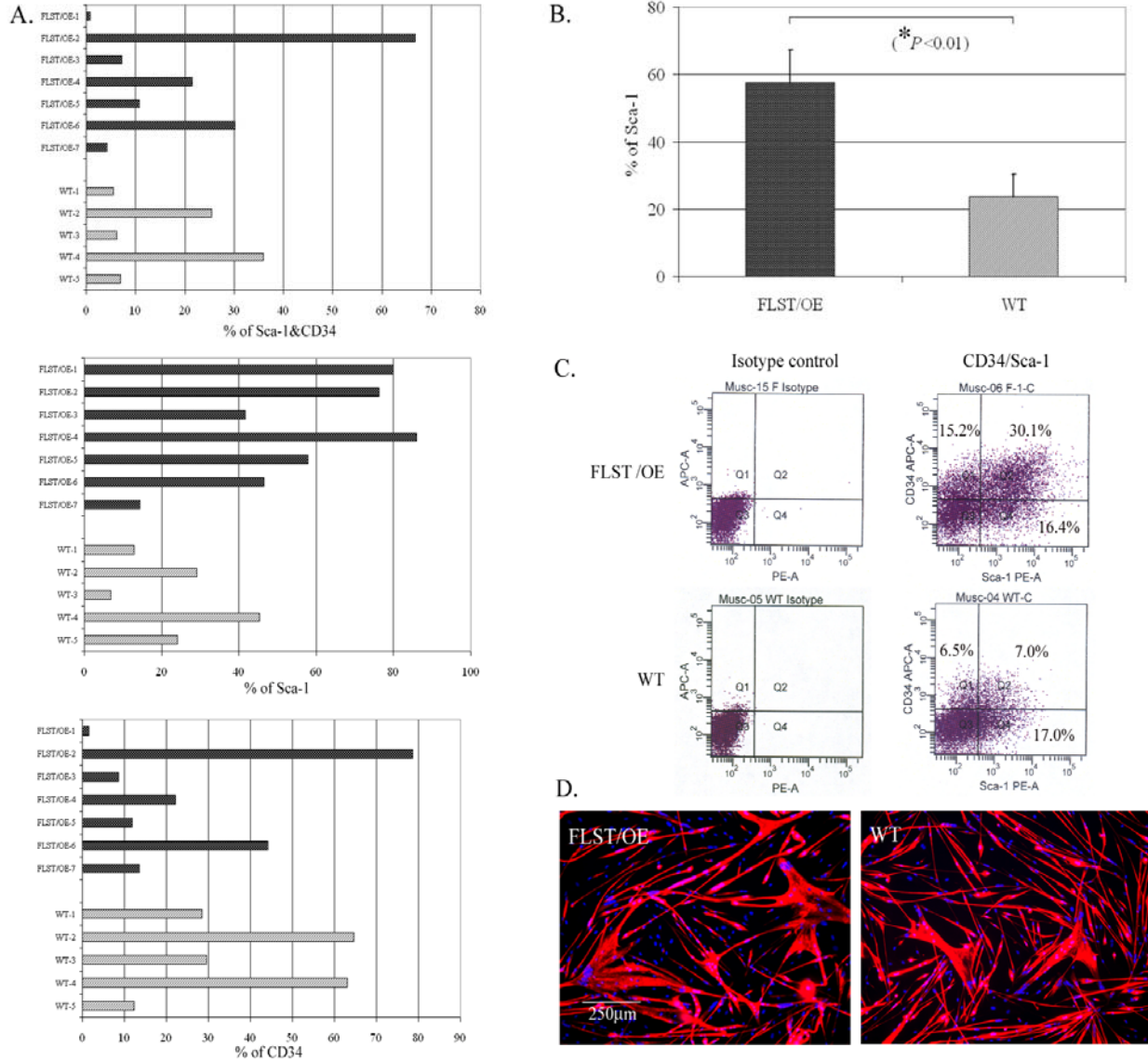


Figure 5-5 *In Vitro* Characterization of WT- and FLST/OE-MPCs

Seven FLST/OE- and 5 WT-MPC populations were examined for Sca-1 expression, CD34 expression, and *in vitro* myogenic differentiation. A, Histograms are showing wide variability in percentages of Sca-1+&CD34+ Sca-1+, and CD34+ cells among MPC populations. B, Quantitation revealed a significant increase in Sca-1+ fraction in FLST/OE-MPC population as compared with WT-MPC populations. C, Images on the left side are isotype control; images on the right side are representative images of flow plot showing that FLST/OE-MPC populations consist of large proportion of Sca-1+ cells than its WT counterpart (46.5% vs. 24%); D, Both FLST/OE- and WT-MPC populations underwent myogenic differentiation as labeled by MyHC (fluorescence red) and Dapi (blue).

To further characterize WT- and FLST/OE- MPCs, we use flow cytometry and immunocytochemistry to analyze the expressions of stem cells (i.e., Sca-1, CD34) and myogenic cell (Desmin) markers by these cells, respectively, and also determined proliferation and myogenic differentiation capacity of cell populations. From the histograms (Sca-1+&CD34+, +Sca-1+, and CD34+) in **Figure 5-5**, the heterogeneous profile of stem cell markers is apparent; cell populations within either FLST/OE or WT group exhibit great variation in the percentages of stem cell marker positive cells. Compared to WT-MPC populations, however, FLST/OE populations possess a significant larger percentage of cells that are positive for Sca-1 (**Figure 5-5 A.B**). The representative images of flow plot showed that one FLST/OE-MPC and one WT-MPC population contained 46.5% and 24% Sca-1 positive cells, respectively (**Figure 5-5 C**). In the low serum containing medium, both FLST/OE- and WT-MPC cells were capable of differentiating and fusing into myotubes as labeled by myosin heavy chain (MyHC) (**Figure 5-5 D**). The percentage of desimin-positive cells, proliferation, and myogenic differentiation capacity were compared between FLST/OE- and WT- MPC population, however, due to a broad variability, no significant difference was found (data not shown).

5.4 DISCUSSION

In this study, we show that the skeletal muscle healing of GMs among FLST/OE mice is superior to that of the GMs among WT mice. Specifically, the mean diameter of regenerating myofibers in injured FLST/OE muscle remain significantly larger than WT counterparts, while fibrosis was significantly lower in the former; these results are comparable to those that we previously obtained for injured MSTN^{-/-} GMs¹²⁷. There are several explanations for this that can be

derived from our results. These include the impact that FLST has on a) downregulating the expression level of MSTN and augmenting vascularity in injured muscle, b) enhancing the ability of MPCs to regenerate skeletal muscle. Although we will discuss these events individually, we highlight that they are not mutually exclusive of one another, but rather, illustrate how FLST can synergistically promote healing through each of these processes.

5.4.1 Mechanism Involved in the Reduced Fibrosis in the Injured FLST/OE Muscle

TGF- β 1 expression in injured skeletal muscle is time dependent; it peaks at 3-5 days and 10-14 days post-injury^{16, 26, 180}. The latter event appears to associate with the formation of fibrosis and ineffective muscle regeneration¹⁶. Blocking the second peak of TGF- β 1 by administering antifibrotic agent at 14 days post-injury led to histological and physiological improvement of injured muscle^{16, 28-32, 148, 149}. Coincidentally, our *in vivo* studies show significant decrease in MSTN immunostaining among injured FLST/OE GMs at 2 weeks after injury. Similar to our previous findings¹²⁷, some small regenerating myofibers without basal lamina were strongly MSTN signal positive in the injured WT and FLST/OE GMs. Li et al reported that some regenerating myofibers appeared to degrade and transform into myofibroblasts to aggravate fibrosis in the injured skeletal muscle¹⁶. If it is the case, these MSTN-positive, lacking basal lamina regenerating fibers may represent a transitional status of regenerating myofibers that are undergoing the differentiation process into myofibroblasts. The decrease in the amount of MSTN at the injured site probably partially account for reduced fibrosis in injured FLST/OE muscle for following reasons: a) there is less MSTN available to trigger fibrosis in injured muscle, b) due to the fact that TGF- β 1 request MSTN's synergistic action to induce fibrosis in muscle¹²⁷, reduced

amount MSTN may reduce TGF- β 1's pro-fibrotic effect. This result also indicates that, in addition to directly inhibiting MSTN, FLST may further decrease the expression of this protein.

Furthermore, while prior reports indicate that FLST upregulates angiogenesis both *in vivo* and *in vitro*, we show that there is significantly more vascularization occurring in injured FLST/OE muscle compared to WT controls¹⁷⁹. As FLST can be expressed by endothelial cells that are activated but not quiescent, these data on the impact of FLST on the cell cycle and angiogenesis are certainly¹⁸¹. It is thereby also noteworthy to point out that angiogenesis correlates with an increase in muscle regeneration and a decrease in fibrosis¹²⁴. Presently, however, there is insufficient evidence to indicate whether FLST directly stimulates angiogenesis in injured skeletal muscle.

5.4.2 Cellular Mechanism by Which FLST Promotes Skeletal Muscle Regeneration after Injury

The development of skeletal muscle during embryogenesis and its regeneration after trauma or in the setting of skeletal muscle disease is largely occurs from the differentiation of satellite cells into myofibers¹⁸²⁻¹⁸⁴. Adult satellite cells enter cellular quiescence within a niche between the basal lamina and sarcolemma of myofibers, thereby forming a pool of myogenic progenitor cells¹⁸⁵. In response to muscle trauma and during disease, these cells are activated to re-enter the cell cycle, migrate from the basal lamina to the zone of injury, and undergo asymmetric divisions. A preponderance of daughter cells are committed to differentiate and fuse into multinucleated myofibers, while a small portion of self-renewing cells replenish the reservoir of satellite cells by re-entering quiescence.

MSTN inhibits satellite cell self-renewal by downregulating the G1 to S progression and retaining satellite cells in a quiescent status^{47, 186}; inversely, MSTN^{-/-} skeletal muscle comprise more satellite cells than WT counterparts, likely resulting from an increase in proliferation and a delay in myogenic differentiation among adult MSTN^{-/-} satellite cells⁴⁷. Based on this information, we sought to determine the impact of FLST on MPCs. MPCs are a heterogeneous population consisting of myoblasts, satellite cells, progenitor cells, and stem cells, which were isolated from the GMs of both FLST/OE and WT mice with the modified pre-plate technique. As the number of dystrophin-positive myofibers is a standard by which the regenerative efficiency of transplanted cells in dystrophic skeletal muscle is measured,^{125, 126, 128} we performed such a comparison between both populations of MPCs. After injecting MPCs isolated from FLST/OE and WT mice into the GMs of *mdx*/SCID mice, we found that overall, FLST/OE-MPC populations regenerate significantly more dystrophin-positive myofibers; however, not all FLST/OE-MPC populations outperformed their WT counterparts. Variation regarding to the regenerative capacity of both types cells is remarkable. Specifically, dystrophin-positive fibers regenerated from FLST/OE-MPC population vary from 200 to 1398, while those produced from WT-MPC populations varying from 27 to 400. The increase in regenerative capacity of FLST/OE MPC populations probably partially accounts for the better regeneration in the injured FLST/OE muscle than WT muscle. These finding may help researchers to develop optimal cell population for cell-based therapy to Duchene Muscular Dystrophy, a lethal sex-linked recessive, muscle-wasting disease stemmed from a mutation of the dystrophin gene. For instance, transplantation of muscle cells carrying FLST transgene into the dystrophic muscle may enhance the success of cell transplantation in comparison to that of normal muscle cells.

We further investigate whether marker profile, proliferation rate, and myogenic differentiation capacity of MPCs can render a clue to their *in vivo* performance. While it is important to note that the regenerative ability of each MPC populations varies, this was true for myoblasts, satellite cells, progenitor cells, and stem cells collectively ¹²⁶. Our group previous found that regenerative capacity of muscle primary cells appears to be negatively related to the level of their *in vitro* myogenic commitments when they compared different fractions among the same muscle primary cell population ¹²⁸. Moreover, they further showed that the CD34+ fraction of MPCs showed significantly improvements in dystrophin restoration after transplanted into dystrophic muscle, when compared to CD34- fraction of the same MPC population ¹²⁸. Nevertheless, these criteria can not be applied to this current study, since we are comparing cell performances among MPC populations isolated from different mice. We instead found that MPC populations isolated from both types of mice exhibited a broad heterogeneity of cell surface markers, proliferation rate, and myogenic capacity *in vitro*. In spite of this heterogeneity, the FLST/OE-MPC populations contain a significantly larger percent of Sca-1+ than WT control. However, our results suggest that the degree of *in vitro* myogenic commitment, proliferation rate, and expression levels of stem cell, and myogenic marker can not be use to predict cell's *in vivo* performance among different cell populations. It is consistent with data collected by others in our group ¹²⁶. Neither myogenic and stem cell marker profile of cells, nor *in vitro* differentiation capacity of cells does appear to correspond to their performance in regenerating dystrophin-positive myofibers ¹²⁶.

5.5 CONCLUSION

We conclude that FLST has great therapeutic potential for the treatment of injured skeletal muscle, as it enhances skeletal muscle healing by inhibiting MSTN. This is illustrated through experiments in which there is an increase in skeletal muscle regeneration and a decrease in fibrosis along the zone of injury among FLST/OE mice, as well as in experiments where MSTN expression is down-regulated in FLST/OE muscles after injury. As expected from these findings, we show that injured FLST/OE muscles undergo significantly more CD31 positive capillary-like structure as compared to controls, and that FLST/OE MPCs have a superior regenerative capacity compared to WT-MPCs.

6.0 OVERALL CONCLUSION

Theoretically, the therapeutic strategy for treating injured skeletal muscle includes down-regulating muscle degeneration, inflammation, up-regulating regeneration, and inhibiting fibrosis. The goals of our projects were to enhance our understanding of the mechanisms involved in the injured skeletal muscle, and to promote the development of biological approaches to improve skeletal muscle healing. We have found that MSTN, a negative regulator of adult skeletal muscle growth, contributes to the formation of fibrosis in injured skeletal muscle. MSTN does not independently induce fibrosis in the skeletal muscle; instead, MSTN and TGF- β 1 appear to synergistically stimulate fibrosis. The following is a list of supporting facts which demonstrate this synergy: 1) MSTN and TGF- β 1 share a TGF- β -like signal transduction pathway^{64, 65}; 2) MSTN and TGF- β 1 reciprocally stimulate myoblasts to express one another; and 3) Blocking the TGF- β 1 signal pathway compromises MSTN's activity, and vice versa; moreover, decorin, which has been known to block fibrosis by inhibiting TGF- β 1, also counteracts the activity of MSTN. Based on this background knowledge and our recent findings, we used MSTN as a therapeutic target to develop biological approaches to improve skeletal muscle healing after injury by inhibiting the action of MSTN.

We found that both MPRO and FLST can effectively inhibit MSTN, which results in improved skeletal muscle healing after injury by enhancing muscle regeneration and inhibiting fibrosis. Blocking MSTN signaling can significantly enhance the regenerative capacity of donor

muscle cells transplanted into the skeletal muscles of *mdx*/SCID mice, by either blocking MSTN expression in the donor cells, which can be done by utilizing muscle progenitor cells (MPC's) isolated from MSTN^{-/-} mice or from FLST/OE mice, or by blocking MSTN expression in the recipient muscle. In conclusion, our results have elucidated that MSTN is an effective therapeutic target for the injured and diseased skeletal muscle, and demonstrated that MPRO and FLST are capable of neutralizing MSTN and improving skeletal muscle healing. Nevertheless, several questions still need to be addressed in the future.

6.1 FUTURE DIRECTION AND LIMITATION

6.1.1 Determine If Blocking MSTN in Injured Skeletal Muscle Leads to Functional Recovery

In the current study we used two histological variables to evaluate the quality of muscle healing, the mean diameter of regenerating myofibers and the percentage of fibrosis. Our results suggested that blocking MSTN signaling improved the healing of injured skeletal muscle when compared to control, as indicated by the enhancement of regeneration and reduction of fibrosis; however, physiological improvements have not yet been determined. It is important to realize that histological improvements do not necessarily correlate with physiological performance. Our group has shown that both insulin-like growth factor-1 (IGF-1) and decorin are capable of enhancing skeletal muscle healing histologically and physiologically. When IGF-1 and decorin were used in combination on injured skeletal muscle, a further improvement was seen histologically, but not functionally²⁸. Another group reported that MSTN blockade increased fiber size, muscle mass, and absolute force, but histopathologically degenerative foci and serum

creatine kinase levels remain unchanged, in a murine model of limb-girdle muscular dystrophy 2C¹⁶². The reasons for the disparity between histological and physiological improvement remain unclear; although, several studies demonstrated that inhibiting MSTN improves muscle function and strength in *mdx* mice^{77, 123, 151, 157}. Future experiments, should utilize physiological testing, such as specific peak force and tetanic force as described previously^{28, 29} to investigate whether blocking MSTN promotes the functional recovery of injured skeletal muscle.

6.1.2 Correlation between Angiogenesis and Improved Muscle Healing

Our data demonstrated an increase in the number of CD31 positive capillary-like structures in the injured skeletal muscle in MSTN^{-/-} mice, AAV-MPRO transduced muscle, and FLST/OE mice. These muscles also showed improvement in skeletal muscle healing when compared to their WT counterparts, which suggests that MSTN appears to inhibit the in-growth of CD31 positive capillary-like structures in the injured skeletal muscle and that MPRO and FLST block MSTN thereby stimulating angiogenesis. In future studies, we need to investigate how MSTN regulates endothelial cell proliferation, migration, and synthesis of vascular endothelial growth factor (VEGF). Using an *in vitro* angiogenesis model, we can investigate whether MSTN has the ability to down-regulate endothelial cells to form von willebrand factor (vWf)-positive capillary-like tubular networks on three dimensional (3D) collagen gel, which will greatly help us to understand the role of MSTN in angiogenesis^{187, 188}. Also in future studies, we will develop techniques to monitor 3D vasculature in the skeletal muscle utilizing a commercially available contrast agent (Fenestra VC™) to quantify vascularization in live animals with our micro computed tomography scanner (VivaCT)). Alternatively, we could use a barium-gelatin mixture as the contrast agent to measure vascularization post-mortem. Micro-CT data can be used to

monitor the vascular supply and indirectly measure the area of fibrosis (non-vascularized area) and can be correlated with histological findings. The evidence that MSTN^{-/-} mice develop a more vascularized network in injured skeletal muscle than WT controls will strongly support the hypothesis that blocking MSTN enhances angiogenesis in skeletal muscle after injury.

6.1.3 Limitation

To the best of our knowledge, MSTN is mainly expressed in the skeletal and cardiac muscle⁴⁹. If it is the case, our findings that MSTN is a fibrotic stimulator, and that MPRO and FLST inhibit MSTN, thereby reducing fibrosis in the injured skeletal muscle may not be applied in other tissues. That is, we don't suggest that our results will be applied to different organs and tissues such as lung, liver, kidney, and skin, which may not express MSTN. Surprisingly, MSTN blockade appears not to attenuate cardiac fibrosis in the *mdx* mice¹⁸⁹. Nevertheless, more evidence showed that MSTN may promote fibrosis in other tissues besides skeletal muscle¹⁹⁰,¹⁹¹. MSTN stimulates synthesis of collagen and TGF- β 1, and phosphorylation of Smad2/3 in C3H 10T1/2 cells, a multipotent mesenchymal mouse cell line¹⁹⁰; FLST blocks MSTN's fibrotic effects on C3H 10T1/2 cells¹⁹⁰. Moreover, MSTN appears to play a role in the Peyronie's disease (PD) characterized by deformity and painful erection¹⁹¹, in which the cavernous body of the penis is encircled by patches or strands of dense fibrous tissue, which mainly mediated by TGF- β 1. The expression level of MSTN was upregulated in the myofibroblasts of the PD plaque as compared to normal tunica albuginea (TA), and MSTN cDNA injected in the normal (TA) led to a fibrotic PD plaque and aggravated the TGF β 1-induced lesion¹⁹¹. Take together, the fibrotic role of MSTN in the different organs and tissues warrants further investigation.

APPENDIX A

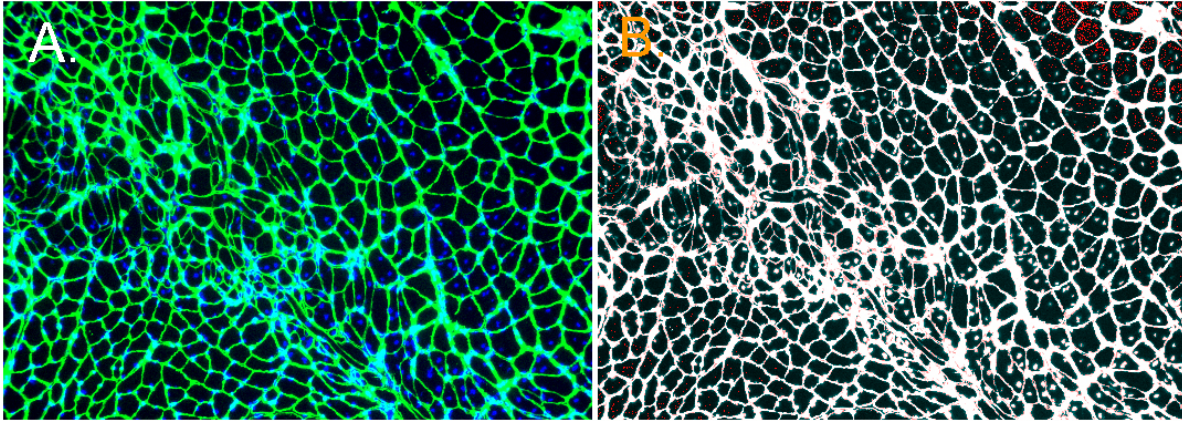
DIAMETER ANALYSIS OF REGENERATED MYOFIBERS USING NORTHERN ECLIPSE

A.1 PHOTOGRAPH FOR SECTIONS WITH IMMUNOHISTOCHEMICAL STAIN

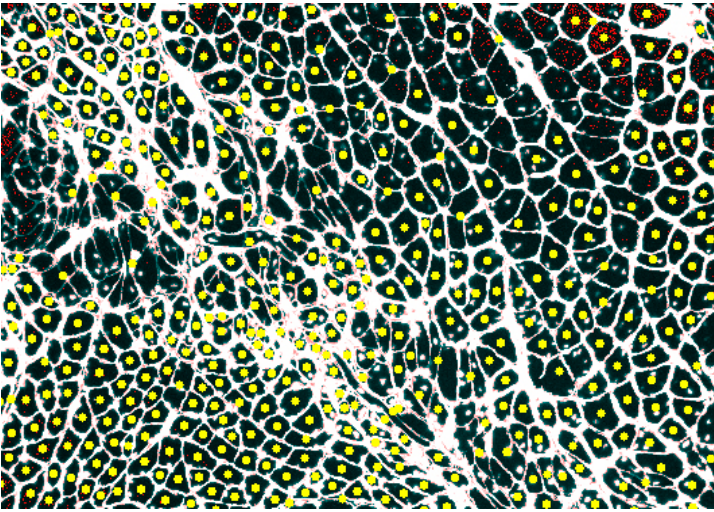
1. Open Northern Eclipse software.
2. Go to **View** to select **User Window** opening “merge window”
 - 1) to select **colors** from “merge window” checking “green” (basal lamina) and “blue” (nuclei) box
 - 2) to chose **loop**
3. Select 10x objective lens from fluorescence microscope, focusing and choosing green and blue filter subsequently to take merged image (green and blue)

A.2 ANALYSIS OF REGENERATED MYOFIBER DIAMETER

1. Go to **View** to select **View Options**
 - 1) Bin (new bin with limited condition: Check “Include these objects” to check new bin, uncheck Default)
 - 2) **Data**: Chose right parameters such as “object Count”, “Minimum axis diameter”
2. Go to **Process** to choose **Conversions** to convert image to 8 bit grayscale
3. * **Threshold** (Monochrome threshold for 8 bit gray image)
4. Go to **Measure** > **Selection Tool** to select the area that you want to measure
5. Go to **View** > **Data** to set “Objects partially inside selection” are “Excluded from selection”
6. Optimize condition using New Bin, based on value of measurement.
7. **View** > **View Options** > **Selection** to set **Object Marker** as yellow dot
8. Click on **Measure** button in Toolbar
9. **LOG to DDE** to export data to Excel spreadsheet



Appendix Figure A. 1 Collagen IV immunohistochemistry stain (green) for basal lamina of regenerated myofibers (A); Image threshold in 8 bit grey (B) using Northern Eclipse software.



Appendix Figure A. 2 Measurement of minimal diameter of regenerated myofibers. Yellow dots in the center of myofiber mean the selected myofibers

Note: 3* the function in this application is used to distinguish the basal lamina of myofibers from background. The value of intensity corresponding to the grayness varies from 0 to 255. When we alter the values, the selected pixels (basal lamina) are shown in red/white, while unselected pixels (background) are indicated in cyan/black.

APPENDIX B

PROCEDURES FOR QUANTIZATION OF FIBROSIS FORMATION USING NORTHERN ECLIPSE

Images of injured muscle stained with Masson's Trichrome stain were photographed with a microscope digital camera system using Qcapture software.

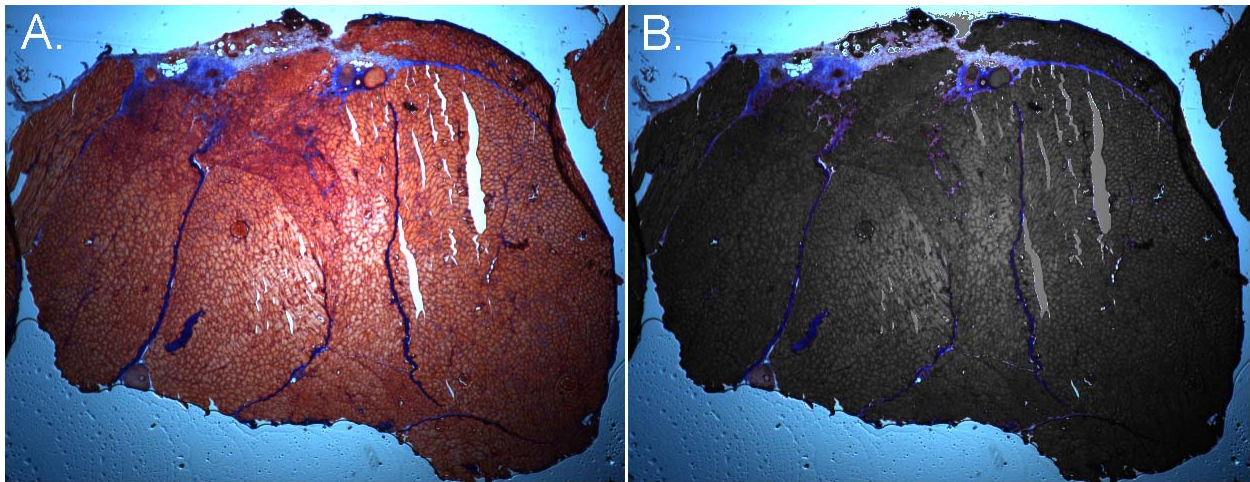
B.1 TAKING BRIGHTFIELD IMAGE AND MASSON'S TRICHROM STAINING

1. Move the beam under camera to the middle position (which should be moved to the left side for fluorescence picture).
2. Open Qcapture software
3. Chose a blank area from slide for white balance
4. Move slide to find area of interest
5. Go **Acquire** and open **Living Preview**
6. Use **Camera Setting** in **Acquire** to adjust color of picture
7. Use **Snap** in **Acquire** to take picture

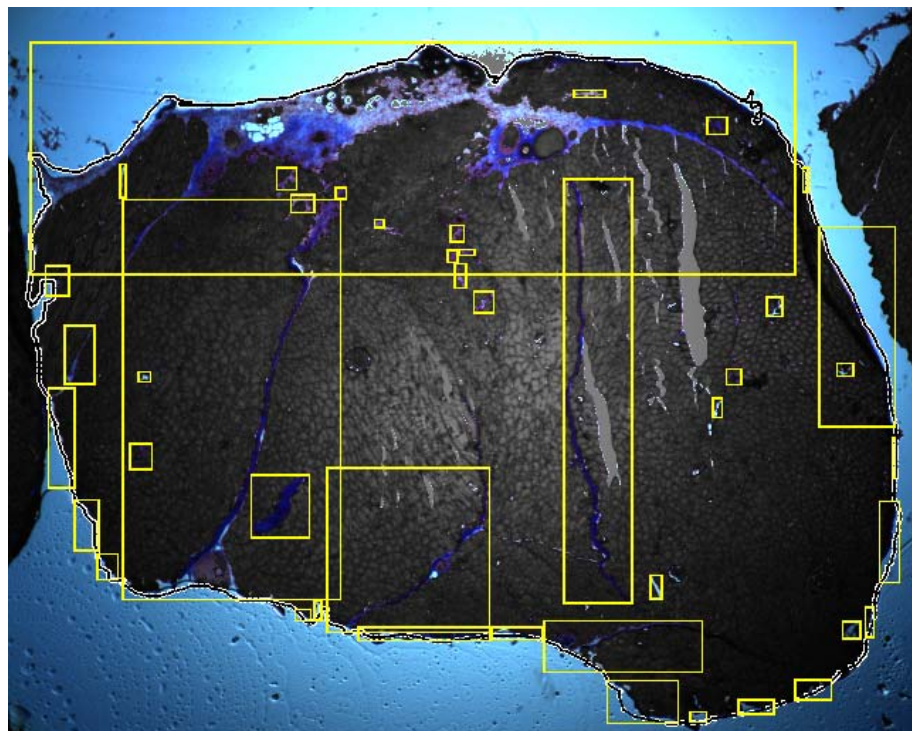
Notes: Images of entire cross-sectional muscles were taken under 2x objective lens to so that entire muscle section was included.

B.2 ANALYSIS OF FIBROSIS FORMATION USING NORTHERN ECLIPSE

1. Open **Northern Eclipse**
2. Open your file and use **Zoom** to adjust size of image (Typically, 50% of image is chosen)
3. Go **Threshold** (color (24 bit) thresholding) to change **RGB model** to **HSV Model** (Hue, Saturation, Value). The muscle fibers turn to be grey, while the collagenous tissue remains blue. And then adjust **Hue, Saturation, Value** separately so that the collagenous tissue area is identical to that in original image (Appendix Figure B.1).
5. Go to **Measure**, **Selection Tool** , and then choose **Trace Tool** to draw a line along the edge of the muscle cross section. Measurement area is cut by selection, meaning that only area selected was measured (Appendix figure B.2)
6. Use Square tool to select bands of interest
7. Click on **Measure** button in Toolbar.
8. **LOG to DDE** to export data to Excel spreadsheet



Appendix Figure B. 1 Image of injured muscle cross section (A), same image in HSV model



Appendix Figure B. 2 Measurement of scar tissue area (9.3426%)

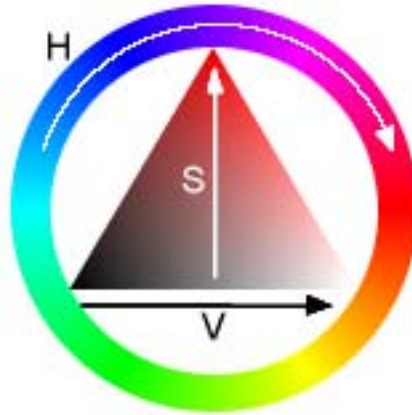
Note:

Threshold is used to distinguish targeted objects from the rest of image by specifying range(s) of values such as hue, saturation, brightness.

HSV is a distinct color space from RGB (red, green, blue), which is non-linear transformation of RGB. Compared to RGB, HSV is more representative for the way that humans perceive color.

Hue refers to the color type arranging from red through the yellows, green, blues, and violets:

- ❖ Ranges from 0-360 (but normalized to 0-255 in Northern Eclipse)
- Saturation indicates the vibrancy of the color:
 - ❖ Ranges from 0-100% (but normalized to 0-255 in Northern Eclipse)
 - ❖ The saturation of a color is correlated to the “grayness”. When the saturation of a color is low, correspondingly, the faded color will appear as a result of low grayness. This function is use to define desaturation as the qualitative inverse of saturation.
- Value depicts the brightness of color:
 - ❖ Ranges from 0-100% (but normalized to 0-255 in Northern Eclipse)



Appendix Figure B. 3 HSV color space as a color wheel

[Http://en.wikipedia.org/wiki/HSV_color_space](http://en.wikipedia.org/wiki/HSV_color_space)

As shown in Appendix Figure B.3 the hue is illustrated by a circular region; Saturation and value are stood for by a triangle region with a vertical axis indicating saturation and horizontal axis representing value. When we do threshold, we began with selecting the hue (color) from the circular region, then pick the optimal saturation and value from the triangular area. The resultant result is shown in appendix Figure B. 1-B.

BIBLIOGRAPHY

1. McLennan IS: Inhibition of prostaglandin synthesis produces a muscular dystrophy-like myopathy, *Exp Neurol* 1985, 89:616-621
2. McLennan IS: Characterization of a prostaglandin dysfunction myopathy, *Muscle Nerve* 1987, 10:801-809
3. Shen W, Li Y, Tang Y, Cummins J, Huard J: NS-398, a Cyclooxygenase-2-Specific Inhibitor, Delays Skeletal Muscle Healing by Decreasing Regeneration and Promoting Fibrosis, *Am J Pathol* 2005, 167:1105-1117
4. Obremsky WT, Seaber AV, Ribbeck BM, Garrett WE, Jr.: Biomechanical and histologic assessment of a controlled muscle strain injury treated with piroxicam, *Am J Sports Med* 1994, 22:558-561
5. Mishra DK, Friden J, Schmitz MC, Lieber RL: Anti-inflammatory medication after muscle injury. A treatment resulting in short-term improvement but subsequent loss of muscle function, *J Bone Joint Surg Am* 1995, 77:1510-1519
6. Rantanen J: Effects of therapeutic ultrasound on the regeneration of skeletal muscle myofibers after experimental muscle injury, *Am J Sports Med* 1999,
7. AOSSM RCot: Hyperbaric oxygen therapy in sports, *Am J Sports Med* 1998,
8. Lehto M, Jarvinen M, Nelimarkka O: Scar formation after skeletal muscle injury. A histological and autoradiographical study in rats, *Arch Orthop Trauma Surg* 1986, 104:366-370
9. Jarvinen M, Sorvari T: Healing of a crush injury in rat striated muscle. 1. Description and testing of a new method of inducing a standard injury to the calf muscles, *Acta Pathol Microbiol Scand [A]* 1975, 83:259-265
10. Menetrey J, Kasemkijwattana C, Day CS, Bosch P, Vogt M, Fu FH, Moreland MS, Huard J: Growth factors improve muscle healing in vivo, *J Bone Joint Surg Br* 2000, 82:131-137
11. Kasemkijwattana C, Menetrey J, Somogyl G, Moreland MS, Fu FH, Buranapanitkit B, Watkins SC, Huard J: Development of approaches to improve the healing following muscle contusion, *Cell Transplant* 1998, 7:585-598

12. Kasemkijwattana C, Menetrey J, Bosch P, Somogyi G, Moreland MS, Fu FH, Buranapanitkit B, Watkins SS, Huard J: Use of growth factors to improve muscle healing after strain injury, *Clin Orthop Relat Res* 2000, 272-285
13. Kasemkijwattana C, Menetrey J, Day CS, Bosch P, Buranapanitkit B, Moreland MS, Fu FH, Huard J: Biological interventions in muscle healing and regeneration., *Sports Med Arthrosc Rev* 1998, 95-102
14. Carlson BM, Faulkner JA: The regeneration of skeletal muscle fibers following injury: a review, *Med Sci Sports Exerc* 1983, 15:187-198
15. Lehto M, Duance VC, Restall D: Collagen and fibronectin in a healing skeletal muscle injury. An immunohistological study of the effects of physical activity on the repair of injured gastrocnemius muscle in the rat, *J Bone Joint Surg Br* 1985, 67:820-828
16. Li Y, Foster W, Deasy BM, Chan Y, Prisk V, Tang Y, Cummins J, Huard J: Transforming growth factor-beta1 induces the differentiation of myogenic cells into fibrotic cells in injured skeletal muscle: a key event in muscle fibrogenesis, *Am J Pathol* 2004, 164:1007-1019
17. Border WA, Noble NA: Transforming growth factor beta in tissue fibrosis, *N Engl J Med* 1994, 331:1286-1292
18. Lijnen PJ, Petrov VV, Fagard RH: Induction of cardiac fibrosis by transforming growth factor-beta(1), *Mol Genet Metab* 2000, 71:418-435
19. Waltenberger J, Lundin L, Oberg K, Wilander E, Miyazono K, Heldin CH, Funai K: Involvement of transforming growth factor-beta in the formation of fibrotic lesions in carcinoid heart disease, *Am J Pathol* 1993, 142:71-78
20. De Bleser PJ, Niki T, Rogiers V, Geerts A: Transforming growth factor-beta gene expression in normal and fibrotic rat liver, *J Hepatol* 1997, 26:886-893
21. Bernasconi P, Torchiana E, Confalonieri P, Brugnoli R, Barresi R, Mora M, Cornelio F, Morandi L, Mantegazza R: Expression of transforming growth factor-beta 1 in dystrophic patient muscles correlates with fibrosis. Pathogenetic role of a fibrogenic cytokine, *J Clin Invest* 1995, 96:1137-1144
22. Gosselin LE, Williams JE, Deering M, Brazeau D, Koury S, Martinez DA: Localization and early time course of TGF-beta 1 mRNA expression in dystrophic muscle, *Muscle Nerve* 2004, 30:645-653
23. Ishitobi M, Haginoya K, Zhao Y, Ohnuma A, Minato J, Yanagisawa T, Tanabu M, Kikuchi M, Iinuma K: Elevated plasma levels of transforming growth factor beta1 in patients with muscular dystrophy, *Neuroreport* 2000, 11:4033-4035
24. Tomasek JJ, Gabbiani G, Hinz B, Chaponnier C, Brown RA: Myofibroblasts and mechano-regulation of connective tissue remodelling, *Nat Rev Mol Cell Biol* 2002, 3:349-363

25. Desmouliere A, Geinoz A, Gabbiani F, Gabbiani G: Transforming growth factor-beta 1 induces alpha-smooth muscle actin expression in granulation tissue myofibroblasts and in quiescent and growing cultured fibroblasts, *J Cell Biol* 1993, 122:103-111
26. Li Y, Huard J: Differentiation of muscle-derived cells into myofibroblasts in injured skeletal muscle, *Am J Pathol* 2002, 161:895-907
27. Bedair HS, Karthikeyan T, Quintero A, Li Y, Huard J: Angiotensin II receptor blockade administered after injury improves muscle regeneration and decreases fibrosis in normal skeletal muscle, *Am J Sports Med* 2008, 36:1548-1554
28. Sato K, Li Y, Foster W, Fukushima K, Badlani N, Adachi N, Usas A, Fu FH, Huard J: Improvement of muscle healing through enhancement of muscle regeneration and prevention of fibrosis, *Muscle Nerve* 2003, 28:365-372
29. Fukushima K, Badlani N, Usas A, Riano F, Fu F, Huard J: The use of an antifibrosis agent to improve muscle recovery after laceration, *Am J Sports Med* 2001, 29:394-402
30. Foster W, Li Y, Usas A, Somogyi G, Huard J: Gamma interferon as an antifibrosis agent in skeletal muscle, *J Orthop Res* 2003, 21:798-804
31. Chan YS, Li Y, Foster W, Horaguchi T, Somogyi G, Fu FH, Huard J: Antifibrotic effects of suramin in injured skeletal muscle after laceration, *J Appl Physiol* 2003, 95:771-780
32. Chan YS, Li Y, Foster W, Fu FH, Huard J: The use of suramin, an antifibrotic agent, to improve muscle recovery after strain injury, *Am J Sports Med* 2005, 33:43-51
33. Jarvinen TA, Jarvinen TL, Kaariainen M, Kalimo H, Jarvinen M: Muscle injuries: biology and treatment, *Am J Sports Med* 2005, 33:745-764
34. Jarvinen MJ, Lehto MU: The effects of early mobilisation and immobilisation on the healing process following muscle injuries, *Sports Med* 1993, 15:78-89
35. Allbrook D: Muscle regeneration, *Physiotherapy* 1973, 59:240-247
36. Carlson BM: Histological observations on the regeneration of mammalian and amphibian muscle. Edited by In Mauro A ea. *Excerpta Medica*, Amsterdam, 1970, p
37. Bailey AJ, Shellswell GB, Duance VC: Identification and change of collagen types in differentiating myoblasts and developing chick muscle, *Nature* 1979, 278:67-69
38. McMinn RM: The cellular morphology of tissue repair, *Int Rev Cytol* 1967, 22:63-145
39. Giri SN, Hyde DM, Braun RK, Gaarde W, Harper JR, Pierschbacher MD: Antifibrotic effect of decorin in a bleomycin hamster model of lung fibrosis, *Biochem Pharmacol* 1997, 54:1205-1216

40. Menetrey J, Kasemkijwattana C, Fu FH, Moreland MS, Huard J: Suturing versus immobilization of a muscle laceration. A morphological and functional study in a mouse model, *Am J Sports Med* 1999, 27:222-229
41. Ulloa L, Doody J, Massague J: Inhibition of transforming growth factor-beta/SMAD signalling by the interferon-gamma/STAT pathway, *Nature* 1999, 397:710-713
42. Allegra S, Li JY, Saez JM, Langlois D: Terminal differentiation of Sol 8 myoblasts is retarded by a transforming growth factor-beta autocrine regulatory loop, *Biochem J* 2004, 381:429-436
43. Olson EN, Sternberg E, Hu JS, Spizz G, Wilcox C: Regulation of myogenic differentiation by type beta transforming growth factor, *J Cell Biol* 1986, 103:1799-1805
44. Florini JR, Roberts AB, Ewton DZ, Falen SL, Flanders KC, Sporn MB: Transforming growth factor-beta. A very potent inhibitor of myoblast differentiation, identical to the differentiation inhibitor secreted by Buffalo rat liver cells, *J Biol Chem* 1986, 261:16509-16513
45. Allen RE, Boxhorn LK: Inhibition of skeletal muscle satellite cell differentiation by transforming growth factor-beta, *J Cell Physiol* 1987, 133:567-572
46. Thomas M, Langley B, Berry C, Sharma M, Kirk S, Bass J, Kambadur R: Myostatin, a negative regulator of muscle growth, functions by inhibiting myoblast proliferation, *J Biol Chem* 2000, 275:40235-40243
47. McCroskery S, Thomas M, Maxwell L, Sharma M, Kambadur R: Myostatin negatively regulates satellite cell activation and self-renewal, *J Cell Biol* 2003, 162:1135-1147
48. Langley B, Thomas M, Bishop A, Sharma M, Gilmour S, Kambadur R: Myostatin inhibits myoblast differentiation by down-regulating MyoD expression, *J Biol Chem* 2002, 277:49831-49840
49. McPherron AC, Lawler AM, Lee SJ: Regulation of skeletal muscle mass in mice by a new TGF-beta superfamily member, *Nature* 1997, 387:83-90
50. Acosta J, Carpio Y, Borroto I, Gonzalez O, Estrada MP: Myostatin gene silenced by RNAi show a zebrafish giant phenotype, *J Biotechnol* 2005, 119:324-331
51. Grobet L, Martin LJ, Poncelet D, Pirottin D, Brouwers B, Riquet J, Schoeberlein A, Dunner S, Menissier F, Massabanda J, Fries R, Hanset R, Georges M: A deletion in the bovine myostatin gene causes the double-muscling phenotype in cattle, *Nat Genet* 1997, 17:71-74
52. Kambadur R, Sharma M, Smith TP, Bass JJ: Mutations in myostatin (GDF8) in double-muscling Belgian Blue and Piedmontese cattle, *Genome Res* 1997, 7:910-916
53. McPherron AC, Lee SJ: Double muscling in cattle due to mutations in the myostatin gene, *Proc Natl Acad Sci U S A* 1997, 94:12457-12461

54. Williams MS: Myostatin mutation associated with gross muscle hypertrophy in a child, *N Engl J Med* 2004, 351:1030-1031; author reply 1030-1031
55. Pirottin D, Grobet L, Adamantidis A, Farnir F, Herens C, Daa Schroder H, Georges M: Transgenic engineering of male-specific muscular hypertrophy, *Proc Natl Acad Sci U S A* 2005, 102:6413-6418
56. Lee SJ, McPherron AC: Regulation of myostatin activity and muscle growth, *Proc Natl Acad Sci U S A* 2001, 98:9306-9311
57. Yang J, Ratovitski T, Brady JP, Solomon MB, Wells KD, Wall RJ: Expression of myostatin pro domain results in muscular transgenic mice, *Mol Reprod Dev* 2001, 60:351-361
58. Joulia D, Bernardi H, Garandel V, Rabenoelina F, Vernus B, Cabello G: Mechanisms involved in the inhibition of myoblast proliferation and differentiation by myostatin, *Exp Cell Res* 2003, 286:263-275
59. Rios R, Carneiro I, Arce VM, Devesa J: Myostatin is an inhibitor of myogenic differentiation, *Am J Physiol Cell Physiol* 2002, 282:C993-999
60. Megeney LA, Rudnicki MA: Determination versus differentiation and the MyoD family of transcription factors, *Biochem Cell Biol* 1995, 73:723-732
61. Oh SP, Seki T, Goss KA, Imamura T, Yi Y, Donahoe PK, Li L, Miyazono K, ten Dijke P, Kim S, Li E: Activin receptor-like kinase 1 modulates transforming growth factor-beta 1 signaling in the regulation of angiogenesis, *Proc Natl Acad Sci U S A* 2000, 97:2626-2631
62. Asahina I, Sampath TK, Hauschka PV: Human osteogenic protein-1 induces chondroblastic, osteoblastic, and/or adipocytic differentiation of clonal murine target cells, *Exp Cell Res* 1996, 222:38-47
63. Attisano L, Wrana JL: Signal transduction by the TGF-beta superfamily, *Science* 2002, 296:1646-1647
64. Zhu X, Topouzis S, Liang LF, Stotish RL: Myostatin signaling through Smad2, Smad3 and Smad4 is regulated by the inhibitory Smad7 by a negative feedback mechanism, *Cytokine* 2004, 26:262-272
65. Rebbapragada A, Benchabane H, Wrana JL, Celeste AJ, Attisano L: Myostatin signals through a transforming growth factor beta-like signaling pathway to block adipogenesis, *Mol Cell Biol* 2003, 23:7230-7242
66. Yamaguchi Y, Ruoslahti E: Expression of human proteoglycan in Chinese hamster ovary cells inhibits cell proliferation, *Nature* 1988, 336:244-246
67. Krusius T, Ruoslahti E: Primary structure of an extracellular matrix proteoglycan core protein deduced from cloned cDNA, *Proc Natl Acad Sci U S A* 1986, 83:7683-7687

68. Hildebrand A, Romaris M, Rasmussen LM, Heinegard D, Twardzik DR, Border WA, Ruoslahti E: Interaction of the small interstitial proteoglycans biglycan, decorin and fibromodulin with transforming growth factor beta, *Biochem J* 1994, 302 (Pt 2):527-534
69. Yamaguchi Y, Mann DM, Ruoslahti E: Negative regulation of transforming growth factor-beta by the proteoglycan decorin, *Nature* 1990, 346:281-284
70. Schonherr E, Broszat M, Brandan E, Bruckner P, Kresse H: Decorin core protein fragment Leu155-Val260 interacts with TGF-beta but does not compete for decorin binding to type I collagen, *Arch Biochem Biophys* 1998, 355:241-248
71. Border WA, Noble NA, Yamamoto T, Harper JR, Yamaguchi Y, Pierschbacher MD, Ruoslahti E: Natural inhibitor of transforming growth factor-beta protects against scarring in experimental kidney disease, *Nature* 1992, 360:361-364
72. Shimizu I: Antifibrogenic therapies in chronic HCV infection, *Curr Drug Targets Infect Disord* 2001, 1:227-240
73. Zimmers TA, Davies MV, Koniaris LG, Haynes P, Esquela AF, Tomkinson KN, McPherron AC, Wolfman NM, Lee SJ: Induction of cachexia in mice by systemically administered myostatin, *Science* 2002, 296:1486-1488
74. Thies RS, Chen T, Davies MV, Tomkinson KN, Pearson AA, Shakey QA, Wolfman NM: GDF-8 propeptide binds to GDF-8 and antagonizes biological activity by inhibiting GDF-8 receptor binding, *Growth Factors* 2001, 18:251-259
75. Jiang MS, Liang LF, Wang S, Ratovitski T, Holmstrom J, Barker C, Stotish R: Characterization and identification of the inhibitory domain of GDF-8 propeptide, *Biochem Biophys Res Commun* 2004, 315:525-531
76. Yang J, Zhao B: Postnatal expression of myostatin propeptide cDNA maintained high muscle growth and normal adipose tissue mass in transgenic mice fed a high-fat diet, *Mol Reprod Dev* 2006, 73:462-469
77. Bogdanovich S, Perkins KJ, Krag TO, Whittemore LA, Khurana TS: Myostatin propeptide-mediated amelioration of dystrophic pathophysiology, *Faseb J* 2005, 19:543-549
78. Nakamura T, Takio K, Eto Y, Shibai H, Titani K, Sugino H: Activin-binding protein from rat ovary is follistatin, *Science* 1990, 247:836-838
79. Patel K: Follistatin, *Int J Biochem Cell Biol* 1998, 30:1087-1093
80. Fainsod A, Deissler K, Yelin R, Marom K, Epstein M, Pillemer G, Steinbeisser H, Blum M: The dorsalizing and neural inducing gene follistatin is an antagonist of BMP-4, *Mech Dev* 1997, 63:39-50

81. Gamer LW, Wolfman NM, Celeste AJ, Hattersley G, Hewick R, Rosen V: A novel BMP expressed in developing mouse limb, spinal cord, and tail bud is a potent mesoderm inducer in *Xenopus* embryos, *Dev Biol* 1999, 208:222-232
82. Amthor H, Nicholas G, McKinnell I, Kemp CF, Sharma M, Kambadur R, Patel K: Follistatin complexes Myostatin and antagonises Myostatin-mediated inhibition of myogenesis, *Dev Biol* 2004, 270:19-30
83. Bonilla E, Samitt CE, Miranda AF, Hays AP, Salviati G, DiMauro S, Kunkel LM, Hoffman EP, Rowland LP: Duchenne muscular dystrophy: deficiency of dystrophin at the muscle cell surface, *Cell* 1988, 54:447-452
84. Carpenter S, Karpati G, Zubrzycka-Gaarn E, Bulman DE, Ray PN, Worton RG: Dystrophin is localized to the plasma membrane of human skeletal muscle fibers by electron-microscopic cytochemical study, *Muscle Nerve* 1990, 13:376-380
85. Engel AG: Duchenne dystrophy. Edited by Engel AG, Banker BQ. New York, McGraw-Hill, 1986, 1185-1202 p
86. Salviati G, Betto R, Ceoldo S, Biasia E, Bonilla E, Miranda AF, Dimauro S: Cell fractionation studies indicate that dystrophin is a protein of surface membranes of skeletal muscle, *Biochem J* 1989, 258:837-841
87. Weller B, Karpati G, Carpenter S: Dystrophin-deficient mdx muscle fibers are preferentially vulnerable to necrosis induced by experimental lengthening contractions, *J Neurol Sci* 1990, 100:9-13
88. Ervasti JM, Campbell KP: Membrane organization of the dystrophin-glycoprotein complex, *Cell* 1991, 66:1121-1131
89. Ibraghimov-Beskrovnaya O, Ervasti JM, Leveille CJ, Slaughter CA, Sernett SW, Campbell KP: Primary structure of dystrophin-associated glycoproteins linking dystrophin to the extracellular matrix, *Nature* 1992, 355:696-702
90. Matsumura K, Campbell KP: Dystrophin-glycoprotein complex: its role in the molecular pathogenesis of muscular dystrophies, *Muscle Nerve* 1994, 17:2-15
91. Ozawa E, Yoshida M, Suzuki A, Mizuno Y, Hagiwara Y, Noguchi S: Dystrophin-associated proteins in muscular dystrophy, *Hum Mol Genet* 1995, 4 Spec No:1711-1716
92. Gorospe JR, Hoffman EP: Duchenne muscular dystrophy, *Curr Opin Rheumatol* 1992, 4:794-800
93. Partridge TA: Invited review: myoblast transfer: a possible therapy for inherited myopathies?, *Muscle Nerve* 1991, 14:197-212

94. Alameddine HS, Dehaupas M, Fardeau M: Regeneration of skeletal muscle fibers from autologous satellite cells multiplied in vitro. An experimental model for testing cultured cell myogenicity, *Muscle Nerve* 1989, 12:544-555
95. Huard J, Labrecque C, Dansereau G, Robitaille L, Tremblay JP: Dystrophin expression in myotubes formed by the fusion of normal and dystrophic myoblasts, *Muscle Nerve* 1991, 14:178-182
96. Morgan JE, Hoffman EP, Partridge TA: Normal myogenic cells from newborn mice restore normal histology to degenerating muscles of the mdx mouse, *J Cell Biol* 1990, 111:2437-2449
97. Partridge TA, Morgan JE, Coulton GR, Hoffman EP, Kunkel LM: Conversion of mdx myofibres from dystrophin-negative to -positive by injection of normal myoblasts, *Nature* 1989, 337:176-179
98. Law PK, Goodwin TG, Fang Q, Chen M, Li HJ, Florendo A, Kirby D, Bertorini T, Herred H, Golden G: Pioneering development of myoblast transfer therapy. Edited by Angelini C, Darrieli GA, Fontanan D. New York, Elsevier Science Inc., 1991, 109-116 p
99. Huard J, Bouchard JP, Roy R, Malouin F, Dansereau G, Labrecque C, Albert N, Richards CL, Lemieux B, Tremblay JP: Human myoblast transplantation: preliminary results of 4 cases, *Muscle Nerve* 1992, 15:550-560
100. Huard J, Roy R, Bouchard JP, Malouin F, Richards CL, Tremblay JP: Human myoblast transplantation between immunohistocompatible donors and recipients produces immune reactions, *Transplant Proc* 1992, 24:3049-3051
101. Gussoni E, Blau HM, Kunkel LM: The fate of individual myoblasts after transplantation into muscles of DMD patients, *Nat Med* 1997, 3:970-977
102. Gussoni E, Pavlath GK, Lanctot AM, Sharma KR, Miller RG, Steinman L, Blau HM: Normal dystrophin transcripts detected in Duchenne muscular dystrophy patients after myoblast transplantation, *Nature* 1992, 356:435-438
103. Mendell JR, Kissel JT, Amato AA, King W, Signore L, Prior TW, Sahenk Z, Benson S, McAndrew PE, Rice R, et al.: Myoblast transfer in the treatment of Duchenne's muscular dystrophy, *N Engl J Med* 1995, 333:832-838
104. Tremblay JP, Malouin F, Roy R, Huard J, Bouchard JP, Satoh A, Richards CL: Results of a triple blind clinical study of myoblast transplantations without immunosuppressive treatment in young boys with Duchenne muscular dystrophy, *Cell Transplant* 1993, 2:99-112
105. Karpati G, Holland P, Worton RG: Myoblast transfer in DMD: problems in the interpretation of efficiency, *Muscle Nerve* 1992, 15:1209-1210

106. Miller RG, Sharma KR, Pavlath GK, Gussoni E, Mynhier M, Lanctot AM, Greco CM, Steinman L, Blau HM: Myoblast implantation in Duchenne muscular dystrophy: the San Francisco study, *Muscle Nerve* 1997, 20:469-478
107. Cao B, Deasy BM, Pollett J, Huard J: Cell therapy for muscle regeneration and repair, *Phys Med Rehabil Clin N Am* 2005, 16:889-907, viii
108. Beauchamp JR, Morgan JE, Pagel CN, Partridge TA: Dynamics of myoblast transplantation reveal a discrete minority of precursors with stem cell-like properties as the myogenic source, *J Cell Biol* 1999, 144:1113-1122
109. Fan Y, Maley M, Beilharz M, Grounds M: Rapid death of injected myoblasts in myoblast transfer therapy, *Muscle Nerve* 1996, 19:853-860
110. Guerette B, Asselin I, Skuk D, Entman M, Tremblay JP: Control of inflammatory damage by anti-LFA-1: increase success of myoblast transplantation, *Cell Transplant* 1997, 6:101-107
111. Hodgetts SI, Beilharz MW, Scalzo AA, Grounds MD: Why do cultured transplanted myoblasts die in vivo? DNA quantification shows enhanced survival of donor male myoblasts in host mice depleted of CD4+ and CD8+ cells or Nk1.1+ cells, *Cell Transplant* 2000, 9:489-502
112. Smythe GM, Hodgetts SI, Grounds MD: Immunobiology and the future of myoblast transfer therapy, *Mol Ther* 2000, 1:304-313
113. Qu-Petersen Z, Deasy B, Jankowski R, Ikezawa M, Cummins J, Pruchnic R, Mytinger J, Cao B, Gates C, Wernig A, Huard J: Identification of a novel population of muscle stem cells in mice: potential for muscle regeneration, *J Cell Biol* 2002, 157:851-864
114. Adachi N, Sato K, Usas A, Fu FH, Ochi M, Han CW, Niyibizi C, Huard J: Muscle derived, cell based ex vivo gene therapy for treatment of full thickness articular cartilage defects, *J Rheumatol* 2002, 29:1920-1930
115. Cao B, Zheng B, Jankowski RJ, Kimura S, Ikezawa M, Deasy B, Cummins J, Epperly M, Qu-Petersen Z, Huard J: Muscle stem cells differentiate into haematopoietic lineages but retain myogenic potential, *Nat Cell Biol* 2003, 5:640-646
116. Kuroda R, Usas A, Kubo S, Corsi K, Peng H, Rose T, Cummins J, Fu FH, Huard J: Cartilage repair using bone morphogenetic protein 4 and muscle-derived stem cells, *Arthritis Rheum* 2006, 54:433-442
117. Lee JY, Qu-Petersen Z, Cao B, Kimura S, Jankowski R, Cummins J, Usas A, Gates C, Robbins P, Wernig A, Huard J: Clonal isolation of muscle-derived cells capable of enhancing muscle regeneration and bone healing, *J Cell Biol* 2000, 150:1085-1100
118. Bosch P, Musgrave D, Ghivizzani S, Latterman C, Day CS, Huard J: The efficiency of muscle-derived cell-mediated bone formation, *Cell Transplant* 2000, 9:463-470

119. Peng H, Wright V, Usas A, Gearhart B, Shen HC, Cummins J, Huard J: Synergistic enhancement of bone formation and healing by stem cell-expressed VEGF and bone morphogenetic protein-4, *J Clin Invest* 2002, 110:751-759
120. Deasy BM, Huard J: Gene therapy and tissue engineering based on muscle-derived stem cells, *Curr Opin Mol Ther* 2002, 4:382-389
121. Floyd SS, Jr., Clemens PR, Ontell MR, Kochanek S, Day CS, Yang J, Hauschka SD, Balkir L, Morgan J, Moreland MS, Feero GW, Epperly M, Huard J: Ex vivo gene transfer using adenovirus-mediated full-length dystrophin delivery to dystrophic muscles, *Gene Ther* 1998, 5:19-30
122. Benabdallah BF, Bouchentouf M, Tremblay JP: Improved success of myoblast transplantation in mdx mice by blocking the myostatin signal, *Transplantation* 2005, 79:1696-1702
123. Wagner KR, McPherron AC, Winik N, Lee SJ: Loss of myostatin attenuates severity of muscular dystrophy in mdx mice, *Ann Neurol* 2002, 52:832-836
124. Nguyen F, Guigand L, Goubault-Leroux I, Wyers M, Cherel Y: Microvessel density in muscles of dogs with golden retriever muscular dystrophy, *Neuromuscul Disord* 2005, 15:154-163
125. Deasy BM, Gharaibeh BM, Pollett JB, Jones MM, Lucas MA, Kanda Y, Huard J: Long-term self-renewal of postnatal muscle-derived stem cells, *Mol Biol Cell* 2005, 16:3323-3333
126. Deasy BM, Lu A, Tebbets JC, Feduska JM, Schugar RC, Pollett JB, Sun B, Urish KL, Gharaibeh BM, Cao B, Rubin RT, Huard J: A role for cell sex in stem cell-mediated skeletal muscle regeneration: female cells have higher muscle regeneration efficiency, *J Cell Biol* 2007, 177:73-86
127. Zhu J, Li Y, Shen W, Qiao C, Ambrosio F, Lavasani M, Nozaki M, Branca MF, Huard J: Relationships between transforming growth factor-beta1, myostatin, and decorin: implications for skeletal muscle fibrosis, *J Biol Chem* 2007, 282:25852-25863
128. Jankowski RJ, Deasy BM, Cao B, Gates C, Huard J: The role of CD34 expression and cellular fusion in the regeneration capacity of myogenic progenitor cells, *J Cell Sci* 2002, 115:4361-4374
129. Grisanti S, Szurman P, Warga M, Kaczmarek R, Ziemssen F, Tatar O, Bartz-Schmidt KU: Decorin modulates wound healing in experimental glaucoma filtration surgery: a pilot study, *Invest Ophthalmol Vis Sci* 2005, 46:191-196
130. Huijun W, Long C, Zhigang Z, Feng J, Muiyi G: Ex vivo transfer of the decorin gene into rat glomerulus via a mesangial cell vector suppressed extracellular matrix accumulation in experimental glomerulonephritis, *Exp Mol Pathol* 2005, 78:17-24

131. Budasz-Rwiderska M, Jank M, Motyl T: Transforming growth factor-beta1 upregulates myostatin expression in mouse C2C12 myoblasts, *J Physiol Pharmacol* 2005, 56 Suppl 3:195-214
132. Yamazaki K, Fukata H, Adachi T, Tainaka H, Kohda M, Yamazaki M, Kojima K, Chiba K, Mori C, Komiyama M: Association of increased type I collagen expression and relative stromal overgrowth in mouse epididymis neonatally exposed to diethylstilbestrol, *Mol Reprod Dev* 2005, 72:291-298
133. Yamanouchi K, Soeta C, Naito K, Tojo H: Expression of myostatin gene in regenerating skeletal muscle of the rat and its localization, *Biochem Biophys Res Commun* 2000, 270:510-516
134. Pierce GF, Mustoe TA, Lingelbach J, Masakowski VR, Griffin GL, Senior RM, Deuel TF: Platelet-derived growth factor and transforming growth factor-beta enhance tissue repair activities by unique mechanisms, *J Cell Biol* 1989, 109:429-440
135. Phan SH: The myofibroblast in pulmonary fibrosis, *Chest* 2002, 122:286S-289S
136. Thannickal VJ, Toews GB, White ES, Lynch JP, 3rd, Martinez FJ: Mechanisms of pulmonary fibrosis, *Annu Rev Med* 2004, 55:395-417
137. McCroskery S, Thomas M, Platt L, Hennebry A, Nishimura T, McLeay L, Sharma M, Kambadur R: Improved muscle healing through enhanced regeneration and reduced fibrosis in myostatin-null mice, *J Cell Sci* 2005, 118:3531-3541
138. Kirk S, Oldham J, Kambadur R, Sharma M, Dobbie P, Bass J: Myostatin regulation during skeletal muscle regeneration, *J Cell Physiol* 2000, 184:356-363
139. Mendler L, Zador E, Ver Heyen M, Dux L, Wuytack F: Myostatin levels in regenerating rat muscles and in myogenic cell cultures, *J Muscle Res Cell Motil* 2000, 21:551-563
140. Cantini M, Massimino ML, Bruson A, Catani C, Dalla Libera L, Carraro U: Macrophages regulate proliferation and differentiation of satellite cells, *Biochem Biophys Res Commun* 1994, 202:1688-1696
141. Chazaud B, Sonnet C, Lafuste P, Bassez G, Rimaniol AC, Poron F, Authier FJ, Dreyfus PA, Gherardi RK: Satellite cells attract monocytes and use macrophages as a support to escape apoptosis and enhance muscle growth, *J Cell Biol* 2003, 163:1133-1143
142. Lescaudron L, Peltekian E, Fontaine-Perus J, Paulin D, Zampieri M, Garcia L, Parrish E: Blood borne macrophages are essential for the triggering of muscle regeneration following muscle transplant, *Neuromuscul Disord* 1999, 9:72-80
143. Merly F, Lescaudron L, Rouaud T, Crossin F, Gardahaut MF: Macrophages enhance muscle satellite cell proliferation and delay their differentiation, *Muscle Nerve* 1999, 22:724-732

144. Robertson TA, Maley MA, Grounds MD, Papadimitriou JM: The role of macrophages in skeletal muscle regeneration with particular reference to chemotaxis, *Exp Cell Res* 1993, 207:321-331
145. Li Y, Cantini M, Huard J: Muscle injury and repair, *Current Opinion in Orthopaedics* 2001, 12:409-415
146. Kocamis H, Killefer J: Myostatin expression and possible functions in animal muscle growth, *Domest Anim Endocrinol* 2002, 23:447-454
147. Chen Y, Luk KD, Cheung KM, Xu R, Lin MC, Lu WW, Leong JC, Kung HF: Gene therapy for new bone formation using adeno-associated viral bone morphogenetic protein-2 vectors, *Gene Ther* 2003, 10:1345-1353
148. Li Y, Negishi S, Sakamoto M, Usas A, Huard J: The use of relaxin improves healing in injured muscle, *Ann N Y Acad Sci* 2005, 1041:395-397
149. Negishi S, Li Y, Usas A, Fu FH, Huard J: The effect of relaxin treatment on skeletal muscle injuries, *Am J Sports Med* 2005, 33:1816-1824
150. Miura T, Kishioka Y, Wakamatsu J, Hattori A, Hennebry A, Berry CJ, Sharma M, Kambadur R, Nishimura T: Decorin binds myostatin and modulates its activity to muscle cells, *Biochem Biophys Res Commun* 2006, 340:675-680
151. Bogdanovich S, Krag TO, Barton ER, Morris LD, Whittemore LA, Ahima RS, Khurana TS: Functional improvement of dystrophic muscle by myostatin blockade, *Nature* 2002, 420:418-421
152. Hill JJ, Davies MV, Pearson AA, Wang JH, Hewick RM, Wolfman NM, Qiu Y: The myostatin propeptide and the follistatin-related gene are inhibitory binding proteins of myostatin in normal serum, *J Biol Chem* 2002, 277:40735-40741
153. Hill JJ, Qiu Y, Hewick RM, Wolfman NM: Regulation of myostatin in vivo by growth and differentiation factor-associated serum protein-1: a novel protein with protease inhibitor and follistatin domains, *Mol Endocrinol* 2003, 17:1144-1154
154. Lee SJ, Reed LA, Davies MV, Girgenrath S, Goad ME, Tomkinson KN, Wright JF, Barker C, Ehrmantraut G, Holmstrom J, Trowell B, Gertz B, Jiang MS, Sebald SM, Matzuk M, Li E, Liang LF, Quattlebaum E, Stotish RL, Wolfman NM: Regulation of muscle growth by multiple ligands signaling through activin type II receptors, *Proc Natl Acad Sci U S A* 2005, 102:18117-18122
155. Li ZB, Kollias HD, Wagner KR: Myostatin directly regulates skeletal muscle fibrosis, *J Biol Chem* 2008, 283:19371-19378
156. Bartoli M, Poupiot J, Vulin A, Fougerousse F, Arandel L, Daniele N, Roudaut C, Noulet F, Garcia L, Danos O, Richard I: AAV-mediated delivery of a mutated myostatin propeptide ameliorates calpain 3 but not alpha-sarcoglycan deficiency, *Gene Ther* 2007, 14:733-740

157. Qiao C, Li J, Jiang J, Zhu X, Wang B, Li J, Xiao X: Myostatin propeptide gene delivery by adeno-associated virus serotype 8 vectors enhances muscle growth and ameliorates dystrophic phenotypes in mdx mice, *Hum Gene Ther* 2008, 19:241-254
158. Xiao X, Li J, Samulski RJ: Production of high-titer recombinant adeno-associated virus vectors in the absence of helper adenovirus, *J Virol* 1998, 72:2224-2232
159. Gharaibeh B, Lu A, Tebbets J, Zheng B, Feduska J, Crisan M, Peault B, Cummins J, Huard J: Isolation of a slowly adhering cell fraction containing stem cells from murine skeletal muscle by the preplate technique, *Nat Protoc* 2008, 3:1501-1509
160. Musaro A, Rosenthal N: Transgenic mouse models of muscle aging, *Exp Gerontol* 1999, 34:147-156
161. Tal J: Adeno-associated virus-based vectors in gene therapy, *J Biomed Sci* 2000, 7:279-291
162. Bogdanovich S, McNally EM, Khurana TS: Myostatin blockade improves function but not histopathology in a murine model of limb-girdle muscular dystrophy 2C, *Muscle Nerve* 2008, 37:308-316
163. Benabdallah BF, Bouchentouf M, Rousseau J, Bigey P, Michaud A, Chapdelaine P, Scherman D, Tremblay JP: Inhibiting myostatin with follistatin improves the success of myoblast transplantation in dystrophic mice, *Cell Transplant* 2008, 17:337-350
164. Grounds MD, Torrisi J: Anti-TNFalpha (Remicade) therapy protects dystrophic skeletal muscle from necrosis, *Faseb J* 2004, 18:676-682
165. Hodgetts S, Radley H, Davies M, Grounds MD: Reduced necrosis of dystrophic muscle by depletion of host neutrophils, or blocking TNFalpha function with Etanercept in mdx mice, *Neuromuscul Disord* 2006, 16:591-602
166. Pierno S, Nico B, Burdi R, Liantonio A, Didonna MP, Cippone V, Fraysse B, Rolland JF, Mangieri D, Andretta F, Ferro P, Camerino C, Zallone A, Confalonieri P, De Luca A: Role of tumour necrosis factor alpha, but not of cyclo-oxygenase-2-derived eicosanoids, on functional and morphological indices of dystrophic progression in mdx mice: a pharmacological approach, *Neuropathol Appl Neurobiol* 2007, 33:344-359
167. McLoughlin TJ, Tsivitse SK, Edwards JA, Aiken BA, Pizza FX: Deferoxamine reduces and nitric oxide synthase inhibition increases neutrophil-mediated myotube injury, *Cell Tissue Res* 2003, 313:313-319
168. Nguyen HX, Tidball JG: Interactions between neutrophils and macrophages promote macrophage killing of rat muscle cells in vitro, *J Physiol* 2003, 547:125-132
169. Pizza FX, McLoughlin TJ, McGregor SJ, Calomeni EP, Gunning WT: Neutrophils injure cultured skeletal myotubes, *Am J Physiol Cell Physiol* 2001, 281:C335-341

170. Cheung EV, Tidball JG: Administration of the non-steroidal anti-inflammatory drug ibuprofen increases macrophage concentrations but reduces necrosis during modified muscle use, *Inflamm Res* 2003, 52:170-176
171. Nguyen HX, Tidball JG: Expression of a muscle-specific, nitric oxide synthase transgene prevents muscle membrane injury and reduces muscle inflammation during modified muscle use in mice, *J Physiol* 2003, 550:347-356
172. Porter JD, Khanna S, Kaminski HJ, Rao JS, Merriam AP, Richmonds CR, Leahy P, Li J, Guo W, Andrade FH: A chronic inflammatory response dominates the skeletal muscle molecular signature in dystrophin-deficient mdx mice, *Hum Mol Genet* 2002, 11:263-272
173. Tews DS, Goebel HH: Cell death and oxidative damage in inflammatory myopathies, *Clin Immunol Immunopathol* 1998, 87:240-247
174. Lundberg IE: The role of cytokines, chemokines, and adhesion molecules in the pathogenesis of idiopathic inflammatory myopathies, *Curr Rheumatol Rep* 2000, 2:216-224
175. Spencer MJ, Tidball JG: Do immune cells promote the pathology of dystrophin-deficient myopathies?, *Neuromuscul Disord* 2001, 11:556-564
176. McGeachie JK, Grounds MD, Partridge TA, Morgan JE: Age-related changes in replication of myogenic cells in mdx mice: quantitative autoradiographic studies, *J Neurol Sci* 1993, 119:169-179
177. Li ZB, Kollias HD, Wagner KR: Myostatin directly regulates skeletal muscle fibrosis, *J Biol Chem* 2008,
178. Jankowski RJ, Haluszczak C, Trucco M, Huard J: Flow cytometric characterization of myogenic cell populations obtained via the preplate technique: potential for rapid isolation of muscle-derived stem cells, *Hum Gene Ther* 2001, 12:619-628
179. Krneta J, Kroll J, Alves F, Prahst C, Sananbenesi F, Dullin C, Kimmina S, Phillips DJ, Augustin HG: Dissociation of angiogenesis and tumorigenesis in follistatin- and activin-expressing tumors, *Cancer Res* 2006, 66:5686-5695
180. Shen W, Li Y, Tang Y, Cummins J, Huard J: NS-398, a cyclooxygenase-2-specific inhibitor, delays skeletal muscle healing by decreasing regeneration and promoting fibrosis, *Am J Pathol* 2005, 167:1105-1117
181. Kozian DH, Ziche M, Augustin HG: The activin-binding protein follistatin regulates autocrine endothelial cell activity and induces angiogenesis, *Lab Invest* 1997, 76:267-276
182. Gros J, Manceau M, Thome V, Marcelle C: A common somitic origin for embryonic muscle progenitors and satellite cells, *Nature* 2005, 435:954-958

183. Kassar-Duchossoy L, Giacone E, Gayraud-Morel B, Jory A, Gomes D, Tajbakhsh S: Pax3/Pax7 mark a novel population of primitive myogenic cells during development, *Genes Dev* 2005, 19:1426-1431
184. Relaix F, Rocancourt D, Mansouri A, Buckingham M: A Pax3/Pax7-dependent population of skeletal muscle progenitor cells, *Nature* 2005, 435:948-953
185. Le Grand F, Rudnicki MA: Skeletal muscle satellite cells and adult myogenesis, *Curr Opin Cell Biol* 2007, 19:628-633
186. McFarlane C, Hennebry A, Thomas M, Plummer E, Ling N, Sharma M, Kambadur R: Myostatin signals through Pax7 to regulate satellite cell self-renewal, *Exp Cell Res* 2008, 314:317-329
187. Bauer SM, Bauer RJ, Liu ZJ, Chen H, Goldstein L, Velazquez OC: Vascular endothelial growth factor-C promotes vasculogenesis, angiogenesis, and collagen constriction in three-dimensional collagen gels, *J Vasc Surg* 2005, 41:699-707
188. Bauer SM, Bauer RJ, Velazquez OC: Angiogenesis, vasculogenesis, and induction of healing in chronic wounds, *Vasc Endovascular Surg* 2005, 39:293-306
189. Cohn RD, Liang HY, Shetty R, Abraham T, Wagner KR: Myostatin does not regulate cardiac hypertrophy or fibrosis, *Neuromuscul Disord* 2007, 17:290-296
190. Artaza JN, Singh R, Ferrini MG, Braga M, Tsao J, Gonzalez-Cadavid NF: Myostatin promotes a fibrotic phenotypic switch in multipotent C3H 10T1/2 cells without affecting their differentiation into myofibroblasts, *J Endocrinol* 2008, 196:235-249
191. Cantini LP, Ferrini MG, Vernet D, Magee TR, Qian A, Gelfand RA, Rajfer J, Gonzalez-Cadavid NF: Profibrotic role of myostatin in Peyronie's disease, *J Sex Med* 2008, 5:1607-1622